

**Translocator protein 18 ligand Emapunil protects against  
neurodegeneration in the MPTP mouse model of  
Parkinsonism**

---

Dissertation

for the award of the degree

“Doctor rerum naturalium” (Dr.rer.nat)

of the Georg-August-Universität Göttingen

within the doctoral program in Biology

of the Georg-August University School of Science (GAUSS)

submitted by

Jing Gong

from Hubei, China

Göttingen, 2019

### Members of the Thesis Committee:

#### **Prof. Dr. Tiago Fleming Outeiro (Reviewer)**

Department of Experimental Neurodegeneration, University Medical Center Göttingen

#### **Prof. Dr. Gerhard Braus (Reviewer)**

Department of Microbiology and Genetics, Georg-August-Universität Göttingen

#### **Prof. Dr. Anja Schneider**

Department of Neurodegenerative Diseases and Geriatric Psychiatry, University Hospital  
Bonn German Center for Neurodegenerative Diseases (DZNE), Bonn

### Members of the Examination Board:

Members of the Thesis Committee and

#### **Prof. Dr. Markus Zweckstetter**

Structure determination using NMR, Max Planck Institute for Biophysical Chemistry,  
Göttingen

German Center for Neurodegenerative Diseases (DZNE), Göttingen

#### **Prof. Dr. André Fischer**

Department of Psychiatry and Psychotherapy, University Medical Center Göttingen

German Center for Neurodegenerative Diseases (DZNE), Göttingen

#### **Prof. Dr. Dr. Hannelore Ehrenreich**

Department of Clinical Neuroscience, Max Planck Institute of Experimental Medicine,  
Göttingen

### Date of the oral examination

02. 07. 2019

## **Affidavit**

I hereby declare that I have written my doctoral thesis entitled “Translocator protein 18 ligand Emapunil protects against neurodegeneration in the MPTP mouse model of Parkinsonism” independently with no other sources and aids than quoted.

Bonn

Jing Gong

21. 03. 2019

## Contents

<b>1 Introduction .....</b>	<b>1</b>
1.1 Parkinson disease (PD) .....	1
1.1.1 Milestones of PD research .....	1
1.1.2 Epidemiology .....	2
1.1.3 Neuropathology .....	3
1.1.4 Genetic risk factors of PD .....	4
1.1.5 $\alpha$ -Synuclein pathology in PD .....	5
1.1.6 Endoplasmic reticulum (ER) stress and response in PD .....	6
1.2 Neuroinflammation in PD .....	8
1.2.1 Microglia origins .....	8
1.2.2 Resting microglia .....	8
1.2.3 Activated Microglia phenotypes .....	9
1.2.3.1 The M1 phenotype .....	9
1.2.3.2 M2 phenotypes .....	11
1.2.4 Microglia activation in PD .....	13
1.2.5 Therapeutic manipulation of microglia in PD .....	15
1.3 Animal models of Parkinson's disease .....	18
1.3.1 The MPTP mouse model of Parkinsonism .....	19
1.3.1.1 Mechanisms of MPTP .....	19
1.3.1.2 Acute versus subacute and chronic MPTP models .....	20
1.3.1.3 Behavior phenotypes in MPTP models .....	22
1.3.1.4 Advantages and disadvantages of MPTP model .....	22
1.4 Translocator protein 18 (TSPO) .....	24
1.4.1 TSPO distribution and function .....	24
1.4.1.1 Role in cholesterol transport .....	25
1.4.1.2 Other functions of TSPO .....	26
1.4.2 TSPO structure .....	26
1.4.3 TSPO ligands .....	28
1.4.3.1 Endogenous ligands of TSPO .....	28
1.4.3.2 Synthetic ligands of TSPO .....	30
1.4.4 TSPO radiotracers applied in PD .....	32
1.4.5 TSPO ligands have therapeutic effects in neurodegenerative diseases .....	33
<b>2 Materials and Methods .....</b>	<b>35</b>
2.1 Materials .....	35

2.1.1	Chemicals and consumables .....	35
2.1.2	Buffer solutions.....	36
2.1.3	Commercial reagents, compounds and consumables.....	38
2.1.4	Cell culture medium.....	39
2.1.4.1	Proliferation medium components .....	39
2.1.4.2	Differentiation medium components.....	39
2.1.5	Commercial kits .....	39
2.1.6	Primers .....	40
2.1.7	Antibodies .....	41
2.1.8	Software .....	42
2.2	Methods.....	42
2.2.1	The experimental schedule .....	42
2.2.1.1	Subacute MPTP treatment .....	43
2.2.1.2	Emapunil treatment.....	43
2.2.1.3	Experimental procedure .....	43
2.2.2	MPTP metabolism .....	44
2.2.3	RT-qPCR .....	44
2.2.3.1	RNA extraction .....	44
2.2.3.2	cDNA synthesis .....	45
2.2.3.3	RT-qPCR amplification .....	45
2.2.4	Behavioral tests.....	46
2.2.4.1	Pole test.....	46
2.2.4.2	Cylinder test.....	47
2.2.5	Neurochemical analysis of dopamine and dopamine metabolites .....	48
2.2.6	Histology.....	48
2.2.6.1	Transcardial Perfusion and tissue cryo-section .....	48
2.2.6.2	Immunohistochemistry .....	49
2.2.6.3	Stereological quantification of substantia nigra neurons .....	50
2.2.6.4	Immunofluorescence .....	50
2.2.6.5	Quantification of microglia activation and astrogliosis .....	51
2.2.6.6	Identification of TSPO expression in TH+ neurons .....	51
2.2.7	RNA-Seq and bioinformatical analysis.....	51
2.2.7.1	Tissue dissection and RNA isolation .....	51
2.2.7.2	RNA sequencing .....	52
2.2.7.3	Bioinformatical analysis .....	52
2.2.8	LUHMES cell culture experiments.....	53
2.2.8.1	Coating of cell culture flasks and dishes.....	53

2.2.8.2	Maintenance and differentiation .....	54
2.2.8.3	siRNA transfection.....	54
2.2.8.4	Toxicity assay .....	55
2.2.8.5	RT-qPCR assay for <i>Xbp1</i> and <i>XBPIs</i> analysis.....	55
2.2.8.6	SDS-PAGE and Western blot analysis .....	55
2.2.9	Statistical Analysis.....	56
<b>3</b>	<b>Results.....</b>	<b>57</b>
3.1	Emapunil protects from dopaminergic neuron loss in the subacute MPTP mouse model of Parkinsonism .....	57
3.1.1	Experimental plan .....	57
3.1.2	Emapunil treatment rescues TH- and Nissl- positive neurons from MPTP intoxication.....	58
3.2	Emapunil improves MPTP-induced motor impairment .....	61
3.2.1	Emapunil treatment improves pole test performance.....	61
3.2.2	Emapunil treatment improves the cylinder test performance .....	62
3.3	Emapunil attenuates alterations of dopamine and its metabolites induced by MPTP toxicity <i>in vivo</i> .....	64
3.4	Emapunil ameliorates IRE1 $\alpha$ /XBP1 pathway activation .....	67
3.5	The effects of Emapunil on XBP1s activation depend on TSPO.....	69
3.5.1	TSPO expression in LUHMES cells.....	69
3.5.2	Emapunil ameliorates MPP <sup>+</sup> and rotenone toxicity and ER stress in LUHMES cells.....	69
3.5.3	siRNA mediated TSPO down-regulation in LUHMES cells.....	72
3.5.4	Emapunil effects on cell viability and <i>XBPIs</i> activation are TSPO dependent .....	73
3.6	Emapunil inhibits microgliosis and astrogliosis <i>in vivo</i> .....	76
3.7	Emapunil induces a shift from pro- to anti-inflammatory microglia activation state .....	79
3.8	Whole-transcriptome analysis.....	82
<b>4</b>	<b>Discussion .....</b>	<b>85</b>
4.1	Physiological function of TSPO.....	85
4.2	Specificity of Emapunil binding to TSPO .....	86
4.3	How are Emapunil's neuroprotective effects mediated? .....	87
4.4	Emapunil shifts activated microglia from M1 to M2.....	88
4.5	Emapunil has additional functional pathways apart from counteracting MPTP toxicity .....	90
4.6	Sex differences in animal models .....	90
4.7	Summary of the mechanisms for the protective effects of Emapunil .....	91
4.8	The possibility to use Emapunil as a potential drug in PD .....	92

4.9 Limitations of this study.....	93
<b>5 Conclusions .....</b>	<b>94</b>
<b>6 Bibliography.....</b>	<b>95</b>
<b>7 Curriculum Vitae .....</b>	<b>118</b>

## Acknowledgments

I would like to express my sincere gratitude to all the people who helped me during my study in Germany.

First, I want to thank my supervisor Prof. Dr. Anja Schneider, who brought me into the field of neurodegenerative diseases research. Thank you for your tremendous support, guidance and teaching in all aspects. You enlighten me with your enthusiasm and dedication for science. Thank you so much.

I would like to thank my Thesis Committee members, Prof. Dr. Tiago Fleming Outeiro and Prof. Dr. Gerhard Braus, for your supports and discussions on this project and my thesis. I also want to thank Prof. Dr. Markus Zweckstetter, Prof. Dr. André Fischer and Prof. Dr. Dr. Hannelore Ehrenreich for being my examination board. Thank you!

Great thanks to the collaborated groups for this project. I want to thank Prof. Dr. Tiago Fleming Outeiro for allowing me to do the most of animal experiments in his lab, and a great thanks to his group members, especially to Dr. Éva M. Szegő, a great mentor who taught and helped me a lot in and out the lab. I also want to thank Prof. Dr. Markus Zweckstetter and Andrei Leonov for preparing Emapunil for us. I am also thankful to Prof. Dr. André Fischer, Susanne Burkhardt and Eva Benito for sequencing and analyzing the NGS data.

Big thanks should be given to all lab members in AG Schneider during I stay, Dr. Marcel Kunadt, Dr. Anne Stündl, Belisa Russo, Dr. Beate Koch, Jiantao Shi, Tanja Kraus, Dr. Anna Antoniou, Björn Zapke, Eva Keß, Dr. Kristin Oberlaender and Dr. Madhurima Chatterjee, for your kind help in and out the lab.

My dear wife Qinqin and my lovely daughter Sophie, thank you for coming into my life and make it colorful. I love you! I also want to thank our parents and friends for supporting us all these years.

## List of Abbreviations

°C	Degree Celsius
6-OHDA	6-hydroxydopamine
AD	Alzheimer's disease
Alpha-synuclein	$\alpha$ -synuclein
ALS	Amyotrophic lateral sclerosis
ANOVA	Analysis of variance
APP	Amyloid precursor protein
Arg1	Arginase 1
ATF6	activating transcription factor 6
BBB	blood-brain-barrier
BDNF	Brain-derived neurotrophic factor
bFGF	Basic fibroblast growth factor
BSA	Bovine serum albumin
CD200R	Cell surface glycoprotein CD200 receptor
CD206	Cluster of Differentiation 206
CD86	Cluster of Differentiation 86
Chi3l3	Chitinase-3-Like-3
CNS	Central nervous system
COX2	cyclo-oxygenase 2
CSF	cerebrospinal fluid
CX3CR1	CX3C chemokine receptor 1
Cxcl10	C-X-C motif chemokine 10
DAPI	4',6-diamidino-2-phenylindole
DAT	dopamine transporter
db-cAMP	Dibutyryl cyclic adenosine-monophosphate
DBS	Deep Brain Stimulation
DMF	Dimethyl fumarate
DMSO	dimethyl sulfoxide
DOPAC	3,4-dihydroxyphenylacetic acid
ER	Endoplasmic reticulum
ERAD	ER-associated degradation
ETC	electron transport chain

FC	Fold change
FCS	Fetal calf serum
FIZZ	Found in inflammatory zone
GABA	gamma-Aminobutyric acid
GAPDH	Glyceraldehyde 3-phosphate dehydrogenase
GDNF	Glial derived neurotrophic factor
GFAP	Glial fibrillary acidic protein
GM-CSF	Granulocyte-modifying colony-stimulating factor
GWAS	genome-wide association studies
HPLC	high performance liquid chromatography
HRP	Horseradish peroxidase
HVA	homovanillic acid
i.p.	intraperitoneal
IBA1	Ionized calcium binding adaptor molecule 1
IFN- $\gamma$	Interferon- $\gamma$
IGF-I	Insulin-like growth factor 1
IgG	Immunoglobulin G
IL-10	interleukin 10
IL-12	interleukin-12
IL-13	Interleukin-13
IL-1 $\beta$	interleukin 1- $\beta$
IL-4	interleukin 4
IL-6	interleukin 6
iNOS	Induced nitric oxide synthase
IP-10	interferon gamma-induced protein-10
IRE $\alpha$	inositol requiring kinase 1 $\alpha$
IRFs	interferon regulatory factors
JAK/STAT	Janus kinase/signal transducer and activator of transcription
LB	Lewy body
Levodopa	L-DOPA
LFC	log fold change
LPS	Lipopolysaccharide
LRRK2	leucine-rich repeat kinase 2
LUHMES	Lund human mesencephalic

MAO B	monoamine-oxidase B
MHC-II	major histocompatibility complex-II
min	Minute(s)
MMR	macrophage mannose receptor
Mpa2l	macrophage activating 2 like protein
MPDP <sup>+</sup>	1-methyl-4-phenyl-2, 3-dihydropyridium
MPP <sup>+</sup>	1-methyl-4-phenylpyridinium
MPTP	1-methyl-4-phenyl-1,2,3,6-tetrahydropyridine
mPTP	mitochondrial permeability transition pore
MS	multiple sclerosis
n	Sample size of a particular group
n.s.	Not significant
NF-κB	nuclear factor kappa beta
NMR	Nuclear magnetic resonance
NO	Nitric oxide
Nos2	Nitric Oxide Synthase 2
NSAID	non-specific target anti-inflammatory drugs
PBR	peripheral-type benzodiazepine receptor
PBS	Phosphate buffered saline
PD	Parkinson's disease
PERK	PRKR-like ER kinase
PET	Positron emission tomography
PFA	Paraformaldehyde
pH	Potential hydrogen
PINK1	PTEN-induced kinase 1
PPAR	peroxisome proliferator-activated receptor
PS1	Presenilin-1
ROS	reactive oxygen species
rpm	Revolutions per minute
RT-qPCR	reverse transcriptase quantitative real-time PCR
Runx1	Runt-related transcription factor 1
SDS-PAGE	sodium dodecyl sulfate–polyacrylamide gel electrophoresis
SEM	Standard error of the mean
SNpc	substantia nigra pars compacta

SOCS3	Suppressor of cytokine signaling 3
SOD1	superoxide dismutase
STAT6	Signal Transducer And Activator Of Transcription 6
TBS	Tris buffered saline
TEMED	N’N’N’-tetramethylethylene diamine
TGF- $\beta$	Transforming growth factor- $\beta$
TH	tyroxine hydroxylase
TLR	toll-like receptor
TNF- $\alpha$	tumor necrosis factor- $\alpha$
toyocamycin	2-hydroxy-1-naphthaldehyde
TREM2	triggering receptor also expressed on myeloid cells-2
Tris	Tris(hydroxymethyl)aminimethane
TSPO	translocator protein 18
UPR	unfolded protein response
VMAT	vesicular monoamine transporter
XBP1	X-box binding protein 1
XBP1s	Spliced X-box binding protein 1
YM1	chitinase-3-like protein 3

## List of Figures

Figure 1.1 Potential activation and response signaling pathways of M1 and M2 states .....	13
Figure 1.2 Schematic mechanisms of MPTP toxicity in CNS .....	24
Figure 1.3 High-resolution of the mTSPO-PK11195 complex .....	27
Figure 1.4 Structures of several representative TSPO ligands. ....	31
Figure 2.1 Emapunil preparation diagram.....	35
Figure 3.1 Schematic view of the experimental procedure. ....	58
Figure 3.2 Emapunil rescues TH- and Nissl- positive neurons. ....	60
Figure 3.3 Emapunil restores motor function.....	63
Figure 3.4 Overview of dopamine synthesis and metabolism. ....	64
Figure 3.5 Levels of dopamine and its metabolites analyzed by HPLC.....	66
Figure 3.6 Emapunil treatment mitigates <i>XBPIs</i> mRNA increase .....	68
Figure 3.7 Co-immunofluorescence staining against TSPO and TH in SN .....	68
Figure 3.8 TSPO is expressed in differentiated LUHMES cells .....	69
Figure 3.9 Cytotoxicity and ER stress were attenuated by Emapunil .....	71
Figure 3.10 siRNA mediated downregulation of TSPO.....	72
Figure 3.11 Emapunil protects from rotenone toxicity in a TSPO dependent manner.....	75
Figure 3.12 Emapunil mitigates ER stress mediated by TSPO in LUHMES.....	76
Figure 3.13 Microgliosis and astrogliosis were attenuated by Emapunil.....	78
Figure 3.14 Emapunil induces microglia from pro- to anti-inflammatory activation .....	81
Figure 3.15 Whole-transcriptome analysis of MPTP and Emapunil effects .....	83
Figure 3.16 GO functional enrichment and network analysis of the most salient Emapunil-specific DE genes.....	84

## List of Tables

Table 2.1 preparation of buffer solutions used in this study .....	36
Table 2.2 Overview of commercial reagents, compounds, and consumables .....	38
Table 2.3 Overview of proliferation medium components.....	39
Table 2.4 Overview of differentiation medium components.....	39
Table 2.5 Overview of commercial kits .....	39
Table 2.6 Overview of the primers for qPCR used in this study.....	40
Table 2.7 Overview of the primary antibodies .....	41
Table 2.8 Overview of the secondary antibodies .....	41
Table 2.9 Overview of software used in this study .....	42
Table 2.10 cDNA synthesis reaction mixture.....	45
Table 2.11 RT-qPCR reaction components.....	46
Table 2.12 Minimal volume of PLO and fibronectin for different well sizes .....	53
Table 2.13 Scheme for preparing siRNA mixture 1 and 2 .....	54
Table 2.14 Components for stacking and resolving gels for SDS-PAGE .....	56

## Abstract

Parkinson's disease (PD) is the second most common neurodegenerative disorder in old age. The presence of akinesia, rigidity and rest tremor caused by dopaminergic neuronal loss in the substantia nigra are the major clinical hallmarks of PD. Although several treatments can temporarily improve motor symptoms and the quality of life in PD patients, it is still incurable until now. PD is neuropathologically characterized by aggregation of misfolded  $\alpha$ -synuclein in dopaminergic neurons, neurodegeneration and neuroinflammation. Translocator protein 18 (TSPO) is a mitochondrial protein which is upregulated in microglia during neuroinflammation, and several TSPO ligands have been shown to exert neuroprotective effects in neurodegenerative diseases. In this study, we investigated the potential neuroprotective effects of Emapunil (also known as AC-5216 or XBD-173), a TSPO ligand, in female mice with subacute 1-methyl-4-phenyl-1,2,3,6-tetrahydropyridine (MPTP) treatment, and in 1-methyl-4-phenylpyridinium ( $\text{MPP}^+$ ) treated human dopaminergic cell line Lund Human Mesencephalic (LUHMES).

We find, that application of Emapunil protects against dopaminergic neuron loss, preserves dopamine metabolism, and also improves motor performance. Furthermore, Emapunil treatment ameliorates  $\text{MPP}^+$  and rotenone toxicity in LUHMES cells.

We identified that Emapunil inhibits endoplasmic reticulum (ER) stress-induced activation of the IRE1 $\alpha$ /XBP1 (X-box binding protein 1) pathway, which can result in apoptosis. In addition, Emapunil induces the shift from pro-inflammatory M1 to anti-inflammatory M2 microglia activation state. Given that Emapunil has been found to be safe and well-tolerated in a phase II clinical trial, our results indicate that Emapunil could be a promising drug for PD patients.

# 1 Introduction

## 1.1 Parkinson disease (PD)

### 1.1.1 Milestones of PD research

PD was first scientifically described by James Parkinson in his monography “An Essay on the Shaking Palsy” in 1817 (Parkinson 2002). Several clinical symptoms which include tremor, rigidity and walking problems were described in this essay (Parkinson 1997). More than 50 years later, Jean-Martin Charcot named this disease “Parkinson's disease” after separating it from other tremor disorders, such as Multiple Sclerosis (MS) (Charcot 1869). The first hypothesis on pathogenesis of PD was proposed by Édouard Brissaud in 1895, who speculated that its pathology starts from subthalamic regions or the cerebral peduncle (Brissaud 1895). Friedrich first described inclusion bodies in PD postmortem tissue, later named “Lewy bodies” (LBs) (Lewy and Handb 1912).

In 1919, Konstantin Tretiakoff proposed that the mainly affected cerebral structure in PD patients was the substantia nigra (Trétiakoff 1919), which was further confirmed by Rolf Hassler in 1938 (Hassler 1938). Later, the Nobel Prize laureate Arvid Carlsson and colleagues elucidated the critical effect of the neurotransmitter dopamine in PD pathogenesis in the late 1950s. L-DOPA as a therapy for PD was subsequently developed, which is still the most commonly prescribed drug for PD (CARLSSON and WALDECK 1958).

In the 1990s, for the first time, a genetic background of PD was revealed as SNCA in autosomal-dominant familial PD, which codes for  $\alpha$ -synuclein (Polymeropoulos et al. 1997). Several days later,  $\alpha$ -synuclein was unveiled as the major component of Lewy bodies within brains of sporadic PD patients (Spillantini et al. 1997).

In the last two decades, unprecedented progress has been made in PD research: Different PD pathological stages were defined (Braak et al. 2003); more and more genetic risk factors have been identified by genetic linkage analysis and large genome-wide association studies (GWAS). Despite the progress in understanding its pathophysiology, PD is still incurable, and all clinical trials with disease-modifying therapies have failed so far. The standard treatment for PD is dopamine or dopamine agonists which is a symptomatic treatment that ameliorates the motor symptoms but does not interfere with the pathogenesis.

### **1.1.2 Epidemiology**

PD is the most common movement disorder and the second-most common neurodegenerative disorder in the world, following AD (Twelves et al. 2003). Its prevalence dramatically increases with aging, and the onset of the disease is usually from 60 years old (Twelves et al. 2003; Savica et al. 2013; Van Den Eeden et al. 2003). PD affects approximately 2-3% of the population aged 65 years or older (Pringsheim et al. 2014), and genetic factors are thought to be involved in 5-10% of all cases (Pinter et al. 2015).

In most populations, men have an approximately 2 fold risk of PD than women (Van Den Eeden et al. 2003; Baldereschi et al. 2000). Female sex hormones might contribute to this male preponderance (Kusumi et al. 1996). The prevalence rates also vary within subgroups defined by ethnicity or environment (Van Den Eeden et al. 2003).

Worldwide, the survival time after PD onset has been rising between 1990 and 2010, because of the improvement in health care. However, the mortality rate of PD patients is still double compared with the age-matched healthy population, starting from the second decade after PD onset (Lix et al. 2010). With the increased aging population worldwide, the estimated number of PD patients and the associated family, societal and economic burden will continuously increase (Dorsey et al. 2007; Vos et al. 2012; Murray et al. 2012; Leibson et al. 2006).

### 1.1.3 Neuropathology

The neuropathological hallmarks of PD include the loss of the dopaminergic neurons in the substantia nigra pars compacta (SNpc) (Dickson et al. 2009; Halliday et al. 2011) and the presence of intraneuronal proteinaceous inclusions within neuronal axons or cell bodies, termed Lewy neurites or Lewy bodies (LBs), respectively.

The selective loss of dopaminergic neurons and their axon terminals which are projected to the dorsal striatum leads to motor symptoms in PD patients, which includes rigidity, bradykinesia, postural instability and resting tremor (Goedert et al. 2013). These motor symptoms normally present when approximately 50% of dopaminergic neurons have been lost (Dijkstra et al. 2014; Iacono et al. 2015; Gibb and Lees 1991). The dopamine replacement therapy (DRT) can temporarily compensate the dopamine loss and is used as the standard treatment for ameliorating motor deficits. However, the long-term DRT can cause aberrant neuronal plasticity by itself, which further results in involuntary dyskinesia (Nishijima et al. 2014; Schapira et al. 2009). Besides, PD patients commonly suffer from a huge range of non-motor symptoms, including hyposmia, pain, somatosensory disturbances, sleep disorders, anxiety, depression, cognitive disorders and dementia, which are also caused by deficits of dopamine or other neurotransmitters in the central and peripheral nervous system (Schapira et al. 2017). Non-motor symptoms can occur before motor deficits and become dominant in advanced PD patients, which severely impairs the quality of life and shortens the life expectancy (Marinus et al. 2018).

LB pathology is another neuropathological hallmark of PD. These intraneuronal proteinaceous inclusions are enriched in aggregated forms of the  $\alpha$ -synuclein and associated with post-translational modifications, like phosphorylation and ubiquitination (Dickson 2012; Spillantini et al. 1997; Ciechanover 2005). By assessing the presence of LBs in a large cohort

of post-mortem tissue, Braak proposed a staging system of the spreading LB pathology to better characterize PD progression (Braak et al. 2003; Braak et al. 2004; Braak et al. 2006; Braak and Del Tredici 2008). Based on Braak's scheme, the LB pathology is divided into six stages: 1-2 are the presymptomatic stages; 3-4 are the early symptomatic stages; and 5-6 are the late symptomatic stages. In stage 1, Lewy neurites and LBs initially start from lower brainstem and olfactory nerves, as well as the dorsal motor nucleus of the vagus nerve in medulla oblongata; in stage 2, Lewy neurites and LBs move up along the brainstem and are presented in medulla oblongata and pontine tegmentum, e.g., caudal raphe nuclei and gigantocellular reticular nucleus; in stage 3, LB pathology enters into midbrain, which presents in SNpc and basal forebrain; in stage 4, the SNpc neurons are severely destructed, while the mesocortex, the allocortex, the subnuclei of the thalamus, and hippocampal formation are also affected; in stage 5, LBs start to appear in higher order association cortex and prefrontal neocortex; in stage 6, LB pathology invades the entire neocortex, affecting the first-order sensory and motor areas (Jellinger 2018).

Based on the progression of LB pathology along anatomic routes and in a stereotypical spatiotemporal pattern, the hypothesis that a prion-like spreading of  $\alpha$ -synuclein pathology might contribute to PD pathogenesis was proposed (Masuda-Suzukake et al. 2013). However, it is still unclear whether LBs and Lewy neurites are neuroprotective or neurotoxic, and to what extent they contribute to clinical symptoms, as some individuals have severe  $\alpha$ -synuclein pathology at autopsy but without any clinical symptoms (Kim et al. 2014).

### **1.1.4 Genetic risk factors of PD**

The majority of diagnosed PD cases are sporadic. However, approximately 5–10% PD are heritable forms, and several genes are reported which can cause monogenic types of PD, for example, mutations in *SNCA* (Polymeropoulos et al. 1996), *LRRK2* (Leucine-rich repeat

kinase 2) (Brice 2005), *VPS35* (Vacuolar Protein Sorting-Associated Protein 35) (Zimprich *et al.* 2011), *Dnajc13* (DnaJ Heat Shock Protein Family (Hsp40) Member C13) and *GBA* (glucosylceramidase gene) (Nalls *et al.* 2014) can cause autosomal-dominant PD forms; mutations in *PARKIN* (Parkin RBR E3 Ubiquitin Protein Ligase) (Lücking *et al.* 2000), *PINK1* (PTEN Induced Kinase 1) (Li *et al.* 2005) and *DJ-1* (Protein Deglycase) (Pankratz *et al.* 2006) are accounted for autosomal recessive PD forms. Besides, many other genes which are identified from genetic linkage analysis and GWAS have shown contribution effects in sporadic PD. These genes are widely located in over 40 loci, e.g., microtubule-associated protein tau (*MAPT*), N-acetyltransferase 2 (*NAT2*), Peroxisome proliferator-activated receptor- $\gamma$  (*PPAR\gamma*), human leukocyte antigen gene complex (*HLA-DRA*), and Apolipoprotein E (*APOE*) (Domingo and Klein 2018; Billingsley *et al.* 2018). These genetic risk factors provide important clues for understanding the potential mechanisms and pathways in the neuropathology of PD. So far, it is known that these genetic risk factors are involved in  $\alpha$ -Synuclein pathology, mitochondrial dysfunction, oxidative stress and neuroinflammation.

### 1.1.5 $\alpha$ -Synuclein pathology in PD

$\alpha$ -Synuclein (*SNCA*) is a 14-kDa protein which is mainly located in presynaptic terminals and highly soluble under normal condition. The physiological function of  $\alpha$ -synuclein is not fully understood so far. It is suggested that  $\alpha$ -synuclein plays a role in SNARE complex assembly, synaptic vesicle release and lipid binding (Burré *et al.* 2010; Bendor *et al.* 2013; Logan *et al.* 2017).  $\alpha$ -Synuclein is the major constituent of LBs which are found in many neurodegenerative diseases, such as PD, DLB (dementia with Lewy bodies) and MSA (multiple system atrophy).

*SNCA* was the first discovered gene in autosomal dominant PD. Several point mutations of  $\alpha$ -synuclein, like A30P (Krüger *et al.* 1998), A53T (Gispert *et al.* 2003), E46K (Zarranz *et al.*

2004), H50Q (Appel-Cresswell et al. 2013) and G51D (Lesage et al. 2013) can cause autosomal dominant PD, as well as the genomic duplication (Chartier-Harlin et al. 2004) and triplication (Singleton et al. 2003) of *SNCA* that significantly increase the protein expression. Furthermore, GWAS revealed that single-nucleotide polymorphisms in *SNCA* which lead to the higher  $\alpha$ -synuclein expression can also increase the risk for sporadic PD (Simon-Sanchez et al. 2009; Nalls et al. 2014; Soldner et al. 2016). This further implicates the crucial role of  $\alpha$ -synuclein in PD pathology.

Mutations of  $\alpha$ -synuclein which favor misfolding or overexpression can accelerate its oligomerization and fibrillation (Bartels et al. 2011; Nuber et al. 2018), which leads to the endoplasmic reticulum (ER) and oxidative stress, mitochondrial dysfunction and cell death (Martinez-Vicente et al. 2008; Kaushik and Cuervo 2015).

Misfolded and aggregated  $\alpha$ -synuclein are assumed to be degraded mainly via chaperone-mediated autophagy (CMA) and macroautophagy (Xilouri et al. 2013; Michel et al. 2016), both of which belong to lysosomal autophagy system (LAS). Many LAS related gene mutations are also associated with PD, for example, *VPS35* (vacuolar protein sorting-35), *LRRK2* (Leucine-rich repeat kinase 2) and *GBA* (glucocerebrosidase), which indicates that impairment of either degradation pathway can contribute to  $\alpha$ -synuclein pathology (Tsika et al. 2014; Volpicelli-Daley et al. 2016).

### **1.1.6 Endoplasmic reticulum (ER) stress and response in PD**

The ER is the major organelle for protein folding in eukaryote cells. Misfolded proteins can cause ER stress (Hetz 2012) and UPR pathway activation. UPR is designed as a protein quality control system which detects misfolded proteins by utilizing three different sensor protein-transcription factor pairs, IRE1 $\alpha$  (inositol requiring kinase 1 $\alpha$ )/XBP1 (X-Box binding protein-1), PERK (protein kinase RNA-like ER kinase)/ATF4 (activating transcription factor

4) and ATF6 $\alpha$  (activating transcription factor 6) (Jiang et al. 2015). The activation of downstream pathways effectively reduces protein translation and induces ER chaperones activities to clear misfolded proteins via autophagy or the ER-associated degradation (ERAD) pathway (Hetz et al. 2011). ER stress is involved in the pathogenesis of PD, mostly caused by misfolded and aggregated  $\alpha$ -synuclein (Matus et al. 2011), which accumulates in the ER of  $\alpha$ -synuclein transgenic mice (Colla et al. 2012). Several postmortem studies also showed that ER stress and active UPR pathways were present in SNpc dopaminergic neurons, and many ER chaperones like BiP (binding immunoglobulin protein) and PDIP (protein disulfide-isomerase) were also upregulated in PD patients as reported previously (Hoozemans et al. 2012; Selvaraj et al. 2012; Colla et al. 2012). Furthermore, in the ATF6 $\alpha$  knockout mouse model, an exacerbated dopaminergic neuronal loss was observed after MPTP treatment, when compared with control mice (Egawa et al. 2011). This suggests that ER stress and active UPR pathways may be neuroprotective. However, chronic ER stress when UPR fails to restore protein homeostasis can induce cell death through apoptosis (Urrea et al. 2013). For instance, in the 6-OHDA mouse model, activation of UPR under ER stress was protective at early stages, whereas chronic UPR activation was shown to result in apoptosis (Mercado et al. 2015).

IRE1 $\alpha$  is a transmembrane ER stress sensor protein. Upon activation either by phosphorylation or dimerization, IRE1 $\alpha$  eliminates a 26-nucleotide intron of the transcription factor XBP1 mRNA. This unconventional splicing leads a shift of the reading frame and results in the active form, *XBPIs* transcription factor. XBP1s activates ER chaperones (Grp78/BiP, Grp58, Grp94) and ERAD components EDEM (ERAD-enhancing a-mannosidase-like proteins) and HRD1 (HMG-CoA reductase degradation protein 1) to refold and degrade misfolded proteins (Valdés et al. 2014). Depending on activation pathways, durations and downstream pathways, XBP1s can be either protective or toxic. It has been

shown that overexpression of XBP1s is neuroprotective in MPP<sup>+</sup> treated dopaminergic neurons (Sado et al. 2009a) and in the 6-OHDA mouse model, whereas down-regulation of XBP1 leads to chronic ER stress and neuronal death (Valdés et al. 2014). However, recent studies showed that XBP1s activation promoted pathogenesis in many neurodegenerative diseases, like AD (Duran-Aniotz et al. 2017a), PD (Hetz and Mollereau 2014), Prion (Moreno et al. 2013) and Huntington's disease (Urrea et al. 2013). Furthermore, inhibition of the IRE1/XBP1 pathway by  $\beta$ -asarone showed therapeutic effects in the 6-OHDA rat model (Ning et al. 2016).

## **1.2 Neuroinflammation in PD**

### **1.2.1 Microglia origins**

Microglia account for approximately 10 – 15% of total cells in brain (Lawson et al. 1990; Mittelbronn et al. 2001) and are derived from primitive yolk sac myeloid progenitors which enter the brain during early development (Alliot et al. 1999; Giunti et al. 2014). As the resident macrophage cells in CNS, microglia have multiple crucial functions which are involved in neural maintenance, pathogen response and promoting repair, and these functions can be altered by interactions with astrocytes, neurons, the blood-brain-barrier (BBB) and migrated T-cells (Stevens et al. 2007; Tremblay et al. 2010; Olah et al. 2011; Paolicelli et al. 2011; González et al. 2014). Microglia have physiological and pathological conditions.

### **1.2.2 Resting microglia**

Under physiological conditions, microglia show a ramified morphology. Resting microglia keep inspecting the microenvironment and receiving signals from neurons or astrocytes (Davalos et al. 2005; Schmid et al. 2009; Nimmerjahn et al. 2005) via CX3CL1,

neurotransmitters, neurotrophins or CD22. Resting microglia is mainly regulated by TREM2 (triggering receptor also expressed on myeloid cells-2), Irf8 (Interferon regulatory factor 8), Runx1 (Runt-related transcription factor 1), chemokine CX3CR1 (CX3C chemokine receptor 1) and CD200R (Cell surface glycoprotein CD200 receptor) (Kierdorf and Prinz 2013). Also, resting microglia express a high level of microRNA-124, which further suppresses the activation of microglia by expression CD46 (cluster of differentiation 46), MHC-II (major histocompatibility complex-II) and CD11b (cluster of differentiation molecule 11B) (Conrad and Dittel 2011).

### **1.2.3 Activated Microglia phenotypes**

Microglia, when activated by different stimuli *in vitro*, can exert numerous functionally distinct activated phenotypes, which can be divided into two polarized phenotypes, named M1 and M2.

#### **1.2.3.1 The M1 phenotype**

The M1 phenotype, which is also termed “classical state”, is an immediate response to injury and infection, acting in the first line to defense against pathogens. The key features of the M1 phenotype are released pro-inflammatory factors and presentation of cell surface markers which are associated with pro-inflammatory and pro-killing functions (Block et al. 2007; Gao et al. 2003). M1 associated pro-inflammatory cytokines include IL(interleukin)-1 $\beta$ , IL-6, IL-12, IL-17, IL-18, IL-23, TNF- $\alpha$  (tumor necrosis factor- $\alpha$ ), IFN- $\gamma$  (Interferon- $\gamma$ ) and NO (nitric oxide). M1 associated pro-inflammatory chemokines include CCL2 (C-C motif chemokine ligand 2) and CXCL10 (C-X-C motif chemokine 10) (Loane and Byrnes 2010; Mahad and Ransohoff 2003; Kawanokuchi et al. 2006; Nakagawa and Chiba 2015; Benarroch 2013). Cell surface markers presented in the M1 phenotype are MHC-II (major histocompatibility

complex-II), CD86 (Cluster of Differentiation 86), CD16/32, iNOS (Induced nitric oxide synthase ), COX-2 (cyclo-oxygenase 2) (Chhor et al. 2013; Franco and Fernandez-Suarez 2015), RNS (reactive nitrogen species), ROS (reactive oxygen species) and prostaglandin E2 (Benarroch 2013; Nakagawa and Chiba 2015).

In experimental models, the M1 phenotype can be classically induced by microbe-associated molecular pattern molecules, such as IFN- $\gamma$  and LPS (Lipopolysaccharide), as depicted in Figure 1.1 (Loane and Byrnes 2010; Boche et al. 2013).

IFN- $\gamma$  activates the M1 phenotype by JAK (Janus kinase)/STAT (Signal Transducer and Activator of Transcription protein) signaling pathway. First, IFN- $\gamma$  activates IFN- $\gamma$  receptors (1 and 2), and the activated receptors then lead to JAK1/2 activation, which then further phosphorylate and activate STATs and IRFs (interferon regulatory factors). This signaling cascade can stimulate the expressions of several pro-inflammatory cytokines, chemokines and other related genes (Hu and Ivashkiv 2009; Boche et al. 2013).

Another M1 stimulus, LPS, activates the M1 phenotype via TLRs (toll-like receptors). LPS first binds to TLR4 along with coupled receptors: LY96 (Lymphocyte antigen 96) and CD14. The binding then stimulates the activation of transcription factors, which include NF $\kappa$ B (nuclear factor kappa-light-chain-enhancer of activated B cells), STAT5, AP1 (Activator protein 1) and IRFs (Hu and Ivashkiv 2009). The TLRs activation cascades, through MyD88 (Myeloid differentiation primary response 88) or TRIF (TIR-domain-containing adapter-inducing interferon- $\beta$ ), cause transcriptional upregulation of M1-associated cytokines and chemokines (Takeda and Akira 2004).

Furthermore, GM-CSF (Granulocyte-modifying colony-stimulating factor) can also activate the M1 phenotype. However, unlike the others, it was reported that GM-CSF could induce pleomorphic activations with both M1 and M2 elements presented (Weisser et al. 2013). Since then, it has increasingly been recognized that the distinction between M1 and M2

activation state is oversimplified and that there is a spectrum of overlapping microglia and macrophage activation states.

### **1.2.3.2 M2 phenotypes**

M2 phenotypes, also named “alternative activation”, are associated with various events including anti-inflammation, tissue repair and extracellular matrix reconstruction. M2 phenotypes can produce several anti-inflammatory cytokines (e.g., IL-4, IL-10 and IL-13) to suppress the pro-inflammatory cytokines (e.g., IL-8, IL-6, TNF- $\alpha$  and IFN- $\gamma$ ). Besides, they also produce extracellular matrix proteins and neurotrophic factors, such as TGF- $\beta$  (Transforming growth factor beta), IGF-1 (Insulin-like growth factor 1) and other substances (Butovsky et al. 2005; Zhou et al. 2012). The typical markers for tissue reconstruction during M2 activation include arginase 1 (Arg1), chitinase-like protein (Ym1), found in inflammatory zone (Fizz1) and peroxisome proliferator activated receptor (PPAR) (Ponomarev et al. 2007; Michelucci et al. 2009).

Based on the different activation mechanisms and cytokines released, M2 phenotypes can be further divided into 3 subforms: M2a, M2b and M2c (as shown in Figure 1.1).

The M2a phenotype can be activated by IL-4 or IL-13 when IL-4/IL-13 binds to its receptor pair (IL-4 binds to the IL4R $\alpha$  receptor and IL-13 binds to the IL13R $\alpha$ 1 receptor). Downstream of the receptors activation, JAK1 and JAK3 are stimulated and then activate STAT6, which further stimulate M2a-associated genes transcription, such as CD206 (mannose receptor), SOCS3 (suppressor of cytokine release 1) and SRs (scavenger receptors). M2a secretes polyamines and IL-10, which are associated with tissue repair and phagocytosis (Martinez et al. 2013; Lu et al. 2013).

The M2b phenotype is not fully understood since it can produce both pro- and anti-inflammatory cytokines (Bell-Temin et al. 2015). This phenotype is normally activated by

immune complexes through the engagement of TLRs and IL-1 receptor. The activated TLRs then interact with Fc $\gamma$  receptors and then bind to Immunoglobulin G to induce the M2b phenotype. The M2b phenotype secretes high amounts of IL10, as well as some pro-inflammatory cytokines at a modest level. CD86 is also a marker for M2b which is highly expressed on the cell surface. M2b is associated with up-regulated phagocytosis and modulation of inflammatory response (Sánchez-Mejorada and Rosales 1998; Takai 2002; Edwards et al. 2006).

Another phenotype, M2c, is activated by IL-10, TGF- $\alpha$  and glucocorticoid hormones. First, IL-10 binds to IL-10 receptors (R1 and R2), which then translocate STAT3 into the nucleus and activate JAK1. The M2c phenotype suppresses many M1-associated pro-inflammatory cytokines (Franco and Fernandez-Suarez 2015; Michell-Robinson et al. 2015) and is associated with tissue regeneration, de-activation of M1/Th1 immune responses and extracellular matrix repairing (Fiorentino et al. 1989; Glocker et al. 2009; Harms et al. 2013).

It is important to note that activated microglia display features of both M1 and M2 phenotypes (Vogel et al. 2013; Martinez and Gordon 2014). The continuum of M1 and M2 phenotypes could be observed in some other neurodegenerative diseases, such as MS (Multiple Sclerosis) (Zhang et al. 2011) and acute CNS injury (Zhang et al. 2012; Kigerl et al. 2009). In spinal cord injury mice, mixed M1 and M2 (defined as Arg1<sup>+</sup> and CD206<sup>+</sup>) phenotypes were co-localized at injury sites (Shechter et al. 2009; Shechter et al. 2013).

The M1/M2 classification of activated microglia provides a basic understanding of the protein expression and the immune response states *in vitro*. However, this classification which is mainly based on the distinct stimuli and released factors is considered as over-simplistic. As discovered from both mouse and human tissue, Single-cell RNA sequencing analysis of microglia also showed that the profiles of each microglia cell were highly diverse in a

dynamic homeostasis state *in vivo* (Li et al. 2019; Masuda et al. 2019). In human microglia, 3 different clusters of transcriptome profiles were identified in healthy human tissues, as “homeostatic microglia”, whereas another 4 clusters were found in early MS patients tissues, as “DAM”. Each cluster has more than one or two markers for identification, which indicates that the microglia are a complex mixture of many different phenotypes.

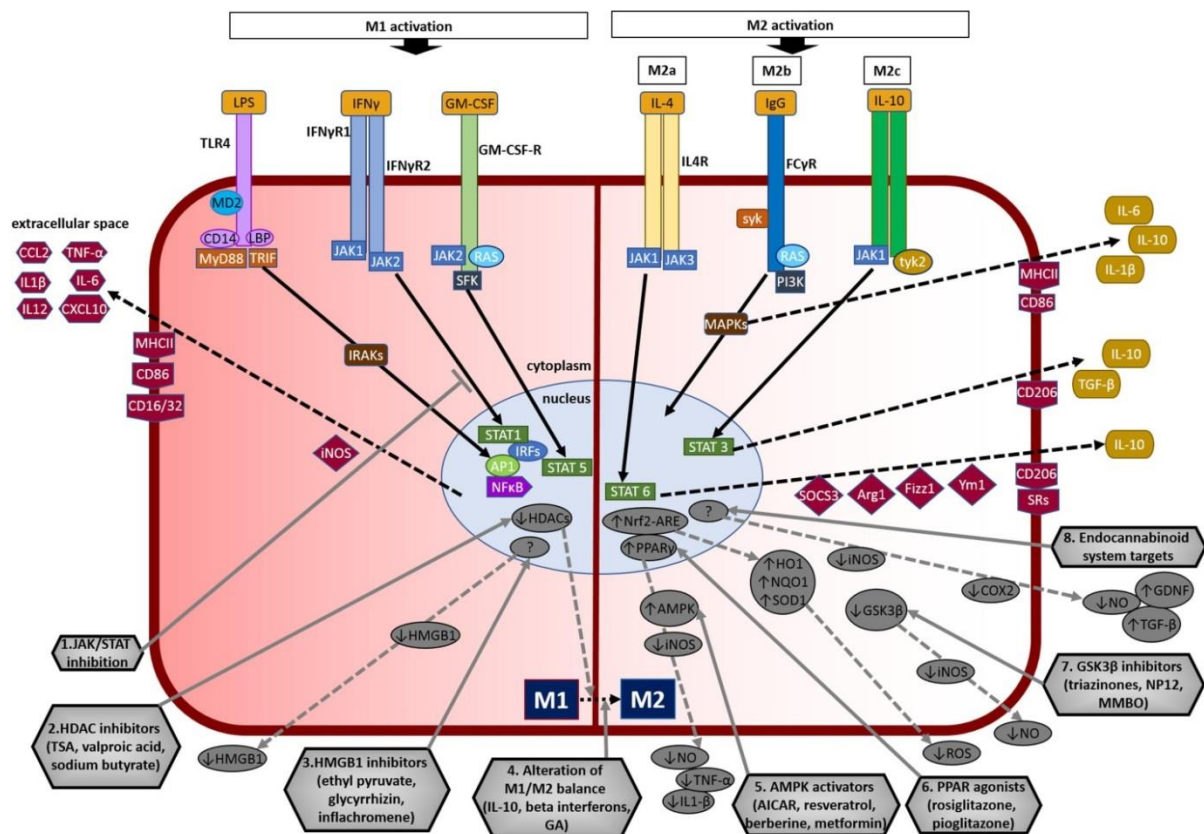


**Figure 1.1 Potential activation and response signaling pathways of M1 and M2 states**

Figure is adapted from (Subramaniam and Federoff 2017)

### 1.2.4 Microglia activation in PD

Although maybe not the initiator, neuroinflammation is implicated to play a crucial role in PD. Activated microglia are acting as the major component of neuroinflammation in the CNS. The classical activation of microglia, the M1 phenotype and its pro-inflammatory effects have been widely studied in PD patients and PD animal models. It was first shown by immune-

histochemistry (IHC) that microglia were activated in SN and striatum in post-mortem tissue of PD patients (McGeer et al. 1988). Several pro-inflammatory cytokines were also elevated in PD patients serum and cerebrospinal fluid (CSF), such as MHC-II, TNF- $\alpha$  and IL-6, and the elevated cytokine levels correlated with severity of motor deficits (Boka et al. 1994; Imamura et al. 2003). Activated microglia in brains of PD patients are suggested to exacerbate dopaminergic neuronal loss and the neurodegeneration process (Hofmann et al. 2009; Scalzo et al. 2010).

In PD, activation of microglia is assumed to be caused by neuromelanin (Wilms et al. 2003b; Zhang et al. 2013), environmental toxins (Rotenone, Paraquat, MPTP) (Goldman 2014), misfolded and aggregated  $\alpha$ -synuclein (Zhang et al. 2005b; Couch et al. 2011; Acosta et al. 2015). Studies suggest that aggregated  $\alpha$ -synuclein released from dying or dead dopaminergic neurons can directly induce microglia activation, mainly through interactions with TLR2 or TLR4 receptors (Béraud et al. 2011; Fellner et al. 2013; Kim et al. 2013). Activated microglia increase NADPH oxidase, ROS and pro-inflammatory cytokines, which can in turn further promote  $\alpha$ -synuclein misfolding and aggregation (Gao et al. 2008), suggesting that the two processes engaged in a self-aggravating cycle (Hirsch and Hunot 2009; Ransohoff 2016).

Recent GWAS studies also linked several genetic risk factors of PD to neuroinflammation, such as *LRRK2* (Schapansky et al. 2014; Akundi et al. 2011; Gillardon et al. 2012; Moehle et al. 2012; Ma et al. 2016), *HLA-DR* (Ahmed et al. 2012; Nalls et al. 2014; Wissemann et al. 2013), *PINK1* (Akundi et al. 2011) and *DJ-1* (Castro et al. 2010). High expression levels of these genes can be found in myeloid cells in PD animal models. It has also been reported that knockdown, knockout, or inhibition these genes in several animal models attenuate M1 microglia inflammatory responses and show protective effects on dopaminergic neuronal loss (Waak et al. 2009; Moehle et al. 2012; Hamza et al. 2010; Kim et al. 2012).

### 1.2.5 Therapeutic manipulation of microglia in PD

Inhibition of microglia activation can attenuate or halt neuroinflammation in multiple PD models. For example, in the MPTP mouse model of Parkinsonism, minocycline<sup>®</sup>, a tetracycline antibiotic, inhibited iNOS expression and NO-induced microglial activation (Du et al. 2001); ibuprofen<sup>®</sup>, one of the nonsteroidal anti-inflammatory drugs (NSAID), decreased the dopamine turnover and inhibited cyclooxygenases (Cox) (Świątkiewicz et al. 2013); bioflavonoid pycnogenol<sup>®</sup>, an effective scavenger of ROS from maritime pine bark (Khan et al. 2013), and peptide carnosine<sup>®</sup>, a natural imidazolic dipeptide, also showed reduced neuroinflammation and attenuated oxidative stress (Tsai et al. 2010). However, most of these anti-inflammatory drugs failed to show benefits in clinical trials with PD patients (Rees et al. 2011; Gao et al. 2011; Becker et al. 2011; Keller et al. 2011; Pena-Altamira et al. 2016). In the  $\alpha$ -syn transgenic model, several other anti-inflammatory drugs also attenuated neuroinflammation and improved behavioral performance, e.g., NF- $\kappa$ B modulator hypoestoxide (Kim et al. 2015) and NF- $\kappa$ B inhibitor lenalidomide (Valera et al. 2015). Furthermore, AZD1480 (an ATP competitive inhibitor of JAK2 kinase) and FK506 (= Tacrolimus or fujimycin), were also able to reduce neuroinflammation and dopaminergic neurodegeneration in the AAV  $\alpha$ -syn overexpression rat model, by inhibiting STAT activation (Qin et al. 2016) and preventing calcineurin phosphorylation (Van der Perren et al. 2015; Qin et al. 2016). Besides, AZD1480 and FK506 can easily cross the BBB (Plimack et al. 2013; Uchino et al. 2002). However, AZD1480 failed the phase I study in myelofibrosis patients due to reversible neurological toxicity (Verstovsek et al. 2015). These results indicate that the inhibition of microglia activation may provide therapeutic effects in PD (Mascarenhas et al. 2014; Wong and Krainc 2017). However, this therapy by globally blocking microglia

activation could also impair host response to pathogens in general and increase infection risk (Kwon et al. 2014; Varley et al. 2013).

Blocking the interaction of pro-inflammatory cytokines with its receptors has been evaluated in PD animal models, for example, anti-TNF- $\alpha$  therapy. Binding TNF- $\alpha$  with neutralizing antibodies (adalimumab), treatment with TNF decoy receptors (etanercept), or AAV injection of dominant negative TNF can attenuate dopaminergic neuron loss in 6-OHDA rat model (Braun et al. 2007; McCoy et al. 2008; Harms et al. 2011; Frankola et al. 2011). Anti-TNF- $\alpha$  therapy was successfully used to reduce systemic inflammation in inflammatory bowel disease (IBD), including Crohn's disease and ulcerative colitis over the last decade (Neurath 2014). Interestingly, a recent retrospective cohort study revealed that the incidence of PD was 28% higher in IBD patients than non-IBD controls. Moreover, among these IBD patients, anti-TNF therapy showed a 78% reduction in the incidence of PD compared with non-treated patients (Peter et al. 2018). The beneficial effect of anti-inflammatory treatments was supported by several other retrospective cohort studies in different countries (Steeland et al. 2018; Weimers et al. 2018; Wu et al. 2018), which strongly indicate that reducing systemic inflammation by anti-TNF- $\alpha$  therapy may provide therapeutic benefits for PD patients. However, large molecules used for counteracting TNF- $\alpha$  are restricted by BBB permeability, which limits the clinical application. The recently developed nanobody TROS (TNF Receptor One Silencer) (Steeland et al. 2015) which can easily cross the BBB may be a promising treatment option for PD, since it showed reduced brain inflammation in APP/PS1 AD mouse model by blocking TNFR1 (TNF signaling receptor 1) (Steeland et al. 2018).

Another promising strategy is to shift activated microglia from pro- to anti-inflammatory state. It has been reported that molecules such as IL-10 and beta interferons can promote the transition of pro- to anti-inflammatory microglia activation state and hence be promising for PD treatment. For instance, injection of AAV expressing human IL-10 into MPTP pre-treated

mice decreased levels of pro-inflammatory mediators including IL-1 $\beta$ , IL-6, TNF- $\alpha$  and iNOS. In addition, it attenuated the loss of striatal dopamine and the decrease of tyrosine hydroxylase (Schwenkgrub et al. 2013; Joniec-Maciejak et al. 2014).

Pioglitazone, a PPAR $\gamma$  (peroxisome proliferator activated receptor-gamma) agonist, is also a promising molecule to induce the transition of M1 to M2 phenotype (Zhao et al. 2016b). PPAR $\gamma$  is a transcription factor in nuclear receptor superfamily that regulates many cellular functions which include lipid metabolism, cell differentiation and inflammatory response (Jafari et al. 2007; Kemp et al. 2012). PPAR $\gamma$  activation by Pioglitazone has been tested in many psychiatric and neurodegenerative diseases where neuroinflammation is involved (Sato et al. 2011; Christine 2015; Liu et al. 2017; Machado et al. 2018). Administration of pioglitazone in the MPTP mouse model decreased proinflammatory microglia activation as well as iNOS- and NO-mediated toxicity in the striatum and substantia nigra (Quinn et al. 2008; Dehmer et al. 2004; Barbiero et al. 2014). However, Pioglitazone treatment failed to modify neuroinflammation in early PD patients in a recent clinical trial (Simuni et al. 2015) and also failed to lower the incidence of PD diagnosis in a large Taiwanese cohort of PD patients with diabetes mellitus (Wu et al. 2018).

Few FDA approved drugs for Multiple Sclerosis (MS) treatment, such as Glatiramer acetate (Giunti et al. 2014; English and Alois 2015) and Dimethyl fumarate (DMF) (Campolo et al. 2017) also showed neuroprotective effects in the MPTP mouse model, presumably by shifting activated microglia from M1 to M2 state and upregulation of GDNF expression.

Besides, several recently reported potential therapeutic drugs in PD are also associated with immune response in PD animal models, e.g., treatment with inhibitors for HMGB1 (Shin et al. 2014), GSK3 $\beta$  (Morales-García et al. 2012; Kondratiuk et al. 2013; Prati et al. 2015), HDACs (Faraco et al. 2009; Wang et al. 2015b) and activators of AMPK (Zhu et al. 2015; Wang et al. 2015a).

Taken together, it is believed that shifting activated microglia from pro- to anti-inflammatory state would restore homeostasis and may have promising therapeutic value in PD and other neurodegenerative diseases.

### **1.3 Animal models of Parkinson's disease**

An ideal animal model of PD should present selective and gradual loss of dopamine neurons during aging, obvious motor deficits,  $\alpha$ -synuclein and Lewy body pathology and neuroinflammation (Beal 2001). Rodents and primates are the most studied species used in PD research, because of the similarity of gene homologs and brain morphology to human (Potashkin et al. 2011). In humans, both genetic and environmental factors, as well as interactions between them contribute to PD pathogenesis. Similarly, animal models of Parkinsonism can also be divided into genetic models, neurotoxin-based models and combination of both (Dawson et al. 2010; Dawson et al. 2018).

Until recently, many transgenic rodents models have been generated with different promoters, mostly focused on SNCA ( $\alpha$ -synuclein), as well as other genes including LRRK2 (leucine-rich repeat kinase 2), Parkin (RBR E3 ubiquitin protein ligase), PINK1 (PTEN-induced putative kinase 1) and DJ-1 (Lee et al. 2012; Poewe et al. 2017; Yun et al. 2018). Most of  $\alpha$ -synuclein transgenic rodents models (A30P, A53T and E46K) exhibit aggregated  $\alpha$ -synuclein and show substantial neurodegeneration (McDowell and Chesselet 2012). However, the absence of DA neurons loss is considered as a major limitation of these models (Visanji et al. 2016). In contrast, conditional or cell-type-specific overexpression of  $\alpha$ -synuclein mutants results in DA neuronal degeneration (Koprich et al. 2017). Lentiviruses or Adeno-associated Viruses (AAV) overexpression of wild type and/or mutated  $\alpha$ -synuclein is widely used for  $\alpha$ -

synucleinopathy investigation. It also causes DA neuronal degeneration if SN is the injection area (Van der Perren et al. 2014; Oliveras-Salvá et al. 2013).

The most widely utilized neurotoxin-based rodents models are two potent complex I inhibitors, 6-hydroxydopamine (6-OHDA) (Iglesias-González et al. 2012) and 1-methyl-1,2,3,6 tetrahydropyridine (MPTP) (Martinez and Greenamyre 2012). Besides, pesticides which induce mitochondrial dysfunction and oxidative stress are also used to mimic PD, such as paraquat and rotenone (Tanner et al. 2011).

### **1.3.1 The MPTP mouse model of Parkinsonism**

#### **1.3.1.1 Mechanisms of MPTP**

The MPTP mouse model is the best characterized neurotoxin-based animal model which mimics many hallmarks of PD, such as dopaminergic neuron loss in the SNpc and striatum, oxidative stress, neuroinflammation and motor deficits (Dauer and Przedborski 2003). MPTP was first discovered to induce Parkinsonism in 1982. 7 US drug-users rapidly emerged with motor symptoms similar to those observed in Parkinson's disease after self-intoxication of 1-methyl-4-phenyl-4-propionoxypiperidine (MPPP) which was contaminated with MPTP, as a byproduct of MPPP synthesis (Langston 1985; Langston et al. 1983). These patients responded to L-Dopa treatment. MPTP was found to selectively destroy dopaminergic neurons in the SNpc (Meredith and Rademacher 2011). In the subsequent years after discovering its neurotoxic potential in humans, neurotoxic effects of MPTP were tested in primates, cats, and several rodents (Kopin and Markey 1988; Jenner 2003; Wichmann and DeLONG 2003). Interestingly, for unknown reasons, rats are highly resistant to the toxicity of MPTP, and different mouse strains also shows widely varieties in their sensitivity to MPTP (Mitra et al. 1994; Riachi and Harik 1988; Hamre et al. 1999). MPTP has been widely used

via subcutaneous, intraperitoneal, intravenous or intramuscular injection into mice and monkeys to mimic motor symptoms of PD. The mouse is the most widely used species for MPTP studies (Schmidt and Ferger 2001).

MPTP itself is not toxic. After crossing the BBB, MPTP is metabolized by monoamine oxidase (MAO)-B in glial cells to the unstable 1-methyl-4-phenyl-2,3-dihydropyridium (MPDP<sup>+</sup>), which is followed by deprotonation to generate its active metabolite, MPP<sup>+</sup> (D'Amato et al. 1987; Friedman and Mytilineou 1990). MPP<sup>+</sup> is preferentially taken up into dopaminergic neurons through the dopamine transporter (DAT) and is thus selectively toxic to dopaminergic neurons (Gainetdinov et al. 1997; Bezard et al. 1999). Once MPP<sup>+</sup> enters the cell, it inhibits complex I of the mitochondrial electron transport chain (ETC), which leads to reduced ATP synthesis and increased oxidative stress, as shown in Figure 1.2 (Nicklas et al. 1985; Pennathur et al. 1999). MPP<sup>+</sup> toxicity results in cell death which induces pro-inflammatory responses with increased levels of pro-inflammatory cytokines, such as IL-6, IFN- $\gamma$  and TNF- $\alpha$ . This pro-inflammatory environment further promotes neurodegeneration (Członkowska et al. 1996; Smeyne and Jackson-Lewis 2005). Blocking TNF receptors by neutralizing antibodies could protect against MPTP-induced neurodegeneration (Sriram et al. 2002; Mount et al. 2007). Therefore, the MPTP model is useful for studying oxidative stress, mitochondrial dysfunction, inflammatory reactions and motor performance in Parkinsonism.

### **1.3.1.2 Acute versus subacute and chronic MPTP models**

It is important to note that the dopaminergic neuronal loss is related to the dose and schemes of MPTP treatment (Schmidt and Ferger 2001). The MPTP mouse model can be categorized into three different schemes: the acute model, the subacute model and the chronic model. The three different schemes mimic different aspects and stages of PD and thus are valuable for PD research.

## Introduction

The acute model was the first invented model, in which C57BL/6 mice received an intermediate dose of MPTP ( $4 \times 15\text{-}20\text{mg/kg}$  body weight) intraperitoneally (i.p.) over 8 h with 2 h intervals. In this model, mice display extensive (40-50%) loss of dopaminergic neurons in SNpc 12 h after administration and rapid cell death which is mainly due to necrosis (Jackson-Lewis et al. 1995) (Sonsalla and Heikkila 1986). This model is widely used to understand the neurotoxic process of MPTP in the brain. However, the necrotic cell death does not mimic the slowly progressive pathology in human. Therefore, the subacute and chronic models were developed to mimic human PD better. In the subacute scheme, 30 mg/kg body weight of free base MPTP is i.p. injected once daily for 5 consecutive days, and the subacute MPTP treated mice show progressive loss of SNpc DA neurons and striatal DA which is mainly due to apoptosis. The degeneration of dopaminergic fibers in the striatum takes place until 7 days after the last MPTP administration, which is named “delayed degeneration”, and the regeneration of dopaminergic fibers starts from 90 days after the last MPTP administration (Tatton and Kish 1997; Vila et al. 2000). Since LBs pathology is absent in both acute and subacute models, chronic blocking complex I was thought to be necessary for LB presence. Thus multiple chronic modes of MPTP application were tested and the schemes vary from weeks to months, including different injection models (low MPTP doses injected 2 or 3 days/injection over weeks or months) or constant MPTP subcutaneous pumping models. However, most of the chronic MPTP treatment failed to achieve LBs (Gibrat et al. 2009; Purisai et al. 2005). Also, the SNpc dopaminergic neuronal loss was very slow and mild in this model as shown in several studies (Fornai et al. 2005). It was even reported that the dopaminergic neuron loss was presented only with extra-treatment of probenecid in the chronic model, which is also neurotoxic itself and used to reduce renal elimination of MPTP (Alvarez-Fischer et al. 2013; Alvarez-Fischer et al. 2008). Furthermore,

the nigrostriatal degeneration was much lower than in PD patients (Meredith and Rademacher 2011; Goldberg et al. 2011). Based on that, this model is mainly used to mimic the very early stage of PD and provides a longer observation period to investigate the pathogenesis before motor symptoms present (Philippens 2018).

### **1.3.1.3 Behavior phenotypes in MPTP models**

The open field box test with infrared beams equipped is widely used to evaluate the general movement of the mice shortly after MPTP intoxication. MPTP injected mice normally show the paucity of movement with longer time for traveling the same distance (Sedelis et al. 2000), but the paucity may disappear over time (Dauer and Przedborski 2003). Another widely used method is the rotarod test, where trained mice stay on a speeding rod until they fail to catch up the speed. MPTP injected mice showed shorter latency to fall off the rod compared with control mice in some studies (Luchtman et al. 2009), while other studies failed to detect the difference (Meredith and Kang 2006).

There are several tests focusing more on the forelimbs activities to detect the subtle degeneration of the dopaminergic system (Ogawa et al. 1985; Chan et al. 2007; Haobam et al. 2005), for example, MPTP treated mice have shown behavior deficits in the pole test (Chan et al. 2007), in the grid test (Tillerson and Miller 2002) and in the forelimb stepping test (Blume et al. 2009).

### **1.3.1.4 Advantages and disadvantages of MPTP model**

MPTP is a potent complex I inhibitor which can cause Parkinsonism both in human and rodents. It induces the loss of DA neurons in SNpc, axons degeneration and eventually the loss of DA in the striatum, in a relatively slow and progressive way, which mimics the occurring of PD during aging.

The MPTP model of Parkinsonism has many advantages compared with other neurotoxin-based models. For example, in the 6-hydroxydopamine (6-OHDA) animal model, 6-OHDA has to be intracerebrally injected because it can not pass the BBB. Besides, 6-OHDA can not only impair DA neurons, but also target noradrenergic transporters and induce neurodegeneration in other regions (Luthman et al. 1989; Meredith and Rademacher 2011). The other two widely used pesticides-based models, rotenone (Fleming et al. 2004) and Paraquat (McCormack et al. 2002; Miller 2007), also show dopaminergic degeneration and intracellular inclusions which resemble LBs in some studies. However, large variabilities with high mortality issues have limited its further application in animals (Sherer et al. 2003; Miller 2007).

It is essential to mention that as an animal model, MPTP model also has some limitations. First, MPP<sup>+</sup> solely inhibits complex I activity in dopamine transporter-expressing cells, like dopaminergic neurons, lacking in mimic the systematic impairments in PD (Betarbet et al. 2002). Second, MPTP model fails to mimic the advanced stage of PD, when the non-dopaminergic neurodegeneration and non-motor symptoms become dominate. Third, MPTP model shows no LBs pathology, which is one of the most important pathological hallmarks in PD. Furthermore, the acute scheme of MPTP treatment is the least frequently used model, since it has severe mortality rate and fails to mimic the progressive pathogenesis of PD, whereas subacute and chronical MPTP treatment overcome this limitation (Dauer and Przedborski 2003).

So far, there is no perfect model for PD research. Neurotoxin-based models are more useful for disease-modifying therapies, as it closely mimics the PD pathology, whereas transgenic animal models are more suitable for investigating the specific mechanisms and processes of neurodegeneration in PD.

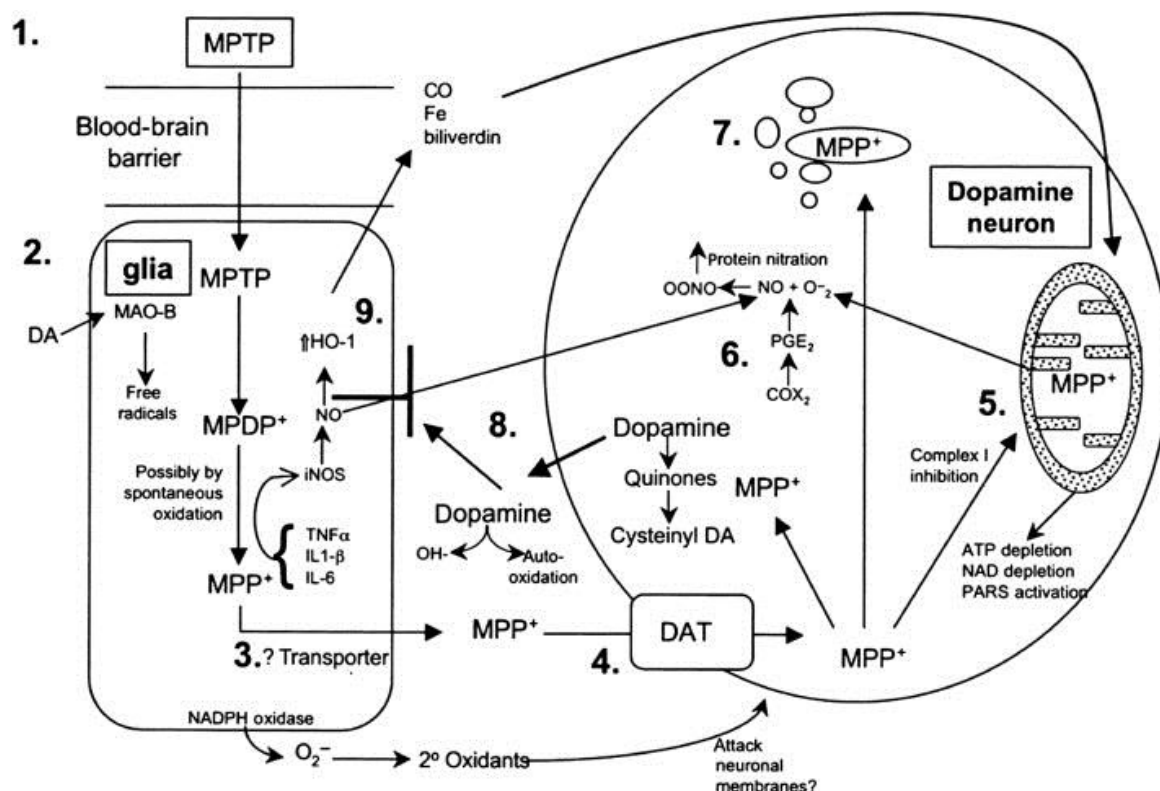


**Figure 1.2 Schematic mechanisms of MPTP toxicity in CNS**

Step 1: transport MPTP into CNS via BBB; Step 2: MPTP is converted into  $MPP^+$  by MAO-B in glial cells, which leads to gliosis, induction of cytokines, and activation of M1 microglia with pro-inflammatory effects; Step 3:  $MPP^+$  is released from the Astrocytes through OCT-3 transporter; Step 4:  $MPP^+$  is transported into the dopaminergic neuron through the DA transporter; Step 5: Once enters the dopaminergic neurons,  $MPP^+$  diffuses into the mitochondria and inhibits complex I of electron transport chain, resulting in ATP and NAD depletion; Step 6:  $MPP^+$  produces peroxynitrite ( $OONO^-$ ), which impairs TH activity, increases dopamine metabolisms and also nitrates many other mitochondrial components; Step 7:  $MPP^+$  is transported from the cytoplasmic space into synaptic vesicle by vesicular monoamine transporter (VMAT); Step 8: Releasing of dopamine into extracellular space caused by cellular ATP depletion leads to dopamine oxidation and hydroxyl radical formation, which further results in cell death; Step 9: increased dopamine in extracellular space upregulates hemeoxygenase-1 (HO-1) expression, a rate-limiting enzyme for heme degradation. HO-1 is postulated to be protective in dopaminergic neurons. Figure is adapted from (Jackson-Lewis et al. 2015)

## 1.4 Translocator protein 18 (TSPO)

### 1.4.1 TSPO distribution and function

TSPO was initially identified in 1977 as a peripheral-type benzodiazepine receptor (PBR), which is a binding site for benzodiazepines outside the CNS whose tissue distribution, function and subcellular localization differ from the CNS benzodiazepine receptors (Braestrup

and Squires 1977). Subsequently, it was reported that TSPO is localized in the outer mitochondrial membrane and is assumed to play a crucial role in the transfer of cholesterol from the outer to the inner mitochondrial membrane (Papadopoulos et al. 1997; Rupprecht et al. 2009). The HUGO Gene Nomenclature Committee redesignated this protein as TSPO in 2006, reflecting its putative function in steroid translocation (Papadopoulos et al. 2006).

TSPO is widely expressed in many organs, including kidney, heart, spleen, lung and brain etc. (Gavish et al. 1999). It is especially abundant in steroid synthesizing cells, such as cells in the adrenal and gonadal tissue (Lacapere and Papadopoulos 2003; Papadopoulos et al. 2006). TSPO was initially reported to be only expressed in microglia (Casellas et al. 2002) and astrocytes (Maeda et al. 2007) in the brain. However, several other studies also showed TSPO expression in neuronal cells, including olfactory bulb neurons (Wadsworth et al. 2012), neuroblastoma and glioblastoma cell lines (Decaudin et al. 2002), cerebellar granule cells (Varga et al. 2009), and rat dorsal root ganglia sensory neurons (Karchewski et al. 2004).

### **1.4.1.1 Role in cholesterol transport**

One of the best-characterized functions of TSPO is its high-affinity binding to cholesterol and its transportation from the outer to the inner mitochondrial membrane in steroidogenic cells, which is the rate-limiting step for steroid synthesis (Papadopoulos et al. 2006; Papadopoulos et al. 2007). After entering mitochondria, cholesterol is then converted to pregnenolone via a side chain oxidative cleavage by cytochrome P450<sub>SCC</sub>, which is the precursor of all other neurosteroids (Rone et al. 2009; Jaipuria et al. 2017). It has been shown that TSPO knockout mice display abnormalities in steroidogenesis in an age-dependent manner (Barron et al. 2018). Thus TSPO is thought to be essential for neurosteroids production. However, some other studies showed conflicting results. For example, Banati and colleagues reported that the cholesterol and pregnenolone biosynthesis was not affected in global TSPO knockout mice

(Banati et al. 2014). Another recent study also showed that the steroidogenesis was not affected in CRISPR/Cas9–TSPO knockout mice (Tu et al. 2014).

### **1.4.1.2 Other functions of TSPO**

TSPO has been reported to be associated with a wide range of cellular functions, e.g., mitochondrial permeability transition pore (mPTP) formation, regulation of mitochondrial reactive oxygen species (ROS) levels, cell proliferation and neuroinflammation (Chen and Guilarte 2008; Cosenza-Nashat et al. 2009; Scarf et al. 2009).

Recently, a study demonstrated that mitochondrial homeostasis and mitochondrial permeability transition pore (mPTP) were affected in TSPO knockout fibroblasts (Tu et al. 2016). Also, an increased mitochondrial fatty acid oxidation and a decreased oxygen consumption rate (OCR) were observed in steroidogenic cells or microglia in TSPO knockout mice (Banati et al. 2014; Zhao et al. 2016a). However, the underlying molecular mechanisms are still unclear and require further investigation.

### **1.4.2 TSPO structure**

TSPO is an evolutionarily conserved ubiquitous 169-amino-acid protein with five transmembrane helices (Fan et al. 2012; Li et al. 2015; Guo et al. 2015). In 2014, the high-resolution structure of recombinant mouse TSPO was determined by using NMR (Jaremko et al. 2014). In this study, Jaremko and colleagues deciphered the 3D structure of the mTSPO, in complex with its synthetic ligand PK11195, in dodecylphosphocholine (DPC) micelles as shown in Figure 1.3. There, the five transmembrane helices of Emapunil were presented in the clockwise order (TM1-TM2-TM5-TM4-TM3) when viewed from the cytosol. The binding sites of Emapunil for cholesterol are located at the C terminus of TM5, through the cholesterol recognition consensus sequence (CRAC) (residues 147 to 159; Ala-Thr-Val-Leu-

Asn-Tyr-Tyr-Val-Trp-Arg-Asp-Asn-Ser). More specifically, The Tyr<sup>152</sup>, Tyr<sup>153</sup>, and Arg<sup>156</sup> residues, which are the side chains of the TSPO structure, are essential for cholesterol binding. The study also revealed that the binding sites for TSPO ligands, PK11195 and cholesterol, are different, in accordance with previous findings that site mutations of these residues block the binding to cholesterol but not to PK11195 (Delavoie et al. 2003). The authors further suggested that monomeric TSPO binds to cholesterol in nanomolar affinity, and that cholesterol binding might modulate the oligomerization of TSPO.

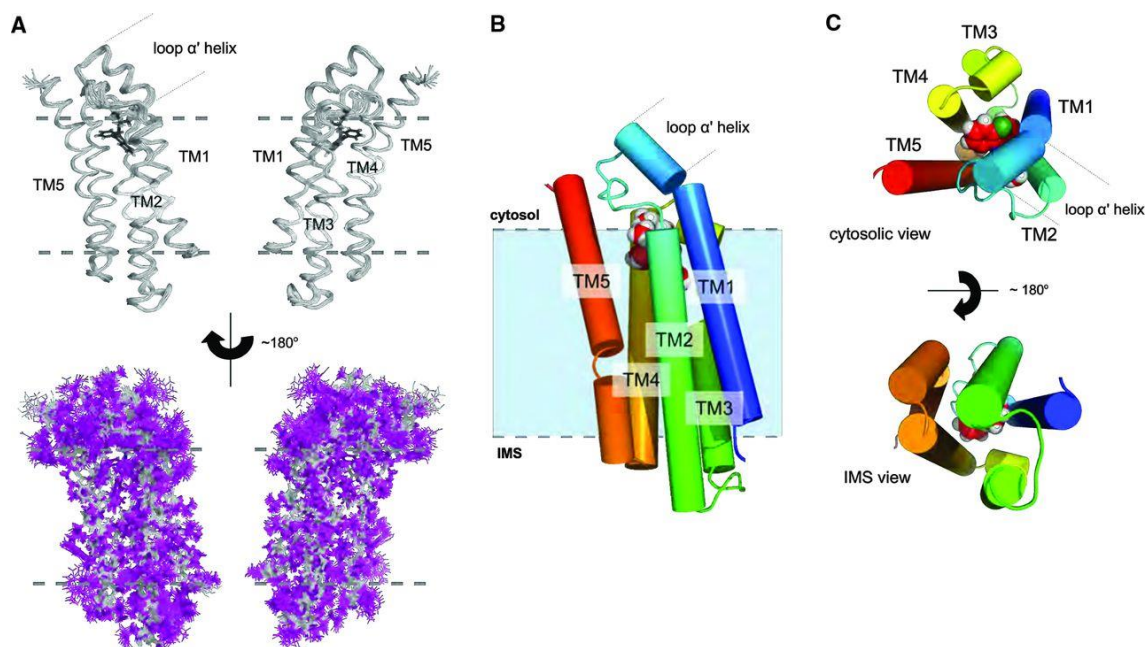


**Figure 1.3 High-resolution of the mTSPO-PK11195 complex**

(A) NMR spectroscopy views of the 20 lowest-energy structures for backbone ribbons (silver, upper panel) and atoms (blue, lower panel), the ligand (black) and membrane boundaries (gray dotted lines); (B) Cylindrical view of the lowest-energy structure represented in spheres; (C) Cytosolic view and the intermembrane space view of the complex, respectively. Figure is adapted from (Jaremko et al. 2014)

Another two recent publications elucidated the crystal structures of bacterial TSPOs by X-ray, with more emphasis on the structural changes caused by the A147T polymorphism (Li et al. 2015; Guo et al. 2015), as individuals with TSPO A147T polymorphism show lower binding affinity to most TSPO PET ligands (Costa et al. 2009). Both studies indicate that the A147T

polymorphism results in tilts and twists between TM1 and TM2 helices with the sterical hindrance of ligands binding by the alanine side chain.

### **1.4.3 TSPO ligands**

#### **1.4.3.1 Endogenous ligands of TSPO**

Many endogenous ligands of TSPO were identified over past decades, such as cholesterol, tetrapyrroles which including (protoporphyrin IX (PPIX), mesoporphyrin IX, deuteroporphyrin IX) and Diazepam Binding Inhibitor (DBI) with its post-translational products (Bovolín et al. 1990) (Wendler et al. 2003; Li et al. 2013; Vanhee et al. 2011). The most famous endogenous ligand is cholesterol which shows nanomolar binding affinity to TSPO, and its binding site located at a conserved CrAC domain in the C-terminus of TSPO (Li et al. 2001b; Jaremko et al. 2014). Porphyrins (cyclic tetrapyrroles with prominent physiological functions) are another class of endogenous TSPO ligands which were reported in 1987 for the first time (Verma et al. 1987; Verma and Snyder 1988). In particular, PPIX, which forms Heme when complexed with  $\text{Fe}^{2+}$  ion in its center (Verma et al. 1987), is suggested to bind to TSPO with the highest affinity in a nanomolar range, via the same binding pocket as PK11195. Interestingly, once bound, TSPO can catalyze PPIX degradation to bilindigin, which resembles biliverdin, a blood breakdown product that functions as an oxyradical scavenger. Since biliverdin suppresses reactive oxygen species (ROS) production, it is plausible that the cleavage of PPIX by TSPO may attenuate oxidative stress, which may, at least, partially explain that the expression levels of TSPO are increased in activated microglia in response to oxidative stress and inflammation (Guo et al. 2015). This is in accordance with a previous report, showing increased ROS in TSPO knockouts (Frank et al.

2007). Altogether, these results suggest that the interaction between TSPO and PPIX plays an important role in heme metabolisms and inflammatory responses (Veenman et al. 2016).

Another class of endogenous ligands is the diazepam-binding inhibitor (DBI). DBI, also known as acyl-CoA-binding protein for the high binding affinity to acyl-CoA esters (Færgeman et al. 2007) or ACbD1 (Fan et al. 2010), is widely expressed in the nervous system (Mocchetti and Santi 1991). DBI can stimulate mitochondrial steroid synthesis by its active peptide fragments, octadecaneuropeptide DbI 33–50 (ODN) and triakontatetranuropeptide DbI 17-50 (TTN) (Papadopoulos et al. 1991; do Rego et al. 2007). Another acyl-CoA-binding domain-containing protein, named PAP7 or ACbD3, can also bind to TSPO, and the binding complex can mediate the transport of cholesterol into mitochondria in steroidogenic cells (Fan et al. 2010; Li et al. 2001a; Liu et al. 2006). These studies suggest that acyl-CoA-binding proteins or acyl-CoA itself could bind to TSPO and further regulate cholesterol transport.

Endozepines are a family of neuropeptides derived from DBI by endogenous proteolysis, which are widely used for prolonged sedation in intensive care units (ICUs) (Martin et al. 2006). The sedative and hypnotic effects are mediated by their binding to GABA<sub>A</sub> (γ-aminobutyric acid type A) receptor (Costa and Guidotti 1991; Sigel and Steinmann 2012). Endozepines can bind to TSPO with multiple binding sites, and they need other partner proteins such as VDAC for maximal binding (Sigel and Steinmann 2012). In the CNS, endozepines are primarily expressed in glial cells and involved in immune response where they exhibit anti-inflammatory effects (Kim et al. 2006). Also, CSF endozepines levels are higher in AD patients than in age-matched healthy controls (Ferrarese et al. 1990). A recent study showed that the amyloid-β peptide could stimulate the synthesis of endozepines in astrocytes *in vitro* (Tokay et al. 2008). Moreover, plasma levels of endozepines are also increased by cecal ligation and puncture treatment, a model characterized by dysregulated

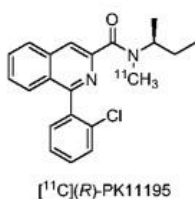
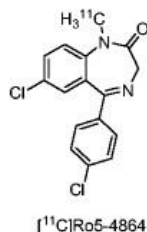
systemic inflammation (Clavier et al. 2014). All these reports suggest that the endogenous ligands of TSPO, at least in part, are involved in the inflammatory response.

### **1.4.3.2 Synthetic ligands of TSPO**

In many neurodegenerative diseases, such as AD and PD, chronic neuroinflammation has been implicated as an important pathological contributor (McManus and Heneka 2017). Several studies demonstrated that the activation of microglia was often associated with increased TSPO expression (Wilms et al. 2003a; Karlstetter et al. 2014). Given that TSPO expression levels are rather low in resting microglia, it was discovered as a potential molecular marker for microglia associated neuroinflammation (Banati 2002). Therefore, many TSPO ligands were synthesized and studied both in human and mouse brain in the last fifteen years.

The first generation of TSPO ligands comprises Ro5-4864 and PK-11195, which belong to Benzodiazepines-class and Isoquinoline Carboxamide derivatives, respectively (Le Fur et al. 1983a; Benavides et al. 1983). Ro5-4864 was classified as an agonist while PK11195 as an antagonist, based on their opposite effects on neuronal seizures rates (Le Fur et al. 1983b; Benavides et al. 1984). PK11195 is so far the best characterized radiotracer of TSPO which is widely used as a reference ligand to compare other newer ligands. It is important to note that binding affinity and selectivity to TSPO is significantly different between TSPO ligands, for example, PK11195 is limited in clinical application, mostly due to its high non-specific binding to plasma protein (highly lipophilic), as well as low brain permeability (Vivash and O'Brien 2016).

## First generation TSPO tracers in neurologic disease



## Second generation and new generation TSPO tracers in neurologic disease

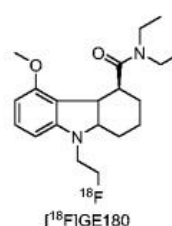
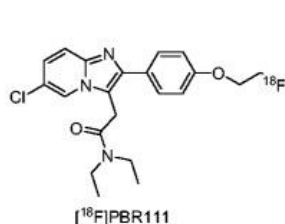
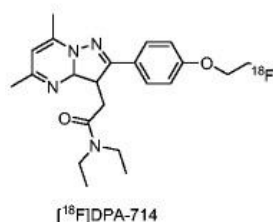
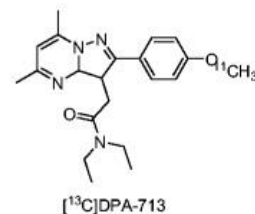
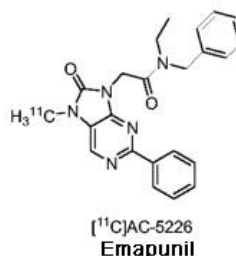
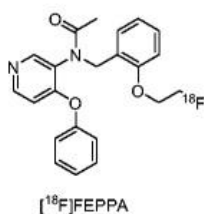
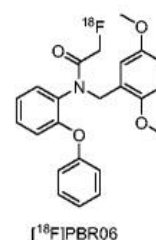
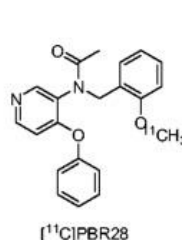
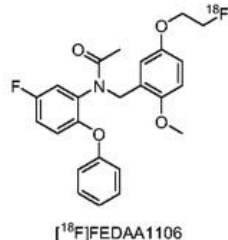
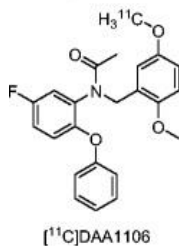


**Figure 1.4 Structures of several representative TSPO ligands.**

Figure is adapted from (Alam et al. 2017)

To improve the signal-to-noise ratio, scientists developed many second and third generation ligands from derivatives of the classical ligands and also from other structural classes (Figure 1.4). The new classes of ligands include acetamides (derivatives with the diazepine ring opening from Ro5-4864, e.g., DAA1106, FEDAA1106 and PBR28), Vinyl alkaloids (e.g., vinpocetine), Aryl-oxodihydropurines (e.g., Emapunil and DAC), Pyrazolopyrimidine (e.g.,

DPA-713 and DPA-714) and Imidazopyridineacetamides (e.g., CLINME, CB148, CB251 and PBR111) (Alam et al. 2017).

All these newly developed ligands showed lower lipophilicity and higher selective affinity to TSPO compared with PK11195. However, most of them still showed non-specific binding to other proteins (Vivash and O'Brien 2016).

Similar to PK11195, these novel ligands with higher specificity exhibit different binding affinities to TSPO due to single nucleotide polymorphism (SNP). The polymorphism (rs6971) of TSPO gene (A147T), which was first identified in 2012 using unlabeled PBR28 (Owen et al. 2011) and was further confirmed by another independent study using [ $^{18}\text{F}$ ]PBR111 (Guo et al. 2013), brings three allele combinations with different binding affinity: AA with the highest affinity, AT with mixed affinity while TT with lowest affinity (Owen et al. 2012; Dickstein et al. 2011). These different binding affinities need to be considered when testing novel ligands.

### **1.4.4 TSPO radiotracers applied in PD**

Most of the TSPO ligands were primarily developed for positron emission tomography (PET) or Single photon emission computed tomography (SPECT) imaging studies. They provide a valuable tool for tracking and quantification of inflammation *in vivo*, e.g., in brain tumors, neurodegenerative diseases and psychiatric disorders. For example, in 6-OHDA-lesioned rodent model of PD, [ $^{11}\text{C}$ ]-(*R*)-PK11195 binding was increased in the substantia nigra and striatum (Bartels and Leenders 2007), which was in line with more widespread activated microglia as assessed by CD68 immunofluorescence staining (Cicchetti et al. 2002) and by other studies in the MPTP mouse model (Belloli et al. 2017; Roussakis and Piccini 2018). PD patients also showed increased [ $^{11}\text{C}$ ]-(*R*)-PK11195 retention in the thalamus, striatum, frontal and cingulate cortex compared with healthy controls (Gerhard et al. 2004; Gerhard et al. 2006). Furthermore, a recent study showed increased striatal [ $^{11}\text{C}$ ]-(*R*)-PK11195 binding in

patients in very early PD stages (mean UPDRS motor score 7.2) (Iannaccone et al. 2013). It is important to note that  $^{18}\text{F}$  have longer half-life compared with  $^{11}\text{C}$ , so the novel ligands with  $^{18}\text{F}$  become more widely used for clinical studies (Schweitzer et al. 2010). The recent study using the second generation ligand [ $^{18}\text{F}$ ]-FEPPA yet showed no significant increase of TSPO tracer retention in PD patients (Koshimori et al. 2015). This may partially be due to the different ligands and patient populations. Interestingly, in several longitudinal studies in PD patients, the retention of TSPO ligands had no significant changes during 4 weeks or 24 months, which indicates that microglia may be activated at an early stage of PD and then remained stable during pathological progression (Ouchi et al. 2005; Gerhard et al. 2006).

### **1.4.5 TSPO ligands have therapeutic effects in neurodegenerative diseases**

Although most of ligands were developed primarily for PET imaging study, some TSPO ligands were found to have neuroprotective and anti-inflammatory effects (Papadopoulos and Lecanu 2009) and TSPO was suggested to be a promising therapeutic target in neurodegenerative diseases (Papadopoulos and Lecanu 2009; Rupprecht et al. 2010; Da Pozzo et al. 2015). For example, the TSPO ligand RO5-4864 could effectively attenuate the neuropathology and behavioral impairment in an AD mouse model (Barron et al. 2013). It has also been reported in several studies that the TSPO ligands modulate microgliosis and show protective effects in retinal degeneration (Scholz et al. 2015; Rashid et al. 2018b), MS (Leva et al. 2017), traumatic brain injury (Papadopoulos and Lecanu 2009), and depression (Gavioli et al. 2003).

It is essential to note that some TSPO ligands can bind to other proteins, apart from binding to TSPO. For example, the synthetic TSPO ligand Etifoxine is a clinically approved drug for anxiety disorder outside Europe and the US. The anxiolytic effects of Etifoxine were caused

by directly binding and activating GABA<sub>A</sub> receptor complex, and by stimulating TSPO-mediated neurosteroids production.

However, another TSPO agonist in aryl-oxodihydropurines class, Emapunil (=AC-5216 or XBD-173, as shown in Figure 1.4), shows nanomolar binding affinity to the mitochondrial purified TSPO (i.e., IC<sub>50</sub> = 3.04 nM or 2.73 nM for TSPO purified from rat or human glioma cells, respectively). It also shows negligible affinity to a total of 90 other transporters, ion channels and receptors, which include GABA<sub>A</sub> receptors (Kita et al. 2004; Rupprecht et al. 2009; Ravikumar et al. 2016). Emapunil has been intensively studied over the past few years and showed neuroprotective and anti-inflammatory effects in MS (Leva et al. 2017) and depression models (Gavioli et al. 2003). It also exerts rapid anxiolytic effects with no sedation and withdrawal symptoms in the CCK4 challenged human volunteers, with enhanced GABAergic neurotransmission (Rupprecht et al. 2009; Kita et al. 2009). Most importantly, Emapunil has already been tested for safety and tolerability in a phase II clinical trial in patients with generalized anxiety disorder (Rupprecht et al. 2010), although it failed to reach positive clinical outcome criteria, partially due to single nucleotide polymorphism (SNP) carriers (Owen et al. 2011; Owen et al. 2012). Given the high affinity and selectivity to TSPO, Emapunil is in a top position for drug development to treat neurodegenerative diseases.

Although the precise molecular and cellular mechanisms of the neuroprotective effects mediated by TSPO ligands in neuropathological conditions are not well defined, stimulation of mitochondrial steroid synthesis and suppression of ROS product in activated microglia have been widely discussed as possible mechanisms (Wang et al. 2014; Guo et al. 2015).

## 2 Materials and Methods

### 2.1 Materials

#### 2.1.1 Chemicals and consumables

In this study, Emapunil was kindly provided by Andrea Leonov and Prof. Dr. Markus Zwechstetter. It was prepared as previously reported (Maeda et al. 2007), as shown in Figure 2.1. All the other chemicals were purchased either from AppliChem GmbH (Germany), Merck group (Germany) or Sigma-Aldrich GmbH (USA). Plastic consumables were purchased from Thermo Fisher Scientific (USA), Eppendorf AG (Germany) and BD Falcon™ (France) unless indicated otherwise.

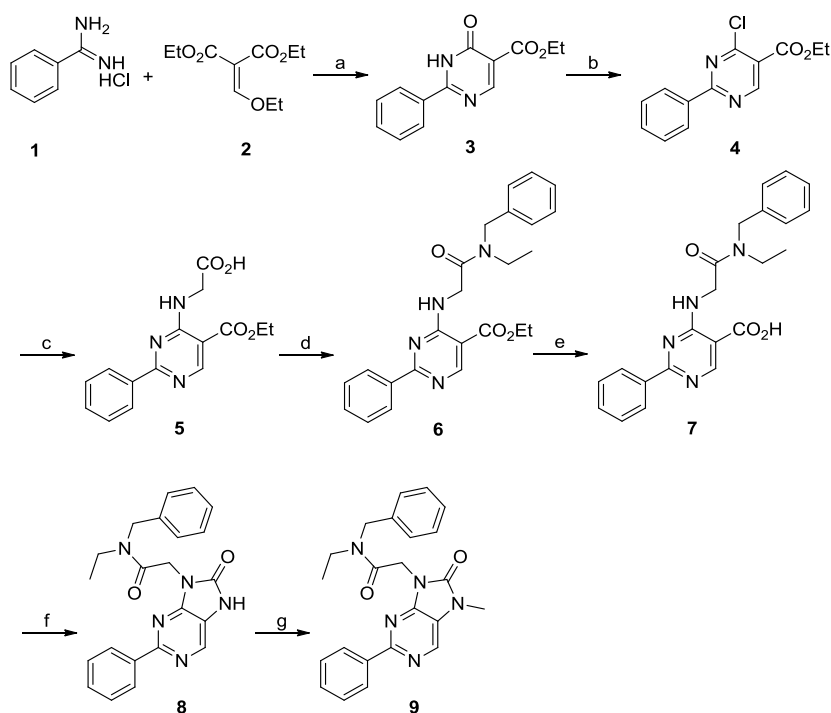


**Figure 2.1 Emapunil preparation diagram**

Reaction reagents and conditions depicted in the diagram: (a) NaOEt with EtOH at 0-80°C for 4 h, 81%; (b) POCl<sub>3</sub> at 90°C for 4 h, 99%; (c) glycine, Et<sub>3</sub>N and EtOH at 78°C for 4 h, 100%; (d) N-ethylbenzylamine, PyBOP, Et<sub>3</sub>N and DMF at 22°C for 2 h, 100%; (e) NaOH, EtOH and water at 78°C for 2 h, 82%; (f) diphenyl phosphorazidate, Et<sub>3</sub>N and DMF at 100°C for 6 h, 55%; (g) MeI, NaH and DMF, at 22°C for 3 h, 78%.

### 2.1.2 Buffer solutions

Buffer solutions used in this study were prepared as shown in Table 2.1

**Table 2.1 preparation of buffer solutions used in this study**

Buffer	formula	concentration	Notes
10x PBS	NaCl KCl Na <sub>2</sub> HPO <sub>4</sub> KH <sub>2</sub> PO <sub>4</sub>	1.37 M 27 mM 100mM 18 mM	pH = 7.4
10x TBS	NaCl KCl Tris	1.37 M 27 mM 248 mM	pH = 7.4
Tissue homogenization buffer for MPTP and dopamine metabolites measurement	perchloric acid	0.1 M	
HPLC mobile phase buffer	sodium phosphate octane sulphonic acid methanol	75mM 275 mg/l 10%	pH = 2.9
16% PFA	PFA ddH <sub>2</sub> O NaOH tablets 10x PBS	16g 70ml to 60°C 2-3 10 ml	pH = 7.4 store at - 20°C
Cryopreservation solution	Glycerol Ethylenoglycol 1x PBS	25% [v/v] 25% [v/v] 1x	pH = 7.4
TBS with 0.1% NaN <sub>3</sub>	NaN <sub>3</sub> TBS	0.1% [w/v] 1x	pH = 7.4
0.1% TBS Tween	Tween-20 TBS	0.1% [v/v] 1x	pH = 7.4
Peroxidases quench buffer	methanol H <sub>2</sub> O <sub>2</sub>	40% 1%	Prepare fresh before use

## Materials and Methods

	TBS	1x	
Blocking buffer for immunohistochemistry	BSA Triton x-100 TBS	3% 0.5% 1x	
Citric buffer	Tri-Sodium Citrate Tween-20	10 mM 0.05% [v/v]	pH = 6.0
Mowiol 488	Mowiol Glycerol Tris HCl DABCO	13.3% [w/v] 33.3% [v/v] 133 mM 24 mg/ml	pH = 8.5 store at - 20°C
Blocking buffer for immunocytochemistry	FBS BSA Fish gelatin PBS	2.5% [v/v] 2.5% [w/v] 2.5% [v/v] 1x	
CHAPS buffer	CHAPS Tris EDTA	1% 50 mM 5 mM	pH = 8.0
5x Protein sample buffer	Glycerol Tris-HCl EDTA SDS $\beta$ -Mercaptoethanol Bromophenol blue	10% 50 mM 2 mM 2% 144 mM 0.05%	pH = 6.8
10x Running buffer	Glycine Tris SDS	1.9 M 192 mM 1% [w/v]	pH = 6.8
10x Transfer buffer	Glycine Tris	1.9 M 192 mM	
1x Transfer buffer	10x Transfer buffer Methanol ddH <sub>2</sub> O	100 ml 200ml 800ml	

### 2.1.3 Commercial reagents, compounds and consumables

The commercial reagents and plastic Consumables are listed in Table 2.2.

**Table 2.2 Overview of commercial reagents, compounds, and consumables**

<b>Commercial reagents, compounds and consumables</b>	<b>Catalog number</b>	<b>company</b>
Nunc™ EasYFlask™ Cell Culture Flasks	10364131	Thermo Scientific™
Nunc™ Cell-Culture Treated Multidishes	10469282	Thermo Scientific™
Poly-L-ornithine	P3655-50MG	Sigma-Aldrich
Fibronectin	F1141-2MG	Sigma-Aldrich
DMEM/F12 medium	D8062-6X500ML	Sigma-Aldrich
N2 supplement	17502048	LIFE Technologies
bFGF	233-FB-025	R und D Systems
db-cAMP	D0627-250MG	Sigma-Aldrich
Tetracycline	T7660-5G	Sigma-Aldrich
GDNF	212-GD-010	R und D Systems
0.05 % Trypsin-EDTA	25300054	LifeTechnologies
Fetal bovine serum	10309433	Fisher Scientific
Cell culture grade DMSO	A3672,0250	AppliChem
MPTP	M0896	Sigma-Aldrich
Rotenone	45656-250MG	Sigma-Aldrich
toyocamycin	Cay17371-5	Biomol
Emapunil	SML1223-5MG	Sigma-Aldrich
MPP <sup>+</sup>	D048	Sigma-Aldrich
Tissue-Tek® O.C.T.	4583	SAKURA
Lipofectamine® RNAiMAX Reagent	13778150	LIFE Technologies
Amersham™ ECL Prime Western Blotting Detection Reagent	GERPN2232	GE Healthcare Life Sciences
cOmplete™ Protease inhibitor cocktail	000Z00011697498001	Roche Diagnostics
ESIRNA HUMAN TSPO	EHU080541-20UG	Sigma-Aldrich

MISSION® siRNA Negative Control	SIC003	Sigma-Aldrich
Negative Control siRNA	1027310	Qiagen
DPX	06522	Sigma-Aldrich

### 2.1.4 Cell culture medium

Lund human mesencephalic (LUHMES) cells were used in this study for *in vitro* experiments. Two different cell culture media (proliferation and differentiation medium) are listed in Table 2.3 and Table 2.4. Proliferation and differentiation medium can be stored at 4°C for 2 weeks and need to be filtered before use.

#### 2.1.4.1 Proliferation medium components

**Table 2.3 Overview of proliferation medium components**

Components	volume
DMEM/F12 medium	495 mL
N2 supplement	5 mL
bFGF stock solution (25 µg/mL)	800 µL

#### 2.1.4.2 Differentiation medium components

**Table 2.4 Overview of differentiation medium components**

components	volume
DMEM/F12 medium	490 mL
N2 supplement	5 mL
db-cAMP stock solution (49 mg/mL)	5 mL
tetracycline stock solution (1 mg/mL)	500 µL
GDNF stock solution (5 µg/mL)	200 µL

### 2.1.5 Commercial kits

Commercial kits used in this study are listed in Table 2.5.

**Table 2.5 Overview of commercial kits**

Commercial Kit	Catalog number	Company
Pierce <sup>™</sup> BCA protein assay	23225	Thermo Fisher Scientific
VECTASTAIN <sup>®</sup> Elite <sup>®</sup> ABC HRP Kit	PK-6200	Vector Laboratories
DAB peroxidase substrate kit	SK-4100	Vector Laboratories
ToxiLight <sup>™</sup> bioassay kit	LT17-217	Lonza Verviers
RNeasy <sup>®</sup> Mini Kit	74104	Qiagen
SuperScript IV VILO Master Mix with ezDNase-50 reactions	11766050	LIFE Technologies
<i>Power</i> SYBR Green PCR Master Mix	4367659	LIFE Technologies

### 2.1.6 Primers

All primers in this study were ordered either from AGCT core facility (Max-Planck Institute of Experimental Medicine, Göttingen, Germany) or from Sigma Aldrich (Munich, Germany) with 50 mM concentration, the working concentrations were diluted to 10 mM or 20 mM, the stock and working solutions were stored at -20°C. The primers are listed in Table 2.6.

**Table 2.6 Overview of the primers for qPCR used in this study**

Gene (protein)	Forward Primer	Reverse Primer
Mrc1 (MMR)	AGTGGCAGGTGGCTTATG	GGTTCAGGAGTTGTTGTGG
Ym1 (YM1)	CATTCAGTCAGTTATCAGATTC C	AGTGAGTAGCAGCCTTGG
Fizz2 (FIZZ2)	TGGAGAATAAGGTCAAGGAAC	GTCAACGAGTAAGCACAGG
Il10 (IL10)	TGGCCCAGAAATCAAGGAGC	CAGCAGACTCAATACACACT
Il4 (IL4)	AGATGGATGTGCCAAACGTCCT CA	AATATGCGAAGCACCTTGGAAG CC
Arg1 (Arg1)	GGAAGACAGCAGAGGAGGTG	TATGGTTACCTCCCGTTGA
Iba1 (IBA1)	GTCCTTGAAGCGAATGCTGG	CATTCTCAAGATGGCAGATC
Tspo (TSPO)	GGGAGCCTACTTTGTGCGTGG	CAGGTAAGGATACAGCAAGCGG G
<i>Tnfa</i> (TNF- $\alpha$ )	TTCCGAATTCAGTGGAGCCTCG AA	TGCACCTCAGGGAAGAATCTGG AA
IP10 (IP10)	TGAGCAGAGATGTCTGAATCCG	TGTCCATCCATCGCAGCA

IL1b (IL1 $\beta$ )	AAGGGCTGCTTCCAAACCTTTG AC	ATACTGCCTGCCTGAAGCTCTTG T
Mpa2l (MPA2l)	CAAGAGGGGAGAAGATTGAACA TGA	CACTTGCCTTCACCCCTTTC
<i>Nos2</i> (iNOS2)	CTGCTGGTGGTGACAAGCACAT TT	ATGTCATGAGCAAAGGCGCAGA AC
Cox2 (COX2)	TTGCTGTACAAGCAGTGGCAAA GG	TGCAGCCATTTCTTCTCTCTCTGT
Il6 (IL6)	TGGCTAAGGACCAAGACCATC CAA	AACGCACTAGGTTTGCCGAGTA GA
<i>Xbp1</i> (XBP1) mouse	CAGCACTCAGACTATGTGCA	GTCCATGGGAAGATGTTCTGG
<i>Xbp1s</i> (XBP1s) mouse	CTGAGTCCGAATCAGGTGCAG	GTCCATGGGAAGATGTTCTGG
<i>XBPI</i> (XBP1) human	CAGCACTCAGACTACGTGCA	ATCCATGGGGAGATGTTCTGG
<i>XBPIs</i> (XBP1s) human	AACCAGGAGTTAAGACAGCGC TT	CTGCACCTGCTGCGGACT
<i>Actb</i> ( $\beta$ -Actin) mouse	TGTGATGGTGGGAATGGGTCA GAA	TGTGGTGCCAGATCTTCTCCATG T
GAPDH human	GAAGGTGAAGGTCTGGAGT	CATGGGTGGAATCATAATGGAA

### 2.1.7 Antibodies

The primary and secondary antibodies are listed in Table 2.7 and Table 2.8, respectively.

**Table 2.7 Overview of the primary antibodies**

Antibody	Host species	Dilution and application	catalog number	company
TH	rabbit polyclonal	1:1000 (IHC)	AB152	Millipore
IBA	rabbit polyclonal	1:2000 (IHC)	019-19741	WAKO
GFAP	Guinea pig polyclonal	1:1000 (IHC)	173004	Synaptic Systems
TSPO	rabbit polyclonal	1:500 (IHC)	ab109497	Abcam
TH	chicken	1:1000 (IHC)	ab76442	Abcam

**Table 2.8 Overview of the secondary antibodies**

Antibody	Host species	Conjugate	Dilution and application	catalog number	Company
anti-rabbit IgG	donkey	biotinylated	1:200 (IHC)	RPN-1004	GE Healthcare
anti-Rabbit IgG	Donkey	Alexa Fluor 488	1:1500 (IHC)	ab150129	Abcam
anti-Guinea pig IgG	Goat	Alexa Fluor 647	1:1000 (IHC)	A-21450	Thermo fisher scientific
anti-Rabbit IgG	Goat	Alexa Fluor	1:1000 (IHC)	A11008	Thermo fisher

		488			scientific
Anti-Chicken IgY	Goat	Cy3	1:500 (IHC)	ab97145	Abcam
Anti-Rabbit IgG	Goat	HRP	1:1000	111-035-003	Dianova

### 2.1.8 Software

The software used in this study is listed in Table 2.9.

**Table 2.9 Overview of software used in this study**

Software	Application	Source
GraphPad Prism 7	Statistical and figure analysis	GraphPad Software Inc.
Stereo Investigator 9.0	Stereology quantification	MicroBrightField Inc.
StepOnePlus™ Real-Time PCR System	qPCR data analysis	Thermo Fisher Scientific
Adobe Illustrator CS5.1	Figure design	Adobe System Inc.
MS Office Excel 2010	Data analysis	Microsoft
EndNote x7	references management	Clarivate Analytics
MS Office Word 2010	Text processing	Microsoft
Zen Blue 2.3 lite	Image acquisition and processing	Zeiss
Fiji/ImageJ	Image analysis	<a href="http://fiji.sc/Fiji">http://fiji.sc/Fiji</a>

## 2.2 Methods

### 2.2.1 The experimental schedule

In this experiment, a total number of 75 C57BL/6JRj female mice were purchased from Janvier Labs, France. They were 8-week-old when the experiment started. They were housed in groups of five in individually ventilated cages in an air-conditioned room and kept under a 12-h light-dark cycle with free access to standard food and water. All animal experiments were carried out under the German animal protection law and legislation of the State of Lower

Saxony. All protocols had been reviewed and approved before experiments by animal welfare board (Landesamt für Verbraucherschutz, Braunschweig, Lower Saxony, Germany, reference number 12/2210). Two mice were sacrificed during the treatment because of severe injuries.

### **2.2.1.1 Subacute MPTP treatment**

Mice were randomly divided into 3 groups with 25 mice per group. Two groups of mice received i.p. injection of 30 mg/kg body weight MPTP (free base from Sigma, dissolved in 0.9% saline) every 24 h for 5 consecutive days. Another group of mice received i.p. injection of saline with the same schedule as saline control (Figure 3.1).

### **2.2.1.2 Emapunil treatment**

From the same day of the first MPTP administration, MPTP injected mice additionally received i.p. injection of either DMSO or 50 mg/kg body weight Emapunil (dissolved in DMSO) every 48 hours for 15 days, named MPTP + DMSO group or MPTP + Emapunil group, individually. Saline-treated mice received i.p. injection of DMSO as control, named NaCl + DMSO group (Figure 3.1).

### **2.2.1.3 Experimental procedure**

The experimental design is shown in Figure 3.1. Experiments started from the first injection of saline, MPTP, DMSO and/or Emapunil. Five mice per group were sacrificed on day 3 for qPCR, HPLC, and transcriptome assays. Two motor tests were conducted on day 11-13 (pole test) and day 14 (cylinder test), separately. On day 15, five mice per group were sacrificed for dopamine and its metabolites quantification. The remaining mice were perfused for IHC and stereological analysis.

### 2.2.2 MPTP metabolism

On day 3, five mice per group were sacrificed 90 min after MPTP or Emapunil injection. Brains were immediately dissected on ice after briefly washing with PBS. The striatum was separated into two hemispheres and collected in cry-stock vials which were filled with ceramic beads at -80°C until further processing.

For the MPTP metabolism measurement, tissue homogenization buffer was added into the vials containing the left striatum hemisphere at a volume of 50ul/mg tissue and then homogenized by Precellys 24 homogenizer. After high-speed centrifugation, supernatants were taken out and stored for MPP<sup>+</sup> concentration measurement by HPLC. The protocol for HPLC measurement was adopted from (Tönges et al. 2012). 10 ul of supernatants were injected onto a reverse-phase column (Nucleosil 100-5 C18; Macherey-Nagel), the flow rate was 0.4 ml/min. The MPP<sup>+</sup> signals were detected by fluorescence, the wavelengths of excitation and emission are 295 nm and 375 nm, respectively (Fluorescence HPLC Monitor; Shimadzu).

### 2.2.3 RT-qPCR

#### 2.2.3.1 RNA extraction

In this study, we extracted RNA from the right hemispheres of the striatum on day 3 and LUHMES cell lysates by using the RNeasy Mini kit according to the manufacturer's instructions. The samples were disrupted and homogenized in buffer RLT with  $\beta$ -ME. After 5 min incubation at RT, the samples were centrifuged at 12000g for 3 min, and supernatants were removed by pipetting. 70% ethanol was added into the pellet and mixed well by pipetting. The samples were transferred into RNeasy Mini spin columns and centrifuged at 10000g for 30 s. Supernatants were discarded and 700  $\mu$ l Buffer RW1 was added into the

## Materials and Methods

column, centrifuged at 10000g for 30 s. This was followed by two Buffer RPE washing steps, and the columns were dried by another centrifuge step at 10000g for 1 min. Finally, RNA was eluted by adding 30–50 µl RNase-free water to the spin column membrane and centrifugation at 10000g for 1 min. From now on, RNA was kept on ice or at -80 °C for storage. The quality and concentration of RNA were measured by NanoDrop.

### 2.2.3.2 cDNA synthesis

The Invitrogen™ SuperScript™ IV VILO™ Master Mix with ezDNase enzyme was used in this study for the first strand cDNA synthesis. The RNA samples were treated with ezDNase enzyme for DNA digestion, the reaction mixture was prepared on ice as shown in Table 2.10. The components were incubated at 37°C for 2 minutes after gently mixed. This was followed by adding 4 µL SuperScript™ IV VILO™ Master Mix and 6 µL Nuclease-free water. Next, the components were incubated at 25°C for 10 min to anneal the primers and then at 50°C for another 10 min to reverse transcribe RNA. After that, the enzyme was inactivated by incubating at 85°C for 5 min. The cDNA was ready for qPCR amplification.

**Table 2.10 cDNA synthesis reaction mixture**

Component	Volume (µL)
10X ezDNase buffer	1
ezDNase enzyme	1
Template RNA (500 pg)	variable
Nuclease-free water	Up to 10

### 2.2.3.3 RT-qPCR amplification

The qPCR amplification was conducted by using Power SYBR® Green PCR Master Mix in StepOnePlus™ Real-Time PCR system. The reaction components were prepared as listed in

Table 2.11. The used primers are shown in Table 2.6. The relative gene expression changes between target genes and the housekeeping gene ( $\beta$ -actin) were analyzed by the  $2^{-\Delta\Delta CT}$  method. The Fold-changes (FC) between groups were analyzed afterward.

**Table 2.11 RT-qPCR reaction components**

Component	Volume ( $\mu$ l)
2x SYBR Green Master Mix	10
Primer-Forward (10 pmol/ $\mu$ l)	1
Primer-Reverse (10 pmol/ $\mu$ l)	1
Template	1
Nuclease-free water	up to 20

### 2.2.4 Behavioral tests

Pole test and cylinder test were used in this study to assess the body coordination and motor function.

#### 2.2.4.1 Pole test

The pole test was initially introduced in 1985 by Ogawa and became a useful tool for evaluating the motor dysfunction caused by striatal dopamine depletion in mouse PD models (Ogawa et al. 1985). A rough-surfaced pole (diameter 12 mm; height 55 cm) was vertically placed in the home cage of the tested mouse, and the mouse was placed on the top of the pole with head-upward. Two parameters were recorded during the test: the time until the mouse orients the head downward, and the time until the mouse descend along the pole to touch the ground with the forelimbs. In this study, mice were trained from day 11 after the initial injection for 2 consecutive days, which include three trials per day with a 10 min interval for

mice to recovery. On day 13, mice performed five consecutive trials with 10 min intervals and the entire procedure was recorded. Time values were calculated and averaged from five consecutive trials. No mice flipped or fell down in this study.

### **2.2.4.2 Cylinder test**

The cylinder test was initially described by Schallert in 2000 for assessing the independent use of forelimbs in unilaterally lesioned mouse models, but it has also been widely used for measuring forelimb akinesia and whole body coordination (Schallert and Tillerson 2000).

In this study, the cylinder test was conducted following the pole test on day 14. The individual mouse was placed in a transparent cylinder (diameter: 11.5 cm; height: 25 cm) for 5 min and all movements were video recorded. The mice had never been habituated to the cylinder before and were free to explore. The number of rearing was counted. A mirror was placed behind the cylinder to make sure that all forelimb movements were recorded when mice turned away from the camera. The rearing activities were normally counted up to thirty times per mouse. The usage of forelimbs against the wall for support after rearing was classified according to the following asymmetry criteria: (i) simultaneous co-using of both left and right forelimbs for contacting the cylinder wall or lateral stepping movements with alternatively using of both left and right forelimbs along the wall, was recorded as ‘both’ forelimbs rearing; (ii) full rearing of the entire body without touching the wall was recorded as ‘free’ rearing; (iii) the first forelimb used to contact the wall for support after full rearing was recorded for that limb, such as either ‘left’ forelimb rearing or ‘right’ forelimb rearing. In addition, mice with too little tendency for exploration (<5 rearings) or too much (jumping over) during a test session were not included in this study. The percentages of ‘both’, ‘right’, ‘left’ or ‘free’ forelimbs rearing within the entire observation time were then subtracted and calculated.

### **2.2.5 Neurochemical analysis of dopamine and dopamine metabolites**

At day 15, all mice were sacrificed. Brains were either freshly prepared for neurochemical analysis of dopamine and metabolites or perfused for histology assays.

In order to analyze the functional impairment of the dopaminergic terminals in the striatum after treatment, five mice per experimental group were sacrificed by cervical dislocation at day 15, and brains were removed immediately after sacrifice. After briefly rinsing with PBS, the left hemispheres of the striatum were dissected on ice and stored into cryo stock vials with ceramic beads at -80°C until further processing. The tissues were then homogenized by Precellys-24 homogenizer, followed by centrifugation at 5000 g for 1 min. Supernatant was transferred into a new vial and again centrifuged at 10000 g for 30 min at 4°C. 50 µl of the supernatant was transferred into an HPLC vial for dopamine, homovanillic acid (HVA) and DOPAC measurement.

The HPLC system contains a C18 reverse-phase HR-80 catecholamine HPLC column (ESA), a Guard cell kept at 600 mV to oxidize impurities in the eluent, and an ESA Coulochem II electrochemical detector equipped with a 5011A analytic model detector (E1 = 50 mV, E2 = 400 mV). The samples were injected into columns (ESA) with a flow rate of 0.4 ml/min mobile phase (filtered and degassed), to prevent pH changing during the mobile phase. Data were analyzed with Chromeleon Chromatography Data System (Dionex) and displayed as ng/mg wet tissue.

### **2.2.6 Histology**

#### **2.2.6.1 Transcardial Perfusion and tissue cryo-section**

At day 15, another cohort of 8-10 mice per experimental group was deeply anesthetized by intraperitoneal injection with 14% chloral hydrate. The whole body including the brain was

## Materials and Methods

perfused with cold PBS and 4% PFA using MPII mini peristaltic pump (flow rate: 3 ml/min). After fixation, brains were removed, post-fixed in 4% PFA overnight and transferred into 30% sucrose for cryopreservation for 48 h at 4°C. After that, brains were snap frozen on dry ice with the protection of Tissue-Tek O.C.T. (Sakura) and stored at -80°C until further processing.

For immunohistochemistry, brains were cryosectioned into 30 µm coronal free-floating sections using a cryostat (CM1900, Leica, Germany), which were stored in 48 well plates containing TBS with 0.1% NaN<sub>3</sub> at 4°C until further use.

### 2.2.6.2 Immunohistochemistry

For quantifying TH- and Nissl- positive neurons in the substantia nigra by stereology, every fifth section in the substantia nigra was stained using the free-floating method. Sections were washed 3 times with 1x TBS for 5 min each to wash the 0.1% NaN<sub>3</sub> away, and the endogenous peroxidases were quenched by 40% methanol and 1% H<sub>2</sub>O<sub>2</sub> in TBS for 15 min. After washing, the sections were blocked with 3% BSA and 0.5% Triton x-100 in TBS (TBST) for 1 h at room temperature. Next, sections were incubated with anti-TH antibody (Table 2.7) in blocking solution for 48 h at 4°C and biotinylated donkey anti-rabbit IgG (Table 2.8) for 2 h at room temperature. This was followed by incubation with VECTASTAIN ABC peroxidase standard kit for 2 h at room temperature. Visualization was performed by using chromogen DAB (DAB peroxidase substrate Kit) for 2 to 5 min at room temperature depending on the color change. The reaction was stopped by washing with TBS 3 times, and the sections were mounted on SuperFrost Plus microscope slides. The slides need to be dried at room temperature for 2 days. After rehydration, Nissl staining was counterstained using 0.5% Cresyl violet at room temperature for 2 to 10 min. This was

followed by dehydration with an ascending concentration series of ethanol and xylene. In the end, slides were mounted with DPX.

### **2.2.6.3 Stereological quantification of substantia nigra neurons**

After drying overnight, the DAB and Nissl stained slides were used for stereological quantification of TH- and Nissl- positive neurons, using Stereo Investigator software. Slides were fixed under a Zeiss Axioplan microscope equipped with a computer-controlled motorized stage (Ludl Electronics, Hawthorne, USA). The substantia nigra region was outlined at 2.5x objective magnification with the optical fractionator method. The number of positive neurons was counted at 100x objective magnification with following criteria: 150x 150  $\mu\text{m}$  grid layout, 50 x 50  $\mu\text{m}$  counting frame, 15  $\mu\text{m}$  dissector height and 3  $\mu\text{m}$  guard. The counting was performed blinded.

### **2.2.6.4 Immunofluorescence**

Immunofluorescence was conducted for quantification of the microgliosis, astrogliosis and identification of TSPO expression in TH positive neurons.

Every tenth section through the striatum (3 slices/brain) was washed with 1x TBS to remove the 1%NaN<sub>3</sub>, and antigen retrieval was performed using citrate buffer for 30 min at 95°C. Sections were still kept in the antigen retrieve buffer for 30 min after moved out from the water bath. Once cooled to room temperature, sections were rinsed with 1x TBS and blocked with 3% BSA in 0.5% TBST for 1 h at room temperature. This was followed by primary antibodies (Table 2.7) incubation for 48 h at 4°C in blocking solution, On the third day, sections were incubated with the corresponding secondary antibodies (Table 2.8) for 2 h at room temperature. DAPI counter-staining was then performed for 10 min at room temperature. Sections were then washed with TBS and mounted with Mowiol 4-88.

### **2.2.6.5 Quantification of microglia activation and astrogliosis**

For quantifying microglia activation and astrogliosis, every tenth section through the striatum from each brain (3 slices/brain) was stained with Iba1 and GFAP. The sections were tile scanned and automatically stitched using Zeiss Axio Observer. Z1 microscope connected to Apotome.2 at 20x objective magnification. The number of Iba1 or GFAP positive cells and the counting area in the striatum were counted using Fiji-ImageJ with a cell counter analysis plug-in, and the result was presented as positive cells normalized to the analyzed area.

### **2.2.6.6 Identification of TSPO expression in TH+ neurons**

To identify the co-localization of TSPO and TH staining, 1 slice containing the substantia nigra from each brain was co-stained with antibodies against TSPO and TH. Fluorescent images were taken using an LSM 700 Zeiss laser scanning confocal microscope under 63x objective magnification, with 16-bit and 1024 x 1024 pixels.

## **2.2.7 RNA-Seq and bioinformatical analysis**

### **2.2.7.1 Tissue dissection and RNA isolation**

For transcriptome assay, another cohort of 8-week-old female C57BL/ 6J Rj mice was purchased from Janvier Lab. They were randomly divided into 3 groups and received the same treatment as previously described. On day 3, 8 mice from each experimental group were sacrificed by cervical dislocation 90 min after the i.p. injection. Brains were quickly isolated on ice and dissected into regions. The striatum tissue was snap-frozen in liquid nitrogen and stored at -80°C. For RNA extraction, tissue was homogenized in TriReagent (Sigma), and RNA was extracted according to the manufacturer's instruction. The extracted RNA was further treated with 2U of DNaseI (Invitrogen) for 20 min at 37°C and re-purified with

Phenol/Chloroform. The purified RNA was resuspended in DEPC water and stored at -80°C until further processing.

### **2.2.7.2 RNA sequencing**

The quality of RNA was measured using Agilent 2100 Bioanalyzer (Agilent Technologies) and Qubit (Life Technologies). RNA library and mRNA sequencing cluster were generated using Illumina HiSeq 2000 according to Illumina standard protocols (TruSeq, Illumina). The Library was mapped to the reference genome (mm10, STAR aligner) with the following parameters: `-outFilterMismatchNmax2-outSAMstrandField intronMotif-sjdbOverhang 49`. The Counts were generated using htseq (Anders et al. 2015).

### **2.2.7.3 Bioinformatical analysis**

To reveal Gene Ontology (GO) biological processes, molecular functions and localizations between the differentially expressed genes in saline control, MPTP + DMSO mice and MPTP + Emapunil mice, the differentially expressed genes between groups were queried using DESeq2 (Love et al. 2014). The threshold for clarifying the differentially expressed genes is:  $\log_2FC > |0.2|$  and adjusted p-value (Benjamini-Hochberg)  $< 0.05$ . Overlaps of the differentially expressed genes were calculated using Venny (Oliveros 2007-2015).

Gene Ontology (GO) functional enrichment analysis was carried out using Webgestalt 2.0 (<http://www.webgestalt.org/option.php/>, (Kirov et al. 2014; Wang et al. 2013; Zhang et al. 2005a). Gene network pathways analysis (p-value  $< 0.1$ ) was conducted using Cytoscape 3.0's plugin ClueGO (Bindea et al. 2009). Transcription factor binding site enrichment analysis was performed with PSCAN using the TRANSFAC database (Zambelli et al. 2009). R was utilized for tracing Heatmaps and individual genes (Team 2008).

### 2.2.8 LUHMES cell culture experiments

All cell culture work was conducted under the S1 security level. The work was carried out entirely under sterile conditions, including 70% ethanol antiseptic cleaning of all equipment, UV- light treatment and sterile filtration of all media and solutions with a 0.22  $\mu\text{m}$  polyethersulfone filter.

#### 2.2.8.1 Coating of cell culture flasks and dishes

The stock solution of PLO was prepared with ddH<sub>2</sub>O to a concentration of 5 mg/mL. The working solution was then diluted 1:100 with ddH<sub>2</sub>O from the stock solution to the final concentration of 0.05 mg/mL. The working solution of Fibronectin was diluted 1:200 from the stock solution (1 mg/mL) with ddH<sub>2</sub>O to the final concentration of 5  $\mu\text{g/mL}$ . The working solution was filtered before use.

The surfaces of multi-well plates, dishes or flasks were coated for LUHMES cells attachment. In the proliferation phase, it is sufficient to coat with PLO only. However, a double coating with PLO and Fibronectin in a row is necessary to allow the outgrowth of cell processes in the differentiation phase. The coating procedure needs to be at least 6 h at 37°C or overnight at room temperature/4°C. The coating solution was added in sufficient volume to cover the surface (see Table 2.12) and rinsed three times with sterile PBS after coating. All residues were removed and air dried before use.

**Table 2.12 Minimal volume of PLO and fibronectin for different well sizes**

Multi-well plates	Size of well (cm <sup>2</sup> )	PLO, fibronectin ( $\mu\text{l}$ )
6	9.6	1750
6 cm dish	28	5000
75 cm <sup>2</sup> flask	75	12000

### 2.2.8.2 Maintenance and differentiation

LUHMES cells is an immortalized human dopaminergic neuronal precursor cell line (Szegő et al. 2017; Scholz et al. 2011). In this experiment, LUHMES cells were first grown and expanded with proliferation medium in pre-coated flasks (see section: Proliferation medium components). The proliferation medium was changed every 2<sup>nd</sup> day. To conduct experiments, the proper amount of LUHMES cells (at a density of 150,000 cells per cm<sup>2</sup>) were transferred to 6-well plates with differentiation medium (see section: Differentiation medium components). 50% of the differentiation medium was changed on the second day after differentiation. From then on, the medium was kept without further changes for six more days.

### 2.2.8.3 siRNA transfection

To down-regulate the expression level of TSPO via siRNA, LUHMES cells were transfected with the esiRNA EHU080541 using Lipofectamine RNAiMAX transfection reagent four days after differentiation. Negative control siRNA from Qiagen was used as control.

The siRNA mixture 1 and 2 were prepared separately, as shown in Table 2.1, and were gently mixed by pipetting. Mixtures were incubated for 5 min at room temperature and then equally distributed into the cell culture medium.

**Table 2.13 Scheme for preparing siRNA mixture 1 and 2**

Component	6-well plates (each well)	Notes
Adherent cells	0.25–1 × 10 <sup>6</sup>	
Opti-MEM <sup>®</sup> medium	150 µL	Mixture 1
Lipofectamine <sup>®</sup> RNAiMAX Reagent	9µL	
Opti-MEM <sup>®</sup> Medium	150 µL	Mixture 2
siRNA (10 µM)	3 µL	

### 2.2.8.4 Toxicity assay

In the toxicity assay experiments, LUHMES cells were transfected with either TSPO or control siRNA at day 4 after differentiation. At day 7, cells were treated with either Emapunil (5  $\mu$ M) or DMSO as control at day 7 after differentiation. 12 h later, LUHMES cells were treated with either DMSO, MPP<sup>+</sup> (10  $\mu$ M in DMSO) or rotenone (10  $\mu$ M in DMSO). After 24 h incubation, supernatants were harvested for toxicity measurements using ToxiLight assay. In brief, 50  $\mu$ l of reagent were added to 50  $\mu$ l of culture supernatants, the pure medium without cells was treated as blank control, after incubation at room temperature for 5 min, luminescence was measured using FLUOstar Omega (BMG labtech, Germany).

### 2.2.8.5 RT-qPCR assay for *Xbp1* and *XBPIs* analysis

For mRNA isolation and qPCR, LUHMES cells were also transfected with either TSPO or control siRNA at day 4 after differentiation. At day 7, LHUMES were treated for 12 h with either DMSO, toyocamycin (Sigma, 1  $\mu$ M in DMSO), Emapunil (5  $\mu$ M) or toyocamycin plus Emapunil. 12 h later, cells were exposed to DMSO or 10  $\mu$ M rotenone. After incubating for another 12 h, cells were harvested for mRNA isolation, cDNA synthesis and qPCR, which were performed as mentioned in section: RT-qPCR.

### 2.2.8.6 SDS-PAGE and Western blot analysis

The TSPO and TH protein expression levels in LUHMES cells were quantified by Western blot. Cell lysates were firstly dissolved in CHAPS buffer and then centrifuged at 4500g for 10 min. Supernatants were then denatured at 95°C for 5 min after adding sample loading buffer. The lysates were loaded into SDS-PAGE gel, which contains 4% stacking gel and 12% resolving gel as prepared in Table 2.14. 20  $\mu$ g protein per sample was loaded into the gel pocket and separated using Bio-Rad Mini-PROTEAN<sup>®</sup> Tetra electrophoresis system at 120 V

for approximately 120 min. The PageRuler<sup>®</sup> Prestained Protein Ladder was used as the molecular weight reference.

**Table 2.14 Components for stacking and resolving gels for SDS-PAGE**

Component	Stacking gel (4%)	Resolving gel (12%)
Acrylamide/Bis Solution 30%	4%	12%
Tris-HCl pH 6.8	125 mM	375 mM
SDS	0.1%	0.1%
Ammonium persulfate (APS)	0.1%	0.1%
N'N'N'-tetramethylethylene diamine (TEMED)	0.15%	0.04%

After electrophoresis, the proteins were transferred from the SDS gel to the Whatman<sup>®</sup> nitrocellulose membrane by using the Mini-Trans Blot cell at 100V for 55 min. Next, the membrane was incubated with blocking solution (4 % non-fat milk powder in PBS) for 40 min at room temperature to reduce the unspecific binding of immunoglobulins. After that, corresponding primary and HRP conjugated secondary antibodies were applied. Proteins were visualized and captured on X-Ray films (CL-XPosure<sup>™</sup> Film, Thermo Fisher Scientific) by chemiluminescence using Pierce ECL or ECL plus substrates (Thermo Fisher Scientific) according to the manufacturer's protocol. TH and TSPO protein expression levels were quantified by the signal intensities using ImageJ and normalized to actin.

### 2.2.9 Statistical Analysis

Data were analyzed with either 2-tailed unpaired t-test (Welch's t-test), one- or two-way analysis of variance followed by Tukey's test (one-way ANOVA) or Holm Sidak test (one- or two-way ANOVA), as mentioned individually. The null hypothesis was rejected at the 0.05 p-value level. Data are presented as mean  $\pm$  SEM.

### 3 Results

Most of the results have been published in:

Translocator protein ligand protects against neurodegeneration in the MPTP mouse model of Parkinsonism.

Gong, Jing\*, Éva M. Szegő\*, Andrei Leonov, Eva Benito, Stefan Becker, Andre Fischer, Markus Zweckstetter, Tiago Outeiro, and Anja Schneider. *Journal of Neuroscience* (2019): 2070-18

\* Contributed equally to this work

#### **3.1 Emapunil protects from dopaminergic neuron loss in the subacute MPTP mouse model of Parkinsonism**

##### **3.1.1 Experimental plan**

To better characterize the potential function of Emapunil and evaluate it as a new therapeutic strategy in PD, we have chosen to use an *in vivo* subacute MPTP mouse model, which mimics many aspects of the disease, including motor deficits, dopaminergic neuron loss and neuroinflammation. Many TSPO ligands were shown to upregulate testosterone production in gonadal tissue (Chung et al. 2013; Le et al. 2014; Verdile et al. 2015), and the increased testosterone level could be a potential risk factor for PD (Garza-Contreras et al. 2017). For instance, gonadectomized male mice showed dopaminergic neuron loss (Khasnavis et al. 2013). In addition, TSPO expression differs between male and female mice (Fairweather et al. 2014). Similar differences in TSPO expression levels were also reported in the brain of *Drosophila* (Lin et al. 2015). Therefore, we chose to study Emapunil effects only in female mice.

The 8 week-old C57BL/ 6J Rj female mice used for this study were randomly divided into 3 groups. Two groups of mice received i.p. injections of 30 mg/kg body weight MPTP on 5 consecutive days. These mice additionally received i.p. injections of either 50mg/kg body weight Emapunil (MPTP + Emapunil group) or DMSO (MPTP + DMSO group) on every second day, starting from the same day as the first MPTP treatment. The control group mice were i.p. injected with only saline and DMSO. Treatment with Emapunil or DMSO was continued until the mice were sacrificed at day 15 after the first MPTP dose (Figure 3.1).

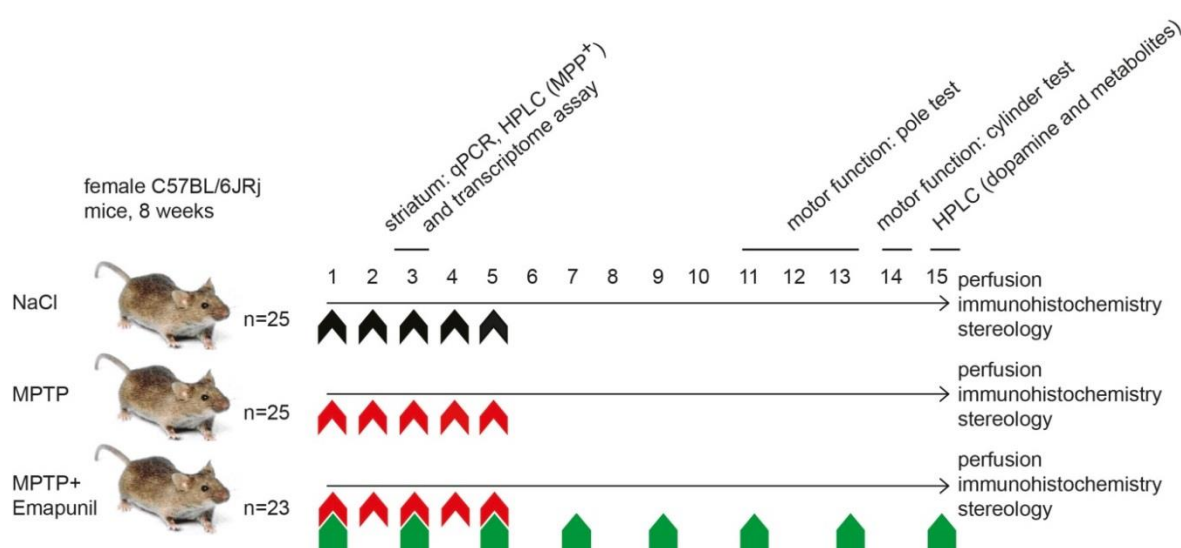


**Figure 3.1 Schematic view of the experimental procedure.**

Top group: NaCl (black color) treated mice, middle group: MPTP (red color) and DMSO treated mice; bottom group: MPTP and Emapunil (green color) treated mice.

### 3.1.2 Emapunil treatment rescues TH- and Nissl- positive neurons from MPTP intoxication

We first evaluated the effects of Emapunil on MPTP induced dopaminergic neuron loss, which resembles the main pathological feature of PD. Tyrosine hydroxylase, which is the key enzyme for catalyzing the rate-limiting step in dopamine biosynthesis, is widely used as a marker for dopaminergic neurons in the CNS (Daubner et al. 2011). At day 15 after the first

MPTP injection, brain slices from 10 mice per group were processed in immunohistochemistry using anti-TH antibody. For each brain, we used thirteen slices among the substantia nigra for stereological quantification of TH- and Nissl- positive neurons (Figure 3.2A). We found that the MPTP + DMSO group showed significantly less TH- positive neurons compared to control group, whereas the loss of TH- positive neurons was significantly prevented by additional Emapunil treatment, which indicates that Emapunil can prevent the MPTP induced dopaminergic neuron loss (Figure 3.2B) (NaCl group =  $21572 \pm 417$ ,  $n = 10$ ; MPTP + DMSO group =  $12047 \pm 246$ ,  $n = 10$ ; MPTP + Emapunil group =  $17547 \pm 391$ ,  $n = 8$ ; one-way ANOVA with Tukey's post hoc test;  $F(2,25) = 192.5$ ,  $p < 0.0001$ ; data are given as means  $\pm$  SEM). To exclude the possibility that the protective effect of Emapunil was caused by up-regulation of TH expression and not by protection of neurons, we also quantified the number Nissl- positive neurons in the substantia nigra, which showed a preservation of neuron counts in the MPTP + Emapunil group compared to the MPTP + DMSO group (Figure 3.2C) (NaCl group =  $27125 \pm 352$ ,  $n = 10$ ; MPTP + DMSO group =  $20258 \pm 401$ ,  $n = 10$ ; MPTP + Emapunil group =  $25662 \pm 423$ ,  $n = 8$ ; one-way ANOVA with Tukey's post hoc test;  $F(2,25) = 90.46$ ,  $p < 0.0001$ ; data are given as means  $\pm$  SEM).

Since MPTP needs to be converted to  $MPP^+$  to exhibit toxicity after crossing the BBB, we further examined whether the protective effect of Emapunil was due to preventing this conversion from MPTP to  $MPP^+$ . We therefore quantified the  $MPP^+$  levels in the striatum by HPLC, which showed no significant differences in the MPTP + DMSO and the MPTP + Emapunil group (HPLC measurements were done by Éva M. Szegő) (Figure 3.2D) ( $MPP^+$  level: MPTP + DMSO group =  $31.13 \pm 2.837$  ng/ml,  $n = 8$ ; MPTP + Emapunil group =  $23.14 \pm 2.3$  ng/ml,  $n = 7$ ; 2-tailed nonparametric Mann-Whitney t-test,  $p = 0.0688$ ; data are given as means  $\pm$  SEM). Taken together, these results suggest that Emapunil protects the dopaminergic neurons from MPTP toxicity.

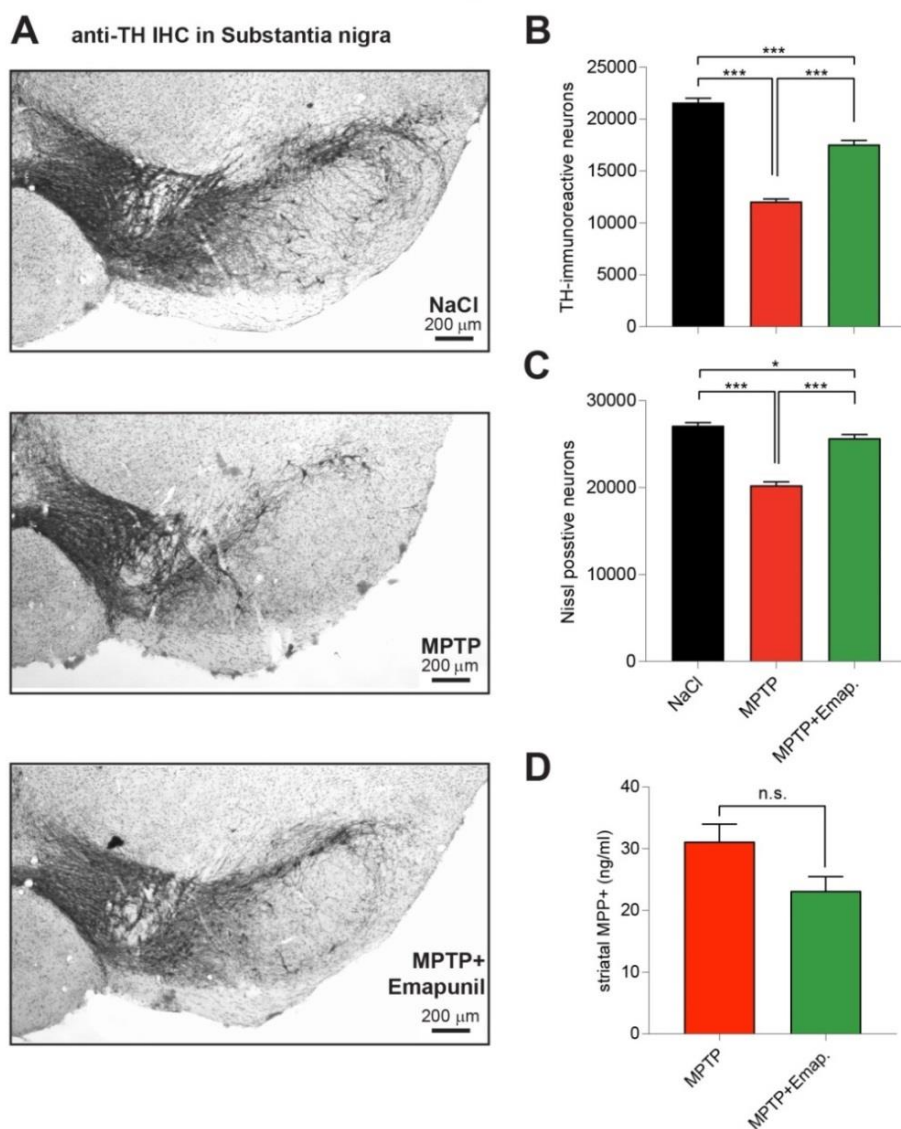


**Figure 3.2 Emapunil rescues TH- and Nissl- positive neurons.**

(A) Representative microscopy images of anti-TH antibody immunohistochemistry. Upper panel: NaCl group; middle panel: MPTP + DMSO group; bottom panel: MPTP + Emapunil group (scale bar = 200  $\mu$ m). Stereological quantification of the number of TH- (B) and Nissl- (C) immunoreactive neurons; one-way ANOVA with Tukey's post hoc test; in between group difference  $P < 0.0001$ . (D) HPLC quantification of MPP<sup>+</sup> levels in striatum from MPTP + DMSO and MPTP + Emapunil groups; 2-tailed nonparametric Mann-Whitney t-test,  $p = 0.0688$ ; All data are given as means + SEM, n.s. = not significant, \* $P < 0.05$ , \*\*\* $P < 0.001$ .

## 3.2 Emapunil improves MPTP-induced motor impairment

After evaluation of the protective effect of Emapunil on dopaminergic neuron survival, we asked whether Emapunil could also improve the motor performance in MPTP-treated animals. To answer this question, we conducted two motor tests.

### 3.2.1 Emapunil treatment improves pole test performance

Firstly, the well-established pole test was used to assess the effects of Emapunil on MPTP induced motor-coordination deficits and bradykinesia. When placing mice on the top of a vertical pole, we recorded the time they used for turning their bodies downward and for climbing down to the ground on day 13 after the first MPTP injection. We found that MPTP + DMSO treated mice needed longer time to turn their heads downward than the saline group, whereas the MPTP + Emapunil group showed no significant difference compared to saline controls (Figure 3.3A) (NaCl group: orientation time =  $1.36 \pm 0.131$  s,  $n = 15$ ; MPTP + DMSO group: orientation time =  $1.545 \pm 0.1008$  s,  $n = 15$ ; MPTP + Emapunil group: orientation time =  $1.152 \pm 0.066$  s,  $n = 13$ ; one-way ANOVA with Tukey's post hoc test; in between group difference  $p = 0.04$ ; data are given as means  $\pm$  SEM). The time to descend from the top of the pole to the ground was also recorded, and MPTP + DMSO treated mice showed a tendency, although not significant, to spend longer time on the pole compared to the control group. MPTP + Emapunil treated mice were faster to reach the ground compared to the MPTP + DMSO treated mice and saline controls (Figure 3.3A) (NaCl group: total time =  $5.27 \pm 0.24$  s,  $n = 15$ ; MPTP + DMSO group: total time =  $5.87 \pm 0.281$  s,  $n = 15$ ; MPTP + Emapunil group: total time =  $4.29 \pm 0.273$  s,  $n = 13$ ; one-way ANOVA with Tukey's post hoc test;  $F(2,40) = 3.366$ ,  $p = 0.004$ ; data are given as means  $\pm$  SEM).

### 3.2.2 Emapunil treatment improves the cylinder test performance

To further assess the effects of Emapunil on motor performance, we performed the cylinder test in the subacute MPTP mouse model. The cylinder test measures sensorimotor coordination and forelimbs usage during free exploratory activity in mice which are placed in a transparent cylinder. It was initially designed to compare motor asymmetry in unilateral CNS lesions (Schallert et al. 2000), but can also be used to study forelimb motor coordination, by evaluating the percentage of free rears with either no, single, or both forelimbs contact to the wall for supporting the body. The cylinder test was previously tested in 6-OHDA (Saal et al. 2015) and MPTP (Tönges et al. 2012) mouse models of Parkinsonism. In this test, 5-minute films were recorded for each mouse when they were freely exploring the cylinder for the first time. The total number of rears was divided into 4 patterns: free rears, rears with either left or right forelimb, and rears with both forelimbs touching the wall and the percentages of each to total rears were calculated.

Mice with MPTP + DMSO treatment showed the highest frequency of rears supported by both forelimbs and the lowest frequency for free rears, which indicated the motor coordination deficiency caused by MPTP. The MPTP + Emapunil treated mice showed a significant higher percentage of free rears and lower percentage of rears with both forelimbs against the wall, when compared to MPTP + DMSO group (Figure 3.3B) (NaCl group: ratio of free rears =  $22.9 \pm 2.37\%$ , ratio of rears with left forelimb =  $4.71 \pm 1.27\%$ , ratio of rears with right forelimb =  $3.48 \pm 0.845\%$ , ratio of rears with both forelimbs =  $68.9 \pm 3.49\%$ , n = 15; MPTP + DMSO group: ratio of free rears =  $13.5 \pm 2.82\%$ , ratio of rears with left forelimb =  $4.07 \pm 0.95\%$ , ratio of rears with right forelimb =  $5.98 \pm 1.37\%$ , ratio of rears with both forelimbs =  $68.9 \pm 3.49\%$ , n = 14; MPTP + Emapunil group: ratio of free rears =  $32 \pm 2.36\%$ , ratio of rears with left forelimb =  $6.79 \pm 0.014\%$ , ratio of rears with right forelimb =  $2.92 \pm$

0.99%, ratio of rears with both forelimbs =  $58.3 \pm 3.66\%$ ,  $n = 13$ ; one-way ANOVA with Tukey's post hoc test; in between group difference: free rears:  $F(2,39) = 12.91$ ,  $p = 0.000108$ ; rears with both forelimbs support:  $F(2,39) = 6.494$ ,  $p = 0.00367$ ; data are given as means  $\pm$  SEM).

In conclusion, Emapunil treatment significantly improves motor behavior in the subacute MPTP mouse model.

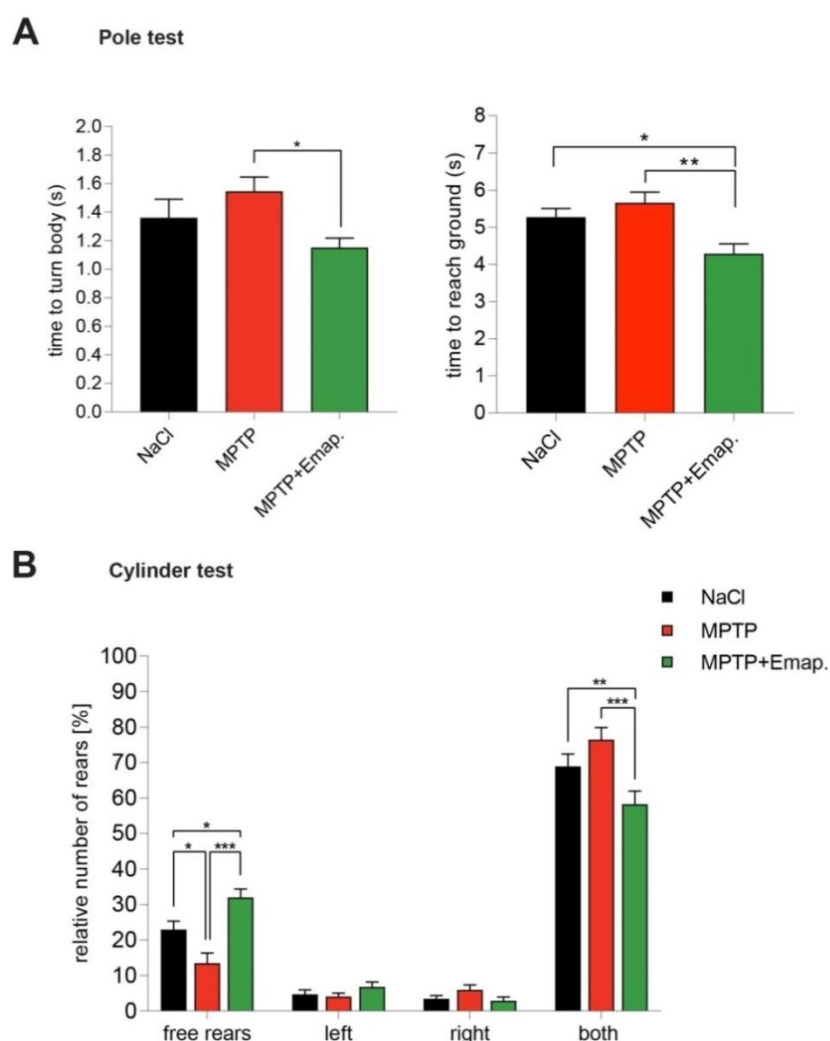


**Figure 3.3 Emapunil restores motor function**

(A) Histograms show the time used for orienting downward and the total time in the pole test for each group. One-way ANOVA with Tukey's post hoc test; in orienting time  $p = 0.04$ , in total time  $p = 0.0024$ ; Data are shown as means  $\pm$  SEM. \* $p < 0.05$ , \*\* $p < 0.01$ . (B) Histogram shows the different patterns mice used during rearing, either with both forelimbs touching the wall for supporting, with only left or right or no forelimb support. One-way ANOVA with Tukey's post hoc test, in free rears  $p = 0.000108$ , in rears with both forelimbs support  $p = 0.00367$ ; data are shown as means  $\pm$  SEM. \* $p < 0.05$ , \*\* $p < 0.01$ , \*\*\* $p < 0.001$ .

### 3.3 Emapunil attenuates alterations of dopamine and its metabolites induced by MPTP toxicity *in vivo*

We next analyzed the effects of Emapunil on the dopamine metabolism at nerve terminals in the striatum by quantifying the levels of dopamine and its metabolites using HPLC. Dopamine is synthesized from tyrosine and serves as an important neurotransmitter. After re-uptake into dopaminergic neurons, it is metabolized to 3,4-Dihydroxyphenylacetic acid (DOPAC) by monoamine oxidase (MAO), which can be further degraded into homovanillic acid (HVA) by COMT in glial cells. Alternatively, dopamine can be directly taken up by glial cells and first degraded to 3-methoxytyramine (3-MT) by catechol-O-methyl transferase (COMT), and 3-MT can be further degraded to HVA by MAO (Figure 3.4) (Winner et al. 2017; Meiser et al. 2013). Therefore, DOPAC and HVA are two major metabolites of dopamine (Juárez Olguín et al. 2016).

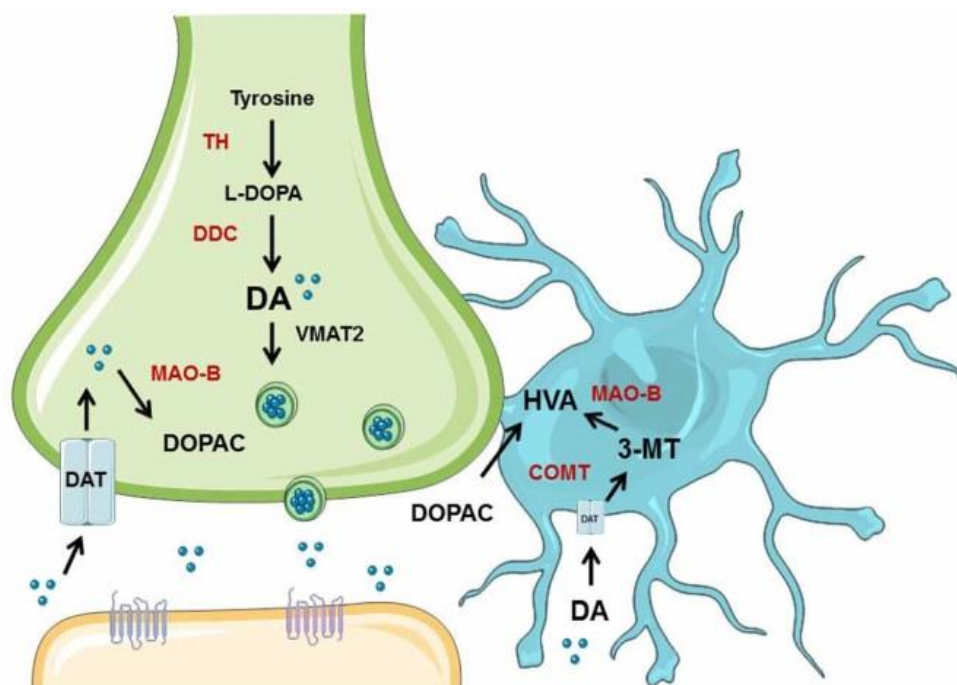


**Figure 3.4 Overview of dopamine synthesis and metabolism.**

Figure is adapted from (Winner et al. 2017)

## Results

To explore the effects of Emapunil in dopamine metabolism, we quantified dopamine, DOPAC and HVA in the striatum from five mice per group at day 3 using HPLC. The results showed that the striatal dopamine levels in MPTP treated mice were significantly lower compared to saline controls, indicating loss of axonal dopamine stores. This reduction was significantly attenuated by Emapunil treatment. Furthermore, we assessed the dopamine metabolic ratio [(HVA + DOPAC)/dopamine], which is an important indicator for oxidative stress. We found that the metabolic ratio was significantly higher in the MPTP + DMSO group compared to saline controls, indicative of a predominantly glial dopamine metabolism and consistent with dopaminergic nerve terminal loss. In contrast, the MPTP + Emapunil treated mice show a significant lower metabolism ratio to a comparable level with saline controls (HPLC analysis was done by Éva M. Szegő) (Figure 3.5) (NaCl group: dopamine =  $8.444 \pm 0.691$  ng/mg, DOPAC =  $7.144 \pm 0.2925$  ng/mg, metabolic ratio =  $1.934 \pm 0.1684$ , n = 5; MPTP + DMSO group: dopamine =  $3.293 \pm 0.3095$  ng/mg, DOPAC =  $5.534 \pm 0.3939$  ng/mg, metabolic ratio =  $3.743 \pm 0.3718$ , n = 5; MPTP + Emapunil group: dopamine =  $5.581 \pm 0.4028$  ng/mg, DOPAC =  $6.691 \pm 0.4018$  ng/mg, metabolic ratio =  $2.304 \pm 0.1942$ , n = 5; one-way ANOVA with Tukey's post hoc test; in between group difference: dopamine p < 0.0001, DOPAC p = 0.02, metabolic ratio p = 0.0008; data are given as means  $\pm$  SEM). Taken together, these data indicate that Emapunil may preserve nigrostriatal innervation by protecting dopaminergic terminals.

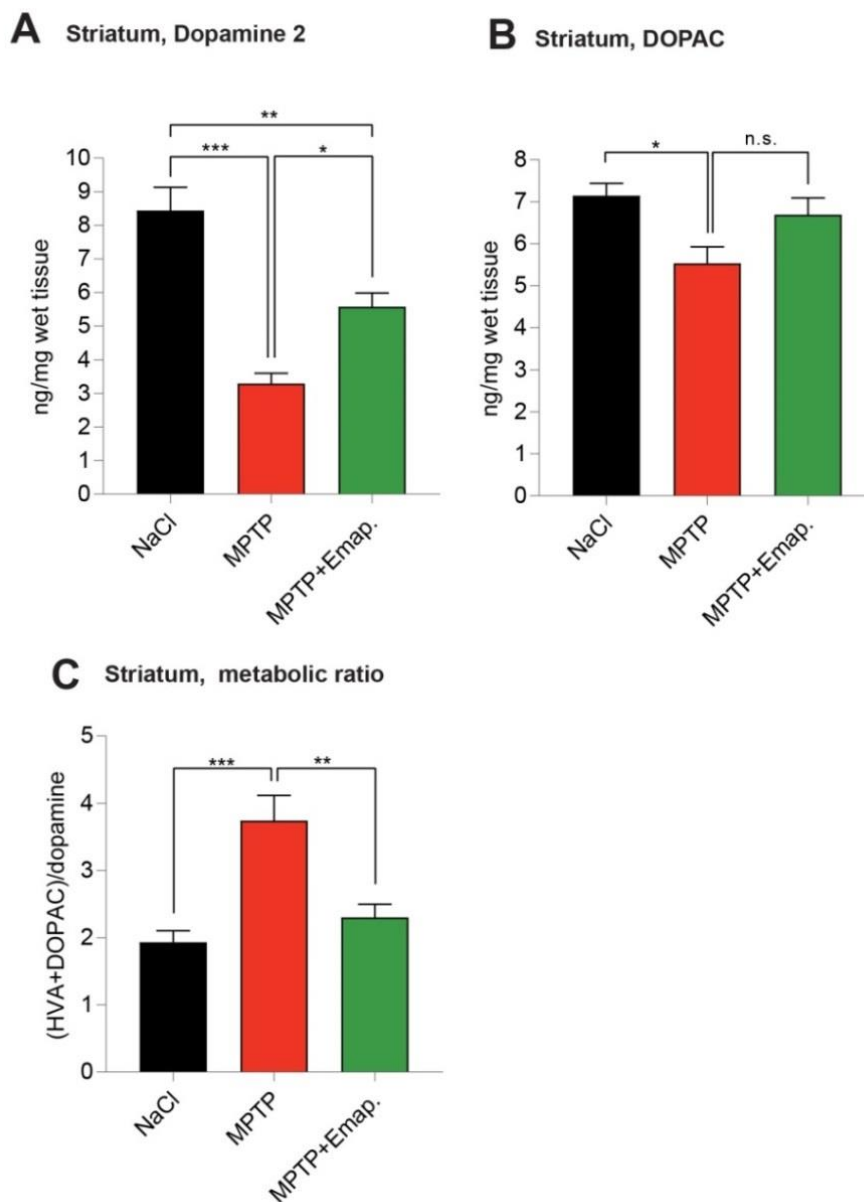


**Figure 3.5 Levels of dopamine and its metabolites analyzed by HPLC**

Levels of dopamine, DOPAC and HVA in the striatum were measured from 5 mice per group at day 3 using HPLC (A) Dopamine levels; (B) DOPAC levels; (C) Metabolic ratios of (HVA + DOPAC)/dopamine. Data are shown as means + SEM; one-way ANOVA with Tukey's post hoc test; in between group difference:  $p < 0.0001$  (dopamine),  $p = 0.02$  (DOPAC),  $p = 0.0008$  (metabolic ratio); n.s. = not significant; \* $p < 0.05$ , \*\* $p < 0.01$ , \*\*\* $p < 0.001$ .

### 3.4 Emapunil ameliorates IRE1 $\alpha$ /XBP1 pathway activation

Numerous studies have shown that endoplasmic reticulum (ER) stress is induced upon MPTP treatment, which leads to the activation of unfolded protein response (UPR) signaling pathways (Kuo et al. 2016). The inositol-requiring enzyme 1  $\alpha$  (IRE1 $\alpha$ )/X-box binding protein 1 (XBP1) pathway is the most conserved UPR signaling pathway, which was also reported to be activated in the subacute MPTP mouse model (Sado et al. 2009a). We assessed *Xbp1s/Xbp1* mRNA ratio *in vivo* by qPCR from striatum at day 3. MPTP + DMSO treated mice showed significantly higher levels of active *XBP1s* mRNA and *XBP1s/Xbp1* mRNA ratio compared to saline controls, whereas additional treatment with Emapunil restored *XBP1s* mRNA and *XBP1s/Xbp1* mRNA ratio to a comparable level with control group (qPCR was done by Éva M. Szegő) (Figure 3.6) (NaCl group were normalized to 1: *Xbp1* =  $1 \pm 0.02093$ , spliced *XBP1s* =  $1 \pm 0.045$ , ratio =  $1 \pm 0.0473$ , n = 5; MPTP + DMSO group: *Xbp1* =  $0.88 \pm 0.067$ , spliced *XBP1s* =  $1.35 \pm 0.0527$ , ratio =  $1.57 \pm 0.155$ , n = 5; MPTP + Emapunil group: *Xbp1* =  $0.904 \pm 0.05349$ , spliced *XBP1s* =  $0.896 \pm 0.036$ , ratio =  $1.01 \pm 0.0834$ , n = 5; one-way ANOVA with Tukey's post hoc test; in between group difference: *Xbp1* p = 0.2532, spliced *Xbp1s* p < 0.0001, ratio *Xbp1s/Xbp1* p = 0.003151; data are given as means  $\pm$  SEM).

The expression of TSPO is mainly in microglia during inflammation. However, the restoration effect of Emapunil on *XBP1s* activation requires the expression of TSPO in neurons, which has never been tested before. As shown in Figure 3.7, we confirmed that TSPO is also expressed in dopaminergic neurons by co-staining of mouse substantia nigra (SN) brain sections with antibodies against TSPO and TH.

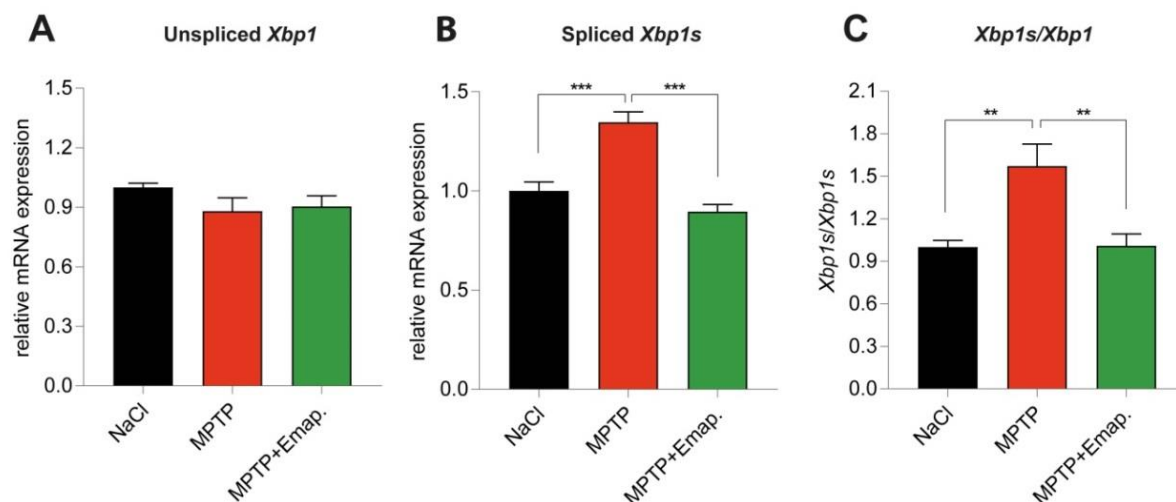


**Figure 3.6 Emapunil treatment mitigates *XBPIs* mRNA increase**

(A) Unspliced *Xbp1* mRNA expression level; (B) spliced *XBPIs* mRNA expression level; (C) ratio of *XBPIs/Xbp1* mRNA expression normalized to control group; in between-group difference: *Xbp1p* = 0.2532, spliced *Xbp1s*  $p < 0.0001$ , and ratio *Xbp1s/Xbp1*  $p = 0.003151$ ; one-way ANOVA with Tukey's post hoc test; \*\* $p < 0.01$ , \*\*\* $p < 0.001$ .

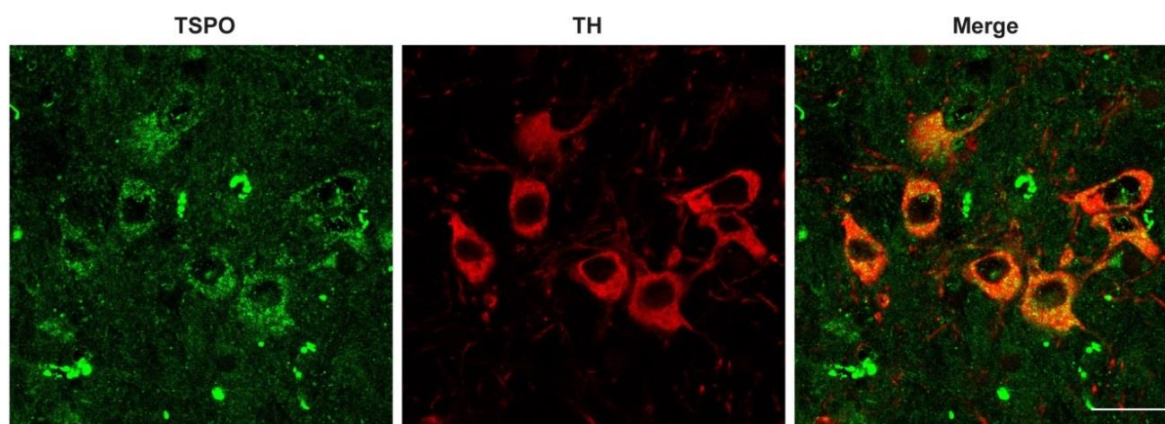


**Figure 3.7 Co-immunofluorescence staining against TSPO and TH in SN**

Substantia nigra sections from control mice were co-immunofluorescence stained against TSPO (left, green color), and TH (middle, red color). The merged image is shown in the right panel, scale bar = 20  $\mu\text{m}$ .

## 3.5 The effects of Emapunil on XBP1s activation depend on TSPO

### 3.5.1 TSPO expression in LUHMES cells

To further study the effects of Emapunil on dopaminergic neurons *in vitro*, we utilized the human dopaminergic neuronal cell line LUHMES (Lotharius et al. 2002). First, the differentiated post-mitotic LUHMES cells were identified by immunostaining against TH and beta-III-tubulin, indicating dopaminergic neurons features (Figure 3.8A). We also confirmed the expression of TSPO in LUHMES cells by co-staining with antibodies against TSPO and beta-III-tubulin (Figure 3.8B).

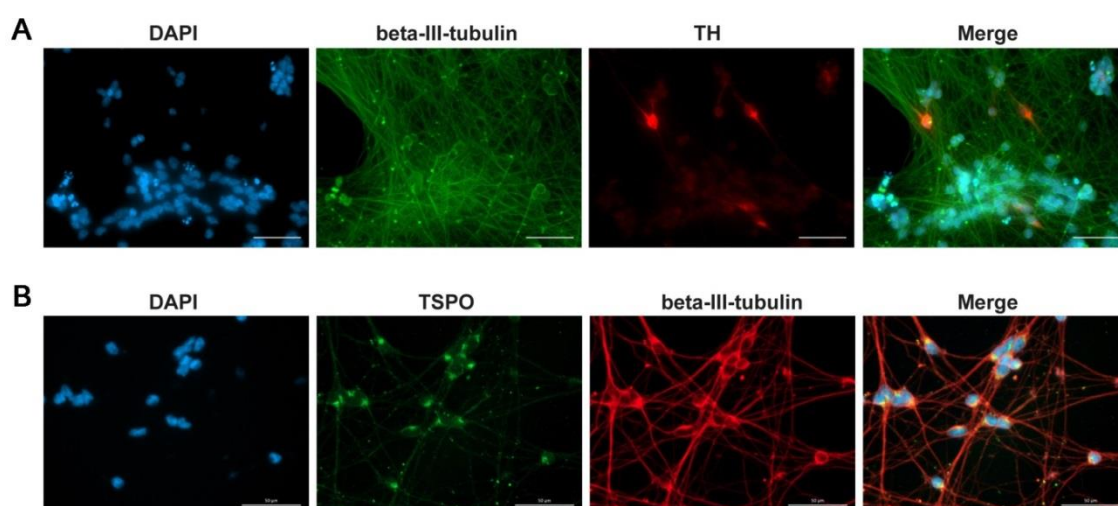


**Figure 3.8 TSPO is expressed in differentiated LUHMES cells**

(A) LUHMES cells were co-stained against beta-III-tubulin (left, green color) and TH (middle, red color); (B) co-immunofluorescence staining against TSPO (left, green color) and beta-III-tubulin (middle, red color). Merged image is in the right panel, scale bar = 20  $\mu$ m.

### 3.5.2 Emapunil ameliorates MPP<sup>+</sup> and rotenone toxicity and ER stress in LUHMES cells

We then quantified cell viability by measuring the released adenylate kinase from cells using ToxiLight assay. LUHMES cells were treated with either MPP<sup>+</sup> or rotenone to induce

## Results

oxidative stress 12 h after Emapunil treatment at day 7 of differentiation (Krug et al. 2014; Giordano et al. 2012). After 24 h incubation, the supernatants were collected for cytotoxicity measurement. LUHMES cells that were exposed to  $\text{MPP}^+$  or rotenone showed significantly increased adenylate kinase compared to DMSO treated control cells, indicating reduced viability and survival rate. The  $\text{MPP}^+$  or rotenone toxicity was markedly ameliorated with Emapunil treatment, which is in line with our *in vivo* results (Figure 3.9A) (DMSO group were normalized to 1: Fold change (FC) =  $1 \pm 0.06748$ ,  $n = 31$ ; DMSO + 5  $\mu\text{M}$  Emapunil group: FC =  $1.216 \pm 0.08$ ,  $n = 31$ ; 10  $\mu\text{M}$   $\text{MPP}^+$  + DMSO group: FC =  $4.877 \pm 0.4397$ ,  $n = 17$ ; 10  $\mu\text{M}$   $\text{MPP}^+$  + 5  $\mu\text{M}$  Emapunil group: FC =  $4.024 \pm 0.3168$ ,  $n = 17$ ; 10  $\mu\text{M}$  rotenone + DMSO group: FC =  $5.624 \pm 0.2506$ ,  $n = 14$ ; 10  $\mu\text{M}$  rotenone + Emapunil group: FC =  $4.042 \pm 0.0871$ ,  $n = 14$ ; in between group difference  $F(2, 118) = 9.856$ ,  $p < 0.0001$ ; two-way ANOVA with Holm Sidak post hoc test; data are given as means  $\pm$  SEM).

Next, we investigated the ratios of *XBPIs*/*XBPI* mRNA expression levels under rotenone induced oxidative stress using qPCR. In accordance with our *in vivo* results with MPTP treated mice, rotenone treatment in LUHMES cells dramatically increased the *XBPIs*/*XBPI* ratio compared to DMSO controls. In contrast, additional Emapunil treatment significantly attenuated the *XBPIs*/*XBPI* ratio, as did the IRE1 $\alpha$ /XBPI inhibitor toyocamycin (Tanabe et al. 2018). Toyocamycin treatment showed lower *XBPIs*/*XBPI* ratio compared to the DMSO treated controls. Notably, there was no additive effect of combined Emapunil and toyocamycin treatment in rotenone exposed cells, which indicates that the protective effect of Emapunil is indeed mediated through the IRE1 $\alpha$ /XBPI pathway. In addition, neither Emapunil nor toyocamycin treatment alone resulted in *XBPIs* alterations in LUHMES cell culture (Figure 3.9B) (Vehicle group were normalized to 1: *XBPI* =  $1 \pm 0.106$ , *XBPIs* =  $1 \pm 0.132$ , ratio =  $1 \pm 0.041$ ,  $n = 9$ ; rotenone group: *XBPI* =  $9.23 \pm 3.41$ , *XBPIs* =  $67.7 \pm 22.6$ ,

ratio =  $8.47 \pm 1$ ,  $n = 9$ ; Toyocamycin group:  $XBPI = 0.681 \pm 0.181$ ,  $XBPIs = 0.607 \pm 0.171$ , ratio =  $0.896 \pm 0.102$ ,  $n = 9$ ; Emapunil group:  $XBPI = 0.679 \pm 0.197$ ,  $XBPIs = 0.68 \pm 0.197$ , ratio =  $1.02 \pm 0.0424$ ,  $n = 9$ ; Toyocamycin + Emapunil group:  $XBPI = 0.879 \pm 0.212$ ,  $XBPIs = 0.823 \pm 0.199$ , ratio =  $0.93 \pm 0.0884$ ,  $n = 9$ ; rotenone + toyocamycin group:  $XBPI = 0.969 \pm 0.175$ ,  $XBPIs = 1.23 \pm 0.188$ , ratio =  $1.46 \pm 0.264$ ,  $n = 9$ ; rotenone + Emapunil group:  $XBPI = 0.599 \pm 0.167$ ,  $XBPIs = 0.756 \pm 0.173$ , ratio =  $1.58 \pm 0.252$ ,  $n = 9$ ; rotenone + toyocamycin + Emapunil group:  $XBPI = 1.41 \pm 0.404$ ,  $XBPIs = 2.2 \pm 0.724$ , ratio =  $1.48 \pm 0.14$ ,  $n = 9$ ; one-way ANOVA with Tukey's post hoc test; in between group difference  $XBPI$ :  $F(7, 64) = 5.835$ ,  $p < 0.0001$ ,  $XBPIs$ :  $F(7, 64) = 8.645$ ,  $p < 0.0001$ , ratio:  $F(7, 64) = 45.43$ ,  $p < 0.0001$ ; data are given as means  $\pm$  SEM).

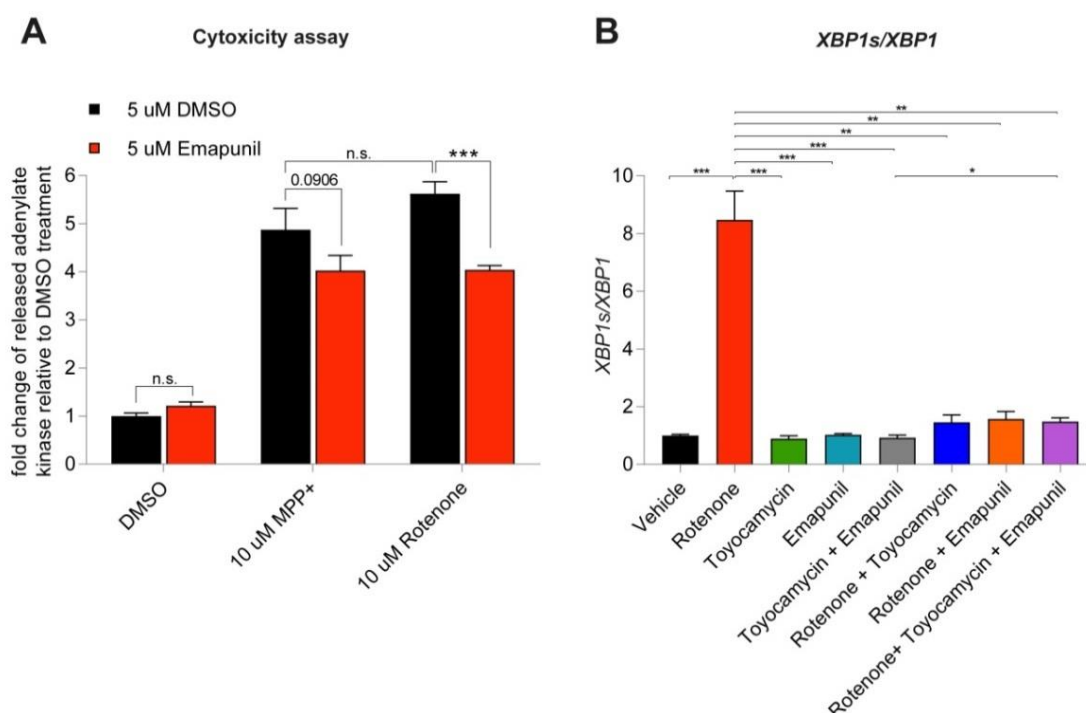


**Figure 3.9 Cytotoxicity and ER stress were attenuated by Emapunil**

(A) LUHMES cells ToxiLight Cytotoxicity assay results. Cells were treated with either MPP<sup>+</sup> or rotenone, with/without additional Emapunil treatment. Control cells were treated with DMSO as solvent control. Data are shown as means + SEM, Two-way ANOVA with Holm Sidak post hoc test,  $p < 0.0001$ , \* $p < 0.05$ , \*\*\* $p < 0.001$ ; (B) Ratio of  $XBPIs/XBPI$  in Luhmes cells of different treatment groups. Data are shown as means + SEM; one-way ANOVA with Tukey's post hoc test, in between group difference  $p < 0.0001$ . \*\* $p < 0.01$ , \*\*\* $p < 0.001$ .

### 3.5.3 siRNA mediated TSPO down-regulation in LUHMES cells

To investigate whether the protective effects of Emapunil observed in MPP<sup>+</sup> and rotenone treated LUHMES cells were mediated by TSPO, we performed siRNA mediated TSPO downregulation. We first quantified the expression level of *TSPO* mRNA in LUHMES cells by qPCR, which showed a ~ 60% reduction in TSPO siRNA treated cells compared to control cells (Figure 3.10A) (TSPO siRNA group: TSPO =  $0.417 \pm 0.027$ , n = 9; control siRNA group were normalized to 1: TSPO =  $1 \pm 0.029$ , n = 9; 2-tailed Welch's t-test, in between group difference p = 0.0048; data are given as means  $\pm$  SEM). Also, the expression level of TSPO protein was reduced to ~ 45% compared to control cells as determined by western blot, while TH protein expression was not affected (Figure 3.10B,C,D) (TSPO siRNA group: TSPO =  $0.445 \pm 0.067$ , TH =  $0.897 \pm 0.096$ , n = 3; control siRNA group were normalized to 1: TSPO =  $1 \pm 0.071$ , TH =  $1 \pm 0.048$ , n = 3; 2-tailed Welch's t-test, in between group difference p = 0.412; data are given as means  $\pm$  SEM).

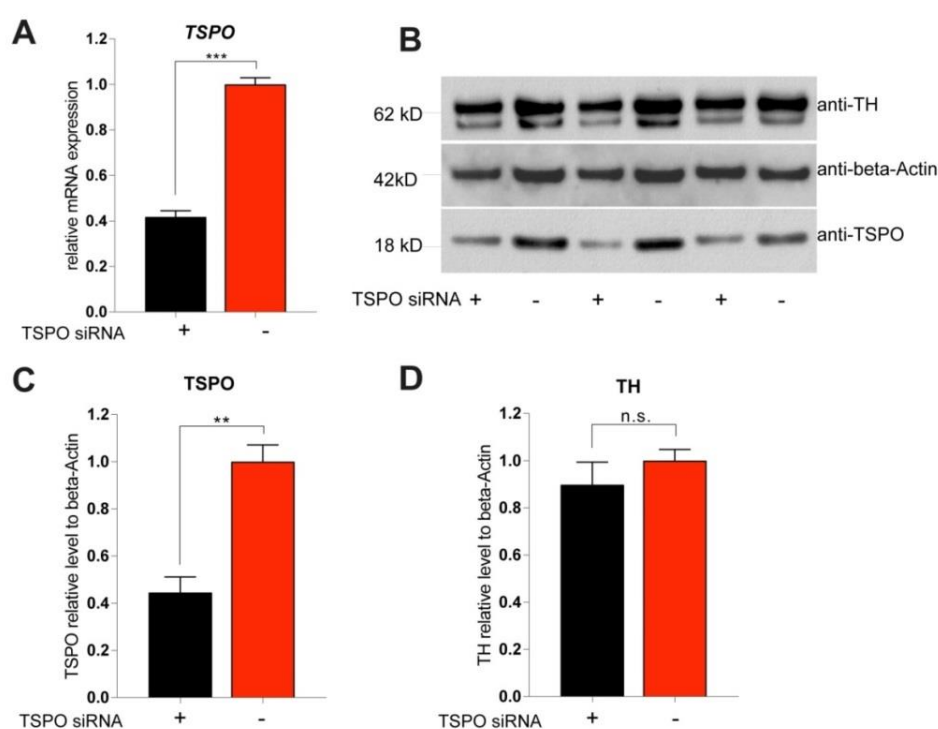


**Figure 3.10** siRNA mediated downregulation of TSPO

(A) *TSPO* mRNA quantification in LUHMES cells after *TSPO* or control siRNA treatment; (B) Representative western blot of *TSPO*, beta-Actin and TH in LUHMES cells treated with either *TSPO* or control siRNA; (C) Quantification of *TSPO* protein levels normalized to beta-Actin from (B), data are shown as means + SEM, 2-tailed Welch's t-test,  $p = 0.0048$ ;  $**p < 0.005$ ; (D) TH protein quantification normalized to beta-Actin from (B), data are shown as means + SEM, 2-tailed Welch's t-test,  $p = 0.412$ ; n.s. = not significant.

### 3.5.4 Emapunil effects on cell viability and *XBPIs* activation are *TSPO* dependent

Next, we investigated whether the protective effects of Emapunil observed in MPP<sup>+</sup> and rotenone treated LUHMES cells were *TSPO* dependent. We performed ToxiLight assays in rotenone treated LUHMES cells either transfected with *TSPO* or control siRNA. In control siRNA transfected cells, Emapunil ameliorated the cytotoxicity induced by rotenone to a similar level as in the DMSO treated control. In contrast, the rescue effect of Emapunil was compromised in *TSPO* siRNA transfected cells (Figure 3.11A) (Groups transfected with control siRNA: Fold change (FC) in the DMSO group was normalized to  $1 = 1 \pm 0.026$ ,  $n = 8$ ; FC in the DMSO + 10  $\mu$ M rotenone group =  $3.682 \pm 0.345$ ,  $n = 8$ ; FC in the 5  $\mu$ M Emapunil + DMSO group =  $1.37 \pm 0.114$ ,  $n = 8$ ; FC in the 5  $\mu$ M Emapunil + 10  $\mu$ M rotenone group =  $1.61 \pm 0.152$ ,  $n = 8$ ; Groups transfected with *TSPO* siRNA: FC in the DMSO group was normalized to  $1 = 1.165 \pm 0.0768$ ,  $n = 8$ ; FC in the DMSO + 10  $\mu$ M rotenone group =  $4.293 \pm 0.357$ ,  $n = 8$ ; FC in the 5  $\mu$ M Emapunil + DMSO group =  $1.385 \pm 0.135$ ,  $n = 8$ ; FC in the 5  $\mu$ M Emapunil + 10  $\mu$ M rotenone group =  $2.908 \pm 0.324$ ,  $n = 8$ ; in between group difference  $F(3, 55) = 3.365$ ,  $p = 0.0251$ ; two-way ANOVA with Tukey post hoc test; data are given as means  $\pm$  SEM). Taken together, we confirmed that the protective effects of Emapunil in LUHMES cells depend on the presence of *TSPO*.

Strikingly, we did not find significant differences between *TSPO* siRNA and control siRNA treated LUHMES cells when exposed to rotenone. We suspected that the toxicity of rotenone

may already have reached maximum effects at the 10  $\mu$ M concentration. Therefore, we performed rotenone titration experiments as shown in Figure 3.11B. Indeed, the maximum toxicity of rotenone was detected at 10  $\mu$ M and did not further increase with higher rotenone concentrations (FC in the DMSO group =  $1 \pm 0.00554$ ,  $n = 6$ ; FC in the 0.5  $\mu$ M rotenone group =  $4.18 \pm 0.195$ ,  $n = 6$ ; FC in the 1  $\mu$ M rotenone group =  $4.55 \pm 0.189$ ,  $n = 6$ ; FC in the 2.5  $\mu$ M rotenone group =  $6.028 \pm 0.229$ ,  $n = 8$ ; FC in the 5  $\mu$ M rotenone group =  $7.246 \pm 0.104$ ,  $n = 8$ ; FC in the 10  $\mu$ M rotenone group =  $8.559 \pm 0.259$ ,  $n = 8$ ; FC in the 20  $\mu$ M rotenone group =  $8.518 \pm 0.317$ ,  $n = 8$ ; one-way ANOVA with Tukey post hoc test; in between group difference  $F(6, 42) = 95.5$ ,  $p < 0.0001$ ; data are given as means  $\pm$  SEM).

Next, to further investigate whether ER stress mitigation by Emapunil is also TSPO dependent, we quantified *XBPIs/XBPI* mRNA ratio by qPCR in rotenone exposed LUHMES cells with additional TSPO or control siRNA treatment. We found that with TSPO siRNA treatment, the ratios of *XBPIs/XBPI* did not significantly differ between the Rotenone + Emapunil group and the Rotenone + DMSO group. This further verified that the Emapunil effects on mitigating ER stress were mediated by TSPO (Figure 3.12) (Fold Change (FC) in the DMSO with control siRNA group =  $1 \pm 0.029$ ,  $n = 12$ ; FC in the DMSO with TSPO siRNA group =  $1.022 \pm 0.069$ ,  $n = 12$ ; FC in the DMSO + 10  $\mu$ M rotenone with control siRNA group =  $3.66 \pm 0.245$ ,  $n = 12$ ; FC in the DMSO + 10  $\mu$ M rotenone with TSPO siRNA group =  $3.178 \pm 0.204$ ,  $n = 12$ ; FC in the 5  $\mu$ M Emapunil + DMSO with control siRNA group =  $0.955 \pm 0.03$ ,  $n = 12$ ; FC in the 5  $\mu$ M Emapunil + DMSO with TSPO group =  $1.141 \pm 0.153$ ,  $n = 12$ ; FC in the 5  $\mu$ M Emapunil + 10  $\mu$ M rotenone with control siRNA group =  $1.573 \pm 0.14$ ,  $n = 12$ ; FC in the 5  $\mu$ M Emapunil + 10  $\mu$ M rotenone with TSPO group =  $2.515 \pm 0.246$ ,  $n = 12$ ; in between group difference  $F(3, 88) = 6.931$ ,  $p = 0.0003$ ; two-way ANOVA with Tukey post hoc test; data are given as means  $\pm$  SEM).

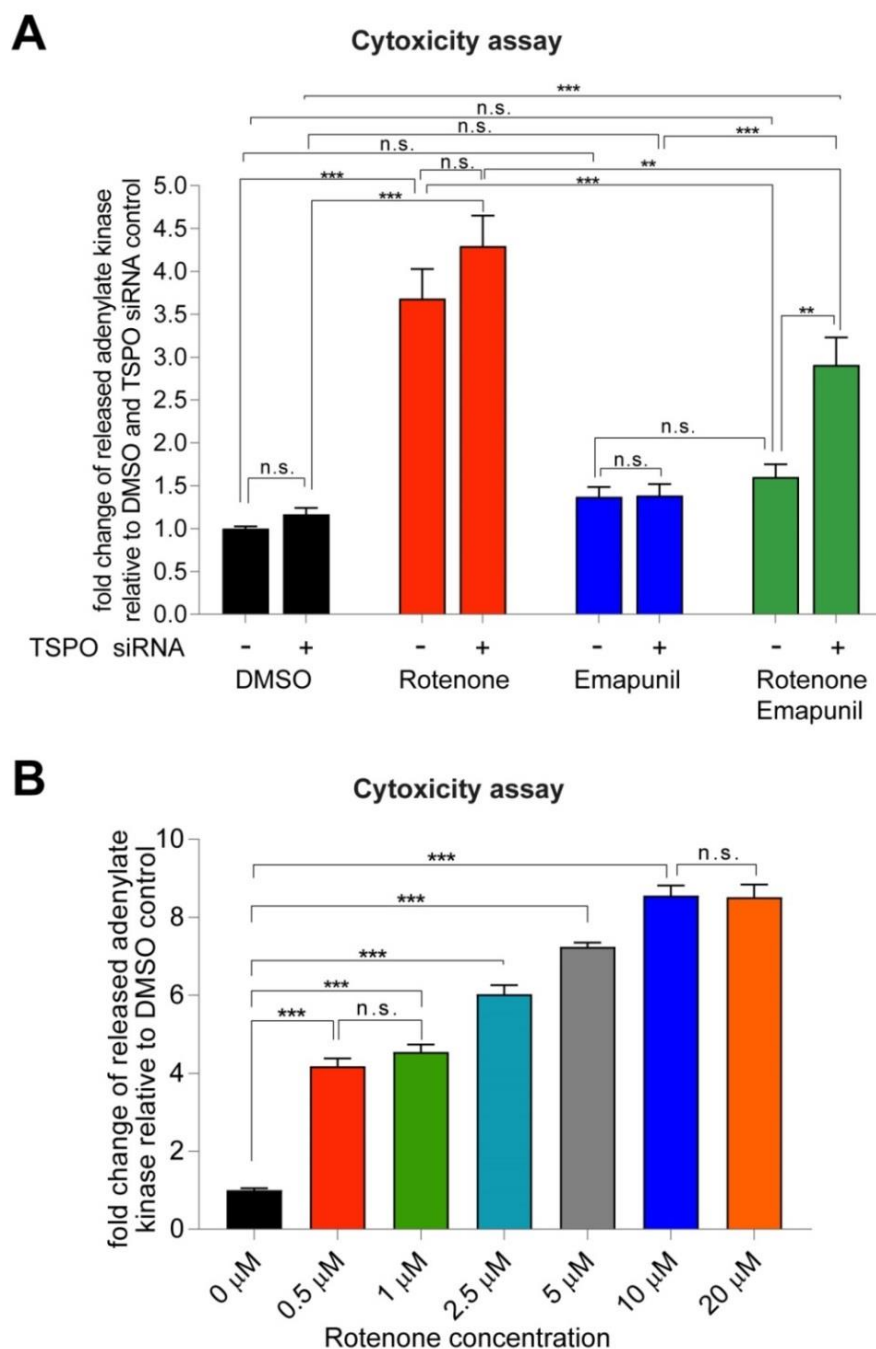


**Figure 3.11 Emapunil protects from rotenone toxicity in a TSPO dependent manner**

(A) ToxiLight cytotoxicity assay in LUHMES cells transfected with either TSPO or control siRNA. Data are shown as means + SEM; Two-way ANOVA with Tukey post hoc test,  $F(3, 55) = 3.365$ ,  $p = 0.0251$ ; \*\* $p < 0.005$ ; \*\*\* $p < 0.001$ ; n.s. = not significant; (B) Rotenone toxicity titration in LUHMES cells. Data are shown as means + SEM, one-way ANOVA with Tukey post hoc test; in between group difference  $F(6, 42) = 95.5$ ,  $p < 0.0001$ ; \*\*\* $p < 0.001$ ; n.s. = not significant.

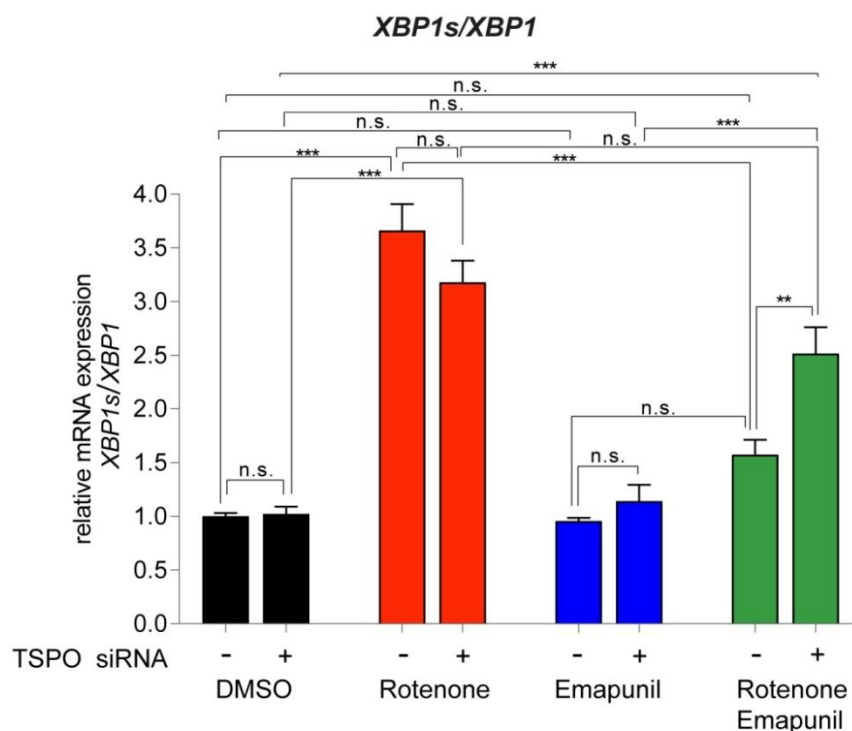


**Figure 3.12 Emapunil mitigates ER stress mediated by TSPO in LUHMES**

The ratios of *XBP1s/XBP1* mRNA expression were quantified by qPCR analysis in LUHMES cells treated with TSPO or control siRNA. Data are shown as means + SEM, Two-way ANOVA with Tukey post hoc test,  $F(3, 88) = 6.931$ ,  $p = 0.0003$ ; n.s. = not significant; \*\* $p < 0.005$ ; \*\*\* $p < 0.001$ .

### 3.6 Emapunil inhibits microgliosis and astrogliosis *in vivo*

In previous studies, neuroprotective effects of TSPO ligands were mediated by anti-inflammatory modulation of microglia, including EAE mouse model and retinal degeneration model (Karlstetter et al. 2014; Scholz et al. 2015; Ravikumar et al. 2016). We thus asked whether Emapunil also provided anti-neuroinflammatory effects in the subacute MPTP mouse model. To this end, we first quantified striatal microgliosis and astrogliosis by immunofluorescence from mice sacrificed at day 15. Three sections containing the striatum per brain were stained with antibodies against IBA1 and GFAP, respectively. The number of IBA1 positive cells per area in the striatum was significantly increased in mice exposed to

MPTP, whereas additional Emapunil treatment showed lower microglia numbers compared to the MPTP + DMSO group and did not significantly differ from the NaCl control group. Similarly, the number of astrocytes was dramatically increased in the MPTP + DMSO group compared to the NaCl controls. However, Emapunil treatment slightly (but significantly) attenuated the astrogliosis, which suggests that Emapunil may only have limited impacts on astrocytes. Because we did not perform longitudinal analysis, we cannot exclude that astrogliosis may need longer recovery time than microgliosis (Figure 3.13) (NaCl group: IBA1 positive cells =  $180.4 \pm 4.125/\text{mm}^2$ ,  $n = 9$ ; GFAP positive cells =  $1.152 \pm 0.1288/\text{mm}^2$ ,  $n = 6$ ; MPTP + DMSO group: IBA1 positive cells =  $234.7 \pm 4.813/\text{mm}^2$ ,  $n = 10$ ; GFAP positive cells =  $133.7 \pm 4.283/\text{mm}^2$ ,  $n = 7$ ; MPTP + Emapunil group: IBA1 positive cells =  $190.8 \pm 6.627/\text{mm}^2$ ,  $n = 8$ ; GFAP positive cells =  $109.4 \pm 3.438/\text{mm}^2$ ,  $n = 6$ ; one-way ANOVA with Tukey's post hoc test; in between group difference IBA1-positive cells:  $F(2,158) = 33.19$ ,  $p < 0.0001$ ; GFAP positive cells  $F(2,111) = 446.5$ ,  $p < 0.0001$ ; data are given as means  $\pm$  SEM).

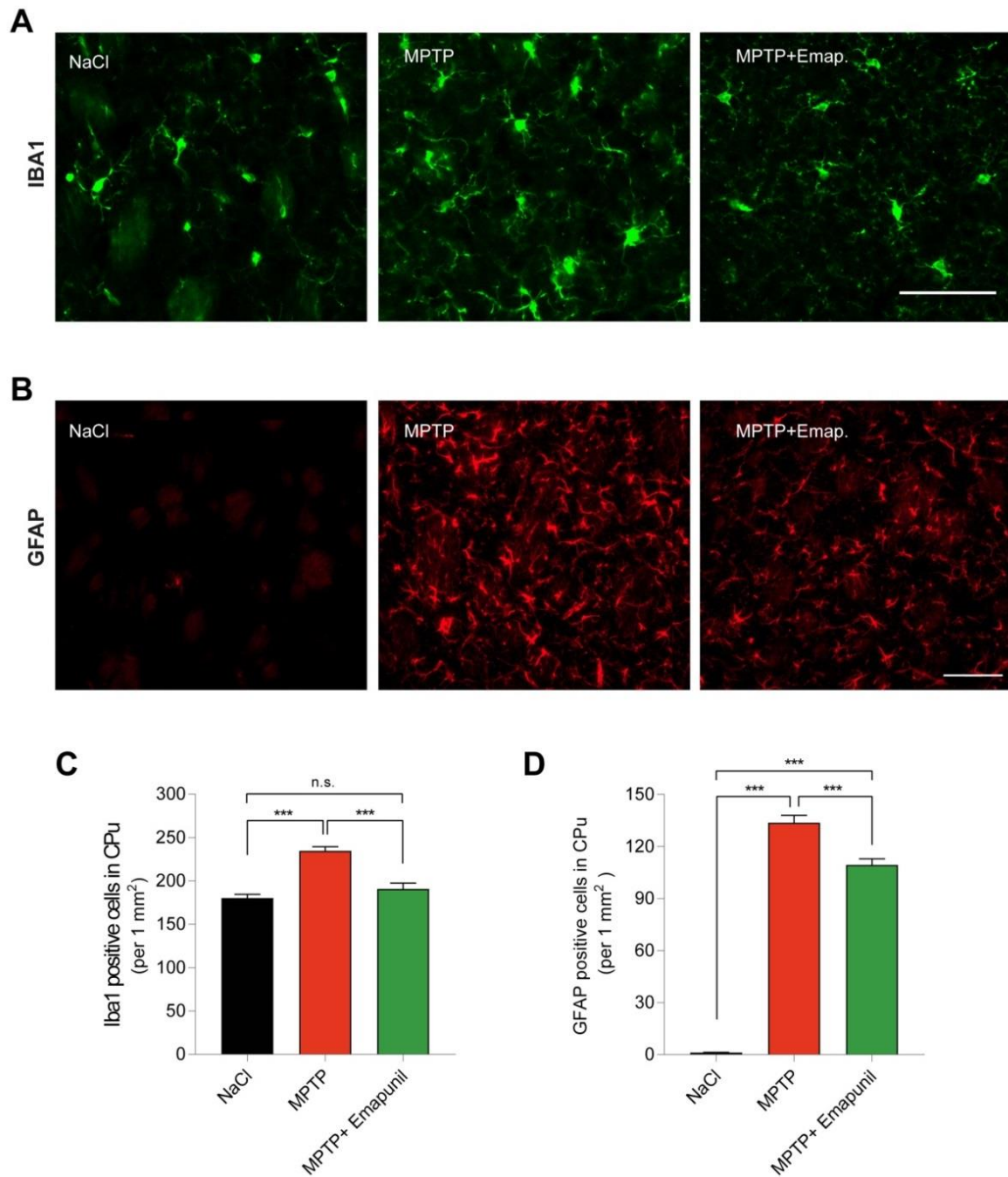


**Figure 3.13 Microgliosis and astrogliosis were attenuated by Emapunil**

Representative immunofluorescence images for Iba1<sup>+</sup> microglia (**A**) and GFAP<sup>+</sup> astrocytes (**B**) from striatal tissues at day 15 in DMSO, MPTP and MPTP + Emapunil treated mice. Quantification results of IBA1+ microglia (**C**) and GFAP+ astrocytes (**D**) from (**A**) and (**B**). Data represents total numbers/mm<sup>2</sup> and are shown as means + SEM; one-way ANOVA with Tukey's post hoc test; IBA1-positive cells:  $F(2,158) = 33.19$ ,  $p < 0.0001$ ; GFAP positive cells  $F(2,111) = 446.5$ ,  $p < 0.0001$ ; n.s. = not significant; \*\*\* $p < 0.001$ ; Scale bars = 50  $\mu$ m (**A**) and 100  $\mu$ m (**B**).

### 3.7 Emapunil induces a shift from pro- to anti-inflammatory microglia activation state

Next, we quantified striatal *Iba1* and *Tspo* mRNA expression levels by qPCR from mice sacrificed at day 3 (qPCR was done by Éva M. Szegő). We found that *Iba1* mRNA level was significant higher in the MPTP + DMSO group compared with controls, whereas no significant differences were found between the MPTP + DMSO and the MPTP + Emapunil group (Figure 3.14A) (The NaCl group was normalized to 1: *Iba1* FC =  $1 \pm 0.1763$ ; MPTP + DMSO group: *Iba1* FC =  $5.633 \pm 0.6228$ ; MPTP + Emapunil group: *Iba1* FC =  $6.842 \pm 1.015$ , n = 5; one-way ANOVA with Tukey's post hoc test; in between group difference  $F(2,12) = 19.68$ , p = 0.000163; data are given as means  $\pm$  SEM). *Tspo* mRNA level was also increased in the MPTP + DMSO group but not in the MPTP + Emapunil or the control group. Because TSPO is known to be upregulated in activated microglia, it indicates less inflammatory activity in the MPTP + Emapunil group (Figure 3.14B) (The NaCl group was normalized to 1: *Tspo* FC =  $1 \pm 0.07894$ , n = 5; MPTP + DMSO group: *Tspo* FC =  $2.342 \pm 0.379$ , n = 5; MPTP + Emapunil group: *Tspo* FC =  $0.7979 \pm 0.1375$ , n = 5; one-way ANOVA with Tukey's post hoc test; in between group difference  $F(2,12) = 12.52$ , p = 0.001157; data are given as means  $\pm$  SEM). To better understand the microglia activation profiles in different groups, we quantified several pro- and anti-inflammatory microglia markers by qPCR using the same striatal tissue as for *Tspo* qPCR. Among the classical M1 microglia activation markers, *Cox2* and *Il10* mRNA expression levels were increased in the MPTP + DMSO group compared to control group, whereas their expression levels were significantly attenuated in MPTP + Emapunil treated animals. Other tested markers, including *Tnfa*, *Il1b* and *Nos2*, also showed a trend towards decreased expression levels in the MPTP + Emapunil group compared to the

## Results

MPTP + DMSO group, whereas the NaCl control group showed the lowest expression levels (Figure 3.14C) (NaCl group normalized to 1: *Tnfa* FC =  $1 \pm 0.3178$ , *Il10* FC =  $1 \pm 0.1652$ , *Il1b* FC =  $1 \pm 0.1329$ , *Mpa2l* FC =  $1 \pm 0.07732$ , *Il6* FC =  $1 \pm 0.1694$ , *Nos2* FC =  $1 \pm 0.1704$ , *Cox2* FC =  $1 \pm 0.1734$ , n = 5; MPTP + DMSO group: *Tnfa* FC =  $5.885 \pm 0.6208$ , *Il10* FC =  $11.6 \pm 0.5612$ , *Il1b* FC =  $1.581 \pm 0.3056$ , *Mpa2l* FC =  $1.111 \pm 0.07614$ , *Il6* FC =  $2.227 \pm 0.3152$ , *Nos2* FC =  $2 \pm 0.1327$ , *Cox2* FC =  $2.746 \pm 0.2961$ , n = 5; MPTP + Emapunil group: *Tnfa* FC =  $4.979 \pm 0.6865$ , *Il10* FC =  $5.365 \pm 1.449$ , *Il1b* FC =  $1.385 \pm 0.1907$ , *Mpa2l* FC =  $1.158 \pm 0.279$ , *Il6* FC =  $3.189 \pm 0.5172$ , *Nos2* FC =  $1.66 \pm 0.305$ , *Cox2* FC =  $1.539 \pm 0.171$ , n = 5; one-way ANOVA with Tukey's post hoc test; in between group difference *Tnfa*:  $F(2,12) = 21.75$ ,  $p = 0.000151$ ; *Cxcl10*:  $F(2,12) = 34.86$ ,  $p = 0.0001$ ; *Il1b*:  $F(2,12) = 1.78$ ,  $p = 0.004$ ; *Mpa2l*:  $F(2,11) = 0.2$ ,  $p = 0.8180$ ; *Il6*:  $F(2,12) = 9.13$ ,  $p = 0.0039$ ; *Nos2*:  $F(2,12) = 5.55$ ,  $p = 0.0197$ ; *Cox2*:  $F(2,12) = 16.32$ ,  $p = 0.00038$ ; data are given as means  $\pm$  SEM). With regards to anti-inflammatory markers, we found that *Arg1*, *Il10*, *Il4*, *Mrc1*, *Ym1* and *Fizz2* were dramatically increased in the MPTP + Emapunil group, whereas most genes showed no alteration or even lower expression levels in MPTP treated mice compared to the NaCl control group (Figure 3.14D) (NaCl group normalized to 1: *Arg1* FC =  $1 \pm 0.06473$ , *Il10* FC =  $1 \pm 0.04799$ , *Il4* FC =  $1 \pm 0.08438$ , *Mrc1* FC =  $1 \pm 0.0555$ , *Ym1* FC =  $1 \pm 0.1139$ , *Fizz2* FC =  $1 \pm 0.2787$ , n = 5; in the MPTP + DMSO group: *Arg1* FC =  $0.8055 \pm 0.001321$ , *Il10* FC =  $0.9218 \pm 0.02449$ , *Il4* FC =  $1.905 \pm 0.4561$ , *Mrc1* FC =  $1.517 \pm 0.06856$ , *Ym1* FC =  $1.357 \pm 0.225$ , *Fizz2* FC =  $1.282 \pm 0.2985$ , n = 5; in the MPTP + Emapunil group: *Arg1* FC =  $1.259 \pm 0.1289$ , *Il10* FC =  $2.478 \pm 0.557$ , *Il4* FC =  $3.082 \pm 0.9407$ , *Mrc1* FC =  $1.955 \pm 0.1961$ , *Ym1* FC =  $2.21 \pm 0.0745$ , *Fizz2* FC =  $4.248 \pm 0.5753$ , n = 5; one-way ANOVA with Tukey's post hoc test; in between group difference *Arg1*:  $F(2,12) = 6.171$ ,  $p = 0.016$ ; *Il10*:  $F(2,12) = 7.36$ ,  $p = 0.008$ ; *Il4*:  $F(2,12) = 2.971$ ,  $p = 0.089$ ; *Mrc1*:  $F(2,12) = 14.84$ ,  $p = 0.00057$ ; *Ym1*:  $F(2,12) =$

16.75,  $p = 0.0003$ ; *Fizz2*:  $F(2,12) = 19.51$ ,  $p = 0.00017$ ; data are given as means  $\pm$  SEM).

Taken together, Emapunil treatment not only mitigates pro-inflammatory microglia activation, but also induces a shift towards anti-inflammatory activation.

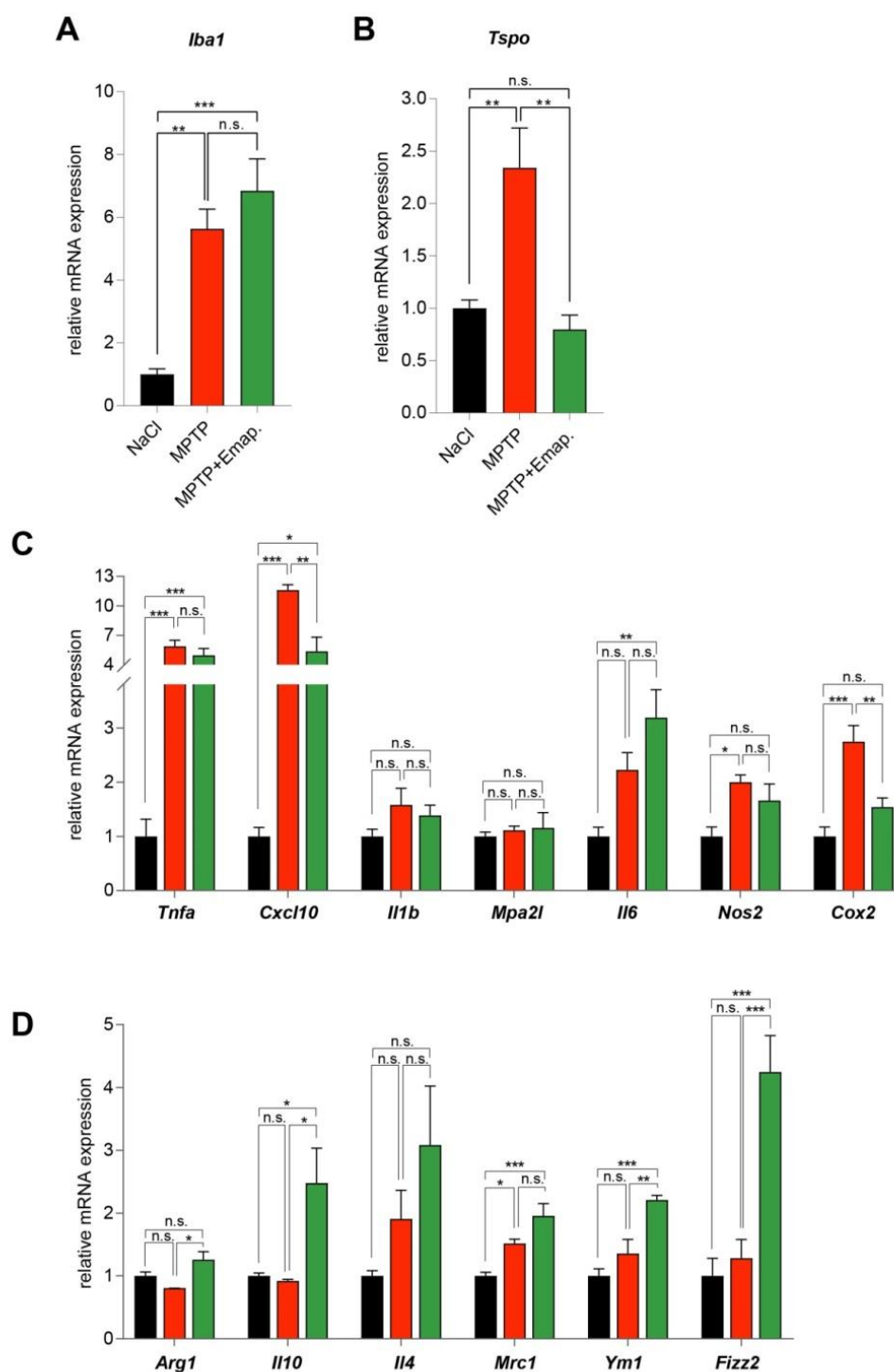


**Figure 3.14 Emapunil induces microglia from pro- to anti-inflammatory activation**

Relative quantification of mRNA expression levels normalized to the NaCl control group (striatum, day

3) (A) pro-inflammatory microglia markers; (B) anti-inflammatory microglia markers; Data are shown as means + SEM. One-way ANOVA with Tukey's post hoc test; in between group difference Tspo:  $F(2,12) = 12.52$ ,  $p = 0.001157$ ; Tnfa:  $F(2,12) = 21.75$ ,  $p = 0.000151$ ; Cxcl10:  $F(2,12) = 34.86$ ,  $p = 0.0001$ ; Il1b:  $F(2,12) = 1.777$ ,  $p = 0.004$ ; Mpa2l:  $F(2,11) = 0.2046$ ,  $p = 0.8180$ ; Il6:  $F(2,12) = 9.131$ ,  $p = 0.0039$ ; Nos2:  $F(2,12) = 5.55$ ,  $p = 0.0197$ ; Cox2:  $F(2,12) = 16.32$ ,  $p = 0.00038$ ; Arg1:  $F(2,12) = 6.171$ ,  $p = 0.016$ ; Il10:  $F(2,12) = 7.36$ ,  $p = 0.008$ ; Il4:  $F(2,12) = 2.971$ ,  $p = 0.089$ ; Mrc1:  $F(2,12) = 14.84$ ,  $p = 0.00057$ ; Yml:  $F(2,12) = 16.75$ ,  $p = 0.0003$ ; Fizz2:  $F(2,12) = 19.51$ ,  $p = 0.00017$ ; \* $p < 0.05$ , \*\* $p < 0.01$ , \*\*\* $p < 0.001$ ; n.s. = not significant.

### 3.8 Whole-transcriptome analysis

To further investigate the potential pathways mediating the effects of Emapunil, another cohort of mice was treated for subsequent transcriptome analysis (done by Eva Benito). Mice were dissected at day 3 after treatment, and the striatum was prepared for RNA-seq. Firstly, we compared the differentially expressed (DE) genes between the MPTP + DMSO group/the MPTP + Emapunil group and the control group (Figure 3.15A). We found 1017 DE genes in the MPTP + DMSO group, and 2464 DE genes in the MPTP + Emapunil group. When we compared these DE genes between the MPTP + DMSO and the MPTP + Emapunil group, we found 834 DE genes were identical, whereas 183 genes were differentially regulated exclusively in the MPTP + DMSO group, but not in the Emapunil treatment group. This indicates that the differential expression of these 183 genes may be attenuated by Emapunil. Interestingly, 1630 genes were differentially expressed in the Emapunil group only. These data suggest that Emapunil is not only able to attenuate part of the DE genes induced by MPTP, but also has additional effects itself (Figure 3.15B, C).

Next, the 183 MPTP-specific DE genes were selected for Gene Ontology (GO) functional enrichment analysis. Among these genes, the up-regulated MPTP-specific DE ones were associated with pathways in innate immune response, ERK and MAPK cascade regulation, vesicle-mediated transport, endocytosis, cytokine production, neuron differentiation and neurogenesis (Figure 3.15C, D). The down-regulated MPTP-specific DE ones were associated

with pathways in cell projection organization and assembly, actin cytoskeleton organization, ion transport, lipid and phospholipid metabolic process, cell migration and motility (Figure 3.15C,D).

We also analyzed the 1630 Emapunil-specific DE genes using GO functional enrichment and network analysis. These genes were linked to a wide range of cellular pathways, including positive response to oxidative stress, steroid hormones, regulation of cell and nuclear division, positive regulation of endocytosis, negative regulation of inflammatory cytokine production, apoptotic signaling pathways, leukocyte-mediated immunity and defense response to bacterial origin molecules (Figure 3.16).

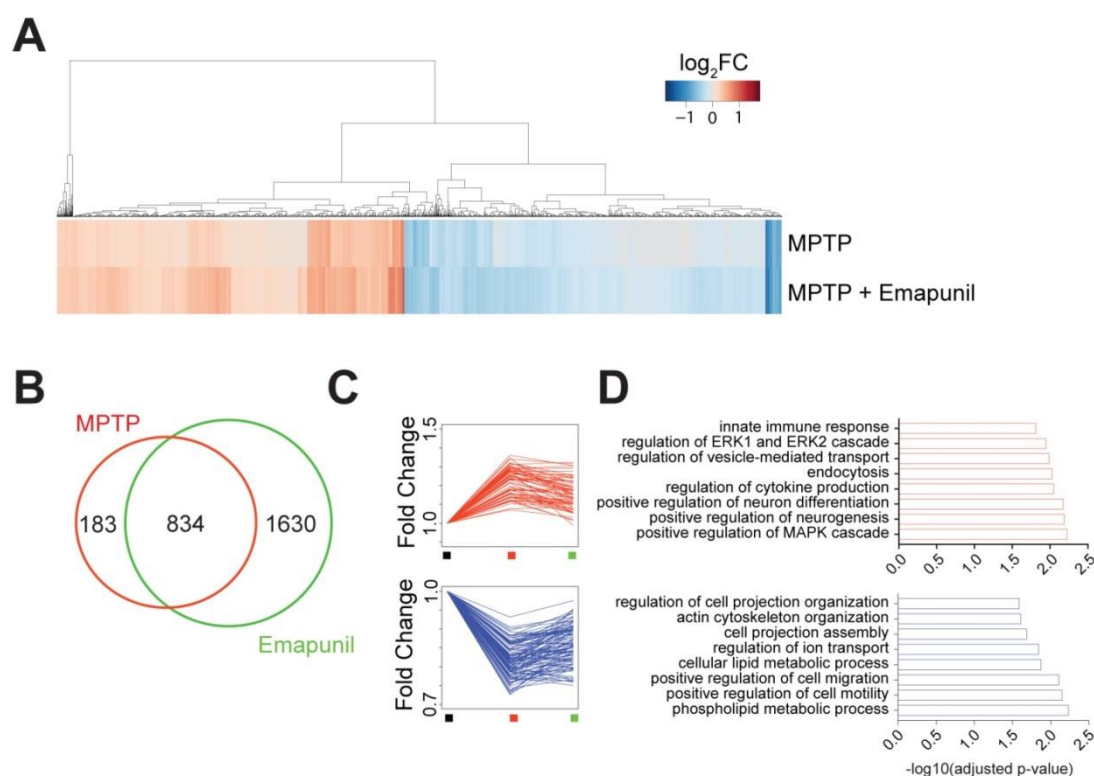
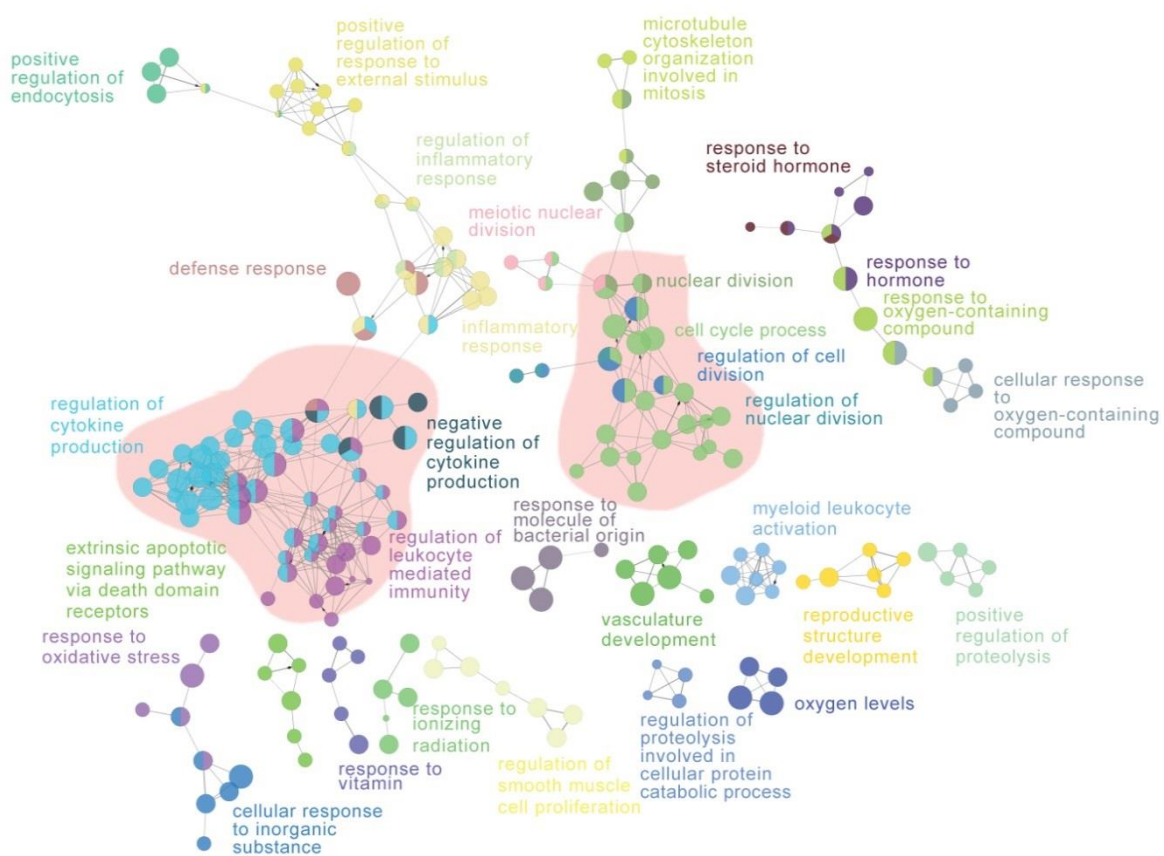


**Figure 3.15 Whole-transcriptome analysis of MPTP and Emapunil effects**

(A) Heatmap and sample clustering for MPTP + DMSO group or MPTP + Emapunil group DE genes compared to NaCl control group; (B) Venn diagram showing the overlaps of DE genes between MPTP + DMSO and MPTP + Emapunil group; (C) Heatmap and sample clustering of the 183 MPTP-specific DE genes, up-regulated genes in red and down-regulated genes in blue; (D) the most salient GO categories from GO functional enrichment analysis of the up-regulated (red, upper panel) and down-regulated (blue, lower panel) DE genes from (C).



Emapunil-specific network (LFC > |0.3|)

**Figure 3.16** GO functional enrichment and network analysis of the most salient Emapunil-specific DE genes

LFC = log fold change

## 4 Discussion

In this preclinical study, we evaluated the effect of Emapunil and its potential pathways in the subacute MPTP mouse model of Parkinsonism as well as in the dopaminergic LUHMES cell line. The MPTP mouse model is a widely used toxin-based animal model since it recapitulates several features of PD, namely dopaminergic neuron degeneration, neuroinflammation and motor deficits.

Here, 8 weeks old C57BL/6JRj female mice were used, with 5 consecutive days of 30 mg/kg MPTP i.p. injection. In addition, 50mg/kg Emapunil were i.p. injected every 48h for 15 days. The results indicated neuroprotective effects of Emapunil against dopaminergic neuron loss in the substantia nigra, against dopaminergic nerve terminals loss in the striatum, and against motor performance impairment. The neuroprotective effect of Emapunil was further confirmed in LUHMES cells which were exposed to MPP<sup>+</sup> and rotenone.

We also investigated the potential pathways which may explain the neuroprotective effects of Emapunil: (i) amelioration of the IRE $\alpha$ /*XBPIs* related UPR pathway; (ii) anti-inflammatory activation of microglia.

### 4.1 Physiological function of TSPO

The notion that TSPO was essential and indispensable for cholesterol transport and steroid homeostasis emerged in 1997, when a study found embryonic lethality in TSPO global knockout mice (Papadopoulos et al. 1997). Subsequent experiments uncovered that the function of TSPO was to transport cholesterol from the outer to the inner mitochondrial membrane, as the rate-limiting step in steroidogenesis (Rupprecht et al. 2010). However, this concept was challenged by the finding that TSPO global knockout mice were viable with normal lifespan, behavior, growth, fertility, and also regular cholesterol transport and plasma

pregnenolone concentration under healthy condition. However, the TSPO global knockout mice in that study showed reduced ATP production when microglia were activated after neuronal injury, indicating that TSPO is involved in mitochondrial metabolic activity (Banati et al. 2014). Until recently, the functional consequences of TSPO knockout are still under debate, as some research groups showed impaired steroid synthesis in TSPO CRISPR/Cas9 deleted MA-10 Leydig cells (Owen et al. 2017; Barron et al. 2018; Fan et al. 2017), whereas others found no significant deficits in the same cells (Tu et al. 2014; Banati et al. 2014; Tu et al. 2015; Tu et al. 2016). One of the limitations of this TSPO knockout mouse model is that compensatory mechanisms can not be ruled out since the knock out is not inducible at a later time point (Papadopoulos et al. 2018). Although the physiological role of TSPO is still unclear, all studies indicate that TSPO is a mitochondrial membrane protein which binds to cholesterol and can stimulate steroidogenesis under certain circumstances, like reduced endogenous steroid levels. This hypothesis is in line with our transcriptome analysis, where we found that Emapunil-related DE genes are strongly linked to the neurosteroidogenesis and hormone-induced steroid production (Figure 3.16).

## 4.2 Specificity of Emapunil binding to TSPO

The selectivity of Emapunil for TSPO binding was previously tested in multiple studies. First, binding affinity of Emapunil to nonselective targets were investigated in concentrations up to 1  $\mu$ M by an *in vitro* screen, which contained a total of 90 different purified receptors (receptors for adenosine, adrenoceptors, bradykinin BK2, dopamine, CCK<sub>A</sub>, GABA, glutamate, histamine, muscarinic, neurokinin, nicotine, opioid, serotonin, sigma, vasopressin V1b and hormones), transporter (dopamine, GABA and monoamines) and ion channels (calcium, potassium and sodium) (Kita et al. 2004). According to the authors, Emapunil

showed “no detectable affinity” to any of these targets tested. Another study also showed that Emapunil had no direct interaction with rat and human GABA<sub>A</sub> receptor subunits at the cellular level (Rupprecht et al. 2009). Ideally, to test whether Emapunil effects are indeed mediated by binding to TSPO, experiments would be repeated in TSPO knockout mice which were not possible within the time frame of this project. Therefore, we recapitulated several aspects in the dopaminergic LUHMES cell line.

We detected that the neuroprotective effects of Emapunil against rotenone induced cytotoxicity and increased *XBPIs*/*XBPI* mRNA ratio, were significantly attenuated when TSPO expression was down-regulated by siRNA (Figure 3.12). Therefore, it is likely that the neuroprotective effects of Emapunil we observed in this study are indeed TSPO dependent and specific, rather than caused by off-target effects, although this could only be excluded using TSPO knockout mice.

### 4.3 How are Emapunil’s neuroprotective effects mediated?

In this study, we detected by qPCR that the spliced *XBPIs*/*XBPI* mRNA ratios were significantly increased both in mice and in LUHMES cells when exposed to MPTP (mice), MPP<sup>+</sup> (cells) or rotenone (cells), and the increased levels were reduced by Emapunil treatment (Figure 3.6, Figure 3.12).

XBPI is one of the major ER stress response factors and key markers through UPR signaling pathways. The active form *XBPIs*, not only directly activates ER chaperones (Grp78/BiP, Grp58, Grp94) and ERAD components to refold and degrade the misfolded proteins, but also indirectly mediates lipids, cholesterol and other steroids synthesis (Valdés et al. 2014).

Most neurodegenerative diseases are characterized by protein misfolding and accumulation, ER stress and activated UPR signaling pathways (Dauer and Przedborski 2003). Activated

UPR signaling pathway is designed for protein degradation through ERAD pathway and for protein translation suppression which would attenuate ER stress (Hetz et al. 2011). Conflicting data have been reported regarding effects of increased XBP1s levels. For example, in MPP<sup>+</sup> treated dopaminergic neuron cultures, adenoviral overexpression of XBP1s was neuroprotective (Sado et al. 2009b). However, the opposite effects, like apoptotic cell death were also reported following chronic activation of XBP1s in multiple diseases, such as AD, PD, Prion and Huntington's disease (Urrea et al. 2013; Tabas and Ron 2011; Moreno et al. 2013). Therefore, a concept named "ER hormesis" was proposed, which concludes that a mild XBP1s activation with efficient downstream pathways may provide neuroprotective effects, whereas the chronic activation of XBP1s with insufficient downstream pathways could lead to apoptosis in diseases (Mercado et al. 2015; Michel et al. 2016). For example, activated IRE1/XBP1 pathway exacerbated pathology in the 5xFAD mouse model of Alzheimer's disease (Duran-Aniotz et al. 2017b). In the 6-OHDA rat model of parkinsonism, treatment with  $\beta$ -asarone, an IRE1/XBP1 pathway inhibitor, was neuroprotective (Ning et al. 2016). In accordance with previous reports, our findings from *in vivo* and *in vitro* experiments show that the neuroprotective effects of Emapunil in MPTP treated mice is associated with attenuated activation of the IRE1/XBP1 signaling pathway, which is also paralleled by lower neurotoxicity in LUHMES cells.

### 4.4 Emapunil shifts activated microglia from M1 to M2

*XBP1s* activation is tightly connected to ROS-mediated oxidative stress and inflammatory response in many neurodegenerative diseases. It was shown that activation of the IRE1/ $\alpha$ /XBP1s pathway itself stimulates the release of several pro-inflammatory cytokines, like TNF- $\alpha$ , IL-6, and IL-1 $\beta$  (Wang et al. 2015c; Chandra et al. 2017). Previously, several TSPO

ligands have already been demonstrated to improve neuron survival and attenuate neuroinflammation in different neurodegenerative and neuroinflammatory diseases, such as Alzheimer's disease (Barron et al. 2013), acute retina degeneration (Scholz et al. 2015), traumatic brain injury (Papadopoulos and Lecanu 2009) and depression (Gavioli et al. 2003). Historically, activated microglia were divided into pro-inflammatory M1 state and anti-inflammatory M2 state, which contained M2a (associated with tissue repair and phagocytosis), M2b (a selective up-regulation of phagocytosis as well as modulation of inflammatory response) and M2c (associated with tissue regeneration, extracellular matrix repairing and de-activation of M1/Th1 immune responses) sub-phenotypes. Although the M1/M2 classification of activated microglia was thought to be over-simplistic and has already been replaced by the new concept proposing that multiple and mixed phenotypes exist in single microglia, they are still useful to evaluate the general states of activated microglia in the disease. The pro-inflammatory M1 activated microglia and its effects have been implicated in the pathogenesis of PD as well as in PD animal models (Hirsch and Hunot 2009; Gao et al. 2008; Wang et al. 2015c).

Following MPTP treatment, we found that several M1 marker mRNA expression levels were upregulated, like *Tnf- $\alpha$* , *Cxcl10*, *Nos2*, and *Cox2*, which is in accordance with a previous report in the subacute MPTP treated mice (Calvello et al. 2017). In contrast, Emapunil treatment significantly attenuated *Il10* and *Cox2* expression. Non-significant reductions were found for *Nos2* and *Tnf- $\alpha$*  (Figure 3.14). In parallel, several M2 microglia markers were significantly upregulated with Emapunil treatment, like *Arg1* (M2a), *Il10*, *Il4* (with only a trend, no significance), *Mrc1*, *Ym1* and *Fizz2* (M2a) (Figure 3.14). As reported previously, *Il10* can stimulate M2c activation, which in turn suppresses M1-associated pro-inflammatory activity (Franco and Fernandez-Suarez 2015; Michell-Robinson et al. 2015). Thus we

concluded that Emapunil treatment induced a shift of the activated microglia from pro- to anti-inflammatory state.

#### **4.5 Emapunil has additional functional pathways apart from counteracting MPTP toxicity**

Analyzing the transcriptome profiles in neurodegenerative diseases is a useful tool for systematically identifying potential mechanisms and pathways. GO functional network analysis of the 1017 genes which were affected by MPTP treatment, revealed that the most salient genes are involved in mitochondrial membrane function, metal transport, calcium signaling, inflammatory response and intracellular transport (Figure 3.15), which is in line with previous transcriptome sequences in MPTP mouse model of PD (Cheng et al. 2016; Klemann et al. 2016). Strikingly, there are only 183 MPTP-specific DE genes which are reinstated by Emapunil treatment. These genes are mostly linked to innate immune response and cytokine production pathways, which is in accordance with previous reports and our findings that Emapunil could alter microglia activation state (Figure 3.15) (Rashid et al. 2018a; Rashid et al. 2018b; Scholz et al. 2015).

However, the majority of Emapunil-associated DE genes are not MPTP related. Network analysis of these Emapunil-specific genes included networks also linked to the regulation of cytokine production and other immune-related pathways. Additionally, they are linked to the positive response to oxidative stress and steroid homeostasis (Figure 3.16).

#### **4.6 Sex differences in animal models**

As previously reported, the expression levels of TSPO between sexes are different, for instance, male mice and men with myocarditis show significant higher TSPO expression

levels compared to female, which are due to testosterone (Fairweather et al. 2014). Male *Drosophila* also exhibit higher TSPO mRNA than females (Lin et al. 2015). Also, TSPO is crucial for steroidogenesis and hormone-induced steroid formation in adrenal and testis as reported in the steroidogenic cell-specific TSPO knockout mice (Fan et al. 2015). Furthermore, it was already reported that several TSPO ligands could upregulate the gonadal testosterone production (Chung et al. 2013; Le et al. 2014). Therefore, it is plausible to speculate that TSPO effects may be different between genders, so we only studied the Emapunil effects in female mice, and the transcriptome results in this study also indicate that the Emapunil is involved in the hormone-related steroid production pathways, which further support the hypothesis that Emapunil effects may differ in male versus female mice.

### **4.7 Summary of the mechanisms for the protective effects of Emapunil**

Several TSPO ligands showed neurosteriodogenesis enhancement, for example, etifoxine treatment correlated with increased concentrations of pregnenolone, progesterone, and allopregnanolone in brain and plasma of male control rat (Verleye et al. 2005). Treatment with another TSPO agonist, FGIN-1-27, has also able to increase the brain pregnenolone concentration in the adrenalectomized rat (Romeo et al. 1993). Previously, Emapunil was proposed to exert anxiolytic effects as a TSPO agonistic ligand (Kita et al. 2004), and its treatment significantly attenuated anxiety symptoms in an induced panic disorder rat model and neuropeptide fragment CCK4 challenged male volunteers (Rupprecht et al. 2009). Both studies have shown that Emapunil induced neurosteriodogenesis (Rupprecht et al. 2009). Furthermore, several recent studies also showed increased neurosteroids production after Emapunil treatment both *in vivo* and *in vitro* models (Wolf et al. 2015; Ravikumar et al.

2016). Therefore, it is likely that Emapunil acts partially by modulating neurosteroidogenesis (Costa et al. 2016).

Importantly, neurosteroids can regulate genes expression by modulating GABA<sub>A</sub>, NMDA and also various other cells surface receptors. However, many different patterns of neurosteroids regulation by different TSPO ligands have been reported across studies, the various readouts of these studies seem to be dependent on the experimental parameters, ligand treatment durations, and brain regions of interest (Giatti et al. 2009; Barron et al. 2013). Because we have not quantified neurosteroids and their concentrations in the brain during this study, the precise effects of Emapunil on neurosteroidogenesis are still unclear and need further investigation. We conclude that the neuroprotective effects of Emapunil may at least partially be mediated by modulation of neurosteroidogenesis.

### **4.8 The possibility to use Emapunil as a potential drug in PD**

Emapunil is orally available and able to cross the blood-brain barrier (Owen et al. 2012; Rupprecht et al. 2009). Also, Emapunil (90 mg/day) was already tested to be safe and tolerable in a clinical trial with healthy volunteers who were challenged with a pharmacological panic disorder paradigm. The reported side effects of Emapunil were comparable with those of the placebo group (Rupprecht et al. 2009). Novartis then launched a clinical phase II trial in patients with generalized anxiety disorder (ClinicalTrials.gov identifier: NCT00108836). This trial was discontinued due to lack of therapeutic efficacy. This may have, at least partially, been caused by polymorphism (A147T) in TSPO which was not controlled for (Owen et al. 2011; Selvaraj and Tu 2016). Homozygous A147T carriers have a much lower binding affinity of TSPO to most of its synthetic ligands (Owen et al. 2012) compared to controls. To overcome this problem, all TSPO ligands have been tested for

sensitivity to this single nucleotide polymorphism (SNP), and the SNP carriers can be genetically identified using blood leukocytes. A147T carriers could then be treated with higher doses to compensate for lower binding affinity (Alam et al. 2017). Taken together, we propose that Emapunil may be an interesting new approach for clinical application in PD treatment.

### 4.9 Limitations of this study

We have shown protective effects of Emapunil in the MPTP mouse model of Parkinsonism, and MPP<sup>+</sup>/Rotenone treated LUHMES cells. However, this study also has several limitations.

First, we have only tested Emapunil effects in MPTP treated female mice. Male mice should also be tested in future studies, which should contain male gonadectomized mice and non-gonadectomized mice.

Secondly, the dose of Emapunil (50 mg/kg body weight) used for *in vivo* study was relatively high, although it was comparable with the concentrations used in previous studies in mice. Ideally, the doses of Emapunil should include multiple concentrations in future studies, from low to high, to comprehensively compare its effects.

Also, since we have not repeated the experiments in TSPO knockout mice, it is impossible to rule out potential off-target effects of Emapunil, which should be studied in future.

Additionally, the neurosteroidogenesis effects of TSPO ligands (including Emapunil) are under intensive research in multiple models, and conflicting results were presented in the last years. Although we provided indirect evidence that Emapunil is involved in steroid production by transcriptome analysis, it would be informative to quantify the neurosteroids concentrations in brain or plasma in future Emapunil studies.

## 5 Conclusions

PD is a devastating neurodegenerative movement disorder. Although symptomatic treatment by the dopamine precursor L-DOPA or dopamine agonists can temporarily improve motor symptoms, no disease-modifying therapy exists yet.

In this study, we used *in vivo* (MPTP) and *in vitro* (MPP<sup>+</sup> and Rotenone) models to investigate the effects of Emapunil (= AC-5216 or XBD-173), a synthetic TSPO ligand. With administration of Emapunil in female MPTP exposed mice and MPP<sup>+</sup> treated LUHMES cells, we quantified: (i) the dopaminergic neurons and total neurons in SNpc by stereology; (ii) the striatal dopamine turnover by HPLC; (iii) the motor performance by pole and cylinder tests; (iv) LUHMES viability by Toxilight assay. We found that Emapunil treatment ameliorates dopaminergic neuron degeneration, preserves striatal dopamine metabolism and attenuates motor deficits.

We further identified potentially protective downstream pathways of Emapunil: (i) we confirmed by qPCR and IF that Emapunil could mitigate ER stress by inhibiting IRE $\alpha$ /XBP1 related UPR *in vivo* and *in vitro*. (ii) we unveiled by qPCR analysis that activated microglia were shifted from pro- to anti-inflammatory state (iii) we also found that Emapunil mitigated MPTP-associated differentially expressed genes by whole transcriptome assay. Interestingly, Emapunil also exhibits other potential effects by altering expression levels of genes which are unaffected by MPTP. These altered genes are related to oxidative stress and negative regulation of inflammatory cytokine production, leukocyte-mediated immunity and defense response to bacterial origin molecules.

Given that Emapunil crosses the BBB and has already been tested to be safe and orally available, it may be an interesting new approach for further clinical studies in PD.

## 6 Bibliography

- Acosta SA, Tajiri N, de la Pena I, Bastawrous M, Sanberg PR, Kaneko Y, Borlongan CV (2015) Alpha-Synuclein as a Pathological Link Between Chronic Traumatic Brain Injury and Parkinson's Disease. *Journal of cellular physiology* 230 (5):1024-1032
- Ahmed I, Tamouza R, Delord M, Krishnamoorthy R, Tzourio C, Mulot C, Nacfer M, Lambert J-c, Beaune P, Laurent-puig P (2012) association Between Parkinson] s Disease And The Hla-drb1 Locus: p374. *Tissue Antigens* 79 (6):585-586
- Akundi RS, Huang Z, Eason J, Pandya JD, Zhi L, Cass WA, Sullivan PG, Bueler H (2011) Increased mitochondrial calcium sensitivity and abnormal expression of innate immunity genes precede dopaminergic defects in Pink1-deficient mice. *PLoS One* 6 (1):e16038. doi:10.1371/journal.pone.0016038
- Alam MM, Lee J, Lee S-Y (2017) Recent Progress in the Development of TSPO PET Ligands for Neuroinflammation Imaging in Neurological Diseases. *Nuclear Medicine and Molecular Imaging* 51 (4):283-296. doi:10.1007/s13139-017-0475-8
- Alliot F, Godin I, Pessac B (1999) Microglia derive from progenitors, originating from the yolk sac, and which proliferate in the brain. *Developmental Brain Research* 117 (2):145-152
- Alvarez-Fischer D, Guerreiro S, Hunot S, Saurini F, Marien M, Sokoloff P, Hirsch EC, Hartmann A, Michel PP (2008) Modelling Parkinson-like neurodegeneration via osmotic minipump delivery of MPTP and probenecid. *Journal of neurochemistry* 107 (3):701-711
- Alvarez-Fischer D, Noelker C, Grünwald A, Vulinović F, Guerreiro S, Fuchs J, Lu L, Lombès A, Hirsch EC, Oertel WH (2013) Probenecid potentiates MPTP/MPP+ toxicity by interference with cellular energy metabolism. *Journal of neurochemistry* 127 (6):782-792
- Anders S, Pyl PT, Huber W (2015) HTSeq--a Python framework to work with high-throughput sequencing data. *Bioinformatics* 31 (2):166-169. doi:10.1093/bioinformatics/btu638
- Appel-Cresswell S, Vilarino-Guell C, Encarnacion M, Sherman H, Yu I, Shah B, Weir D, Thompson C, Szu-Tu C, Trinh J (2013) Alpha-synuclein p. H50Q, a novel pathogenic mutation for Parkinson's disease. *Movement disorders* 28 (6):811-813
- Baldereschi M, Di Carlo A, Rocca W, Vanni P, Maggi S, Perissinotto E, Grigoletto F, Amaducci L, Inzitari D, Group IW (2000) Parkinson's disease and parkinsonism in a longitudinal study Two-fold higher incidence in men. *Neurology* 55 (9):1358-1363
- Banati RB (2002) Visualising microglial activation in vivo. *Glia* 40 (2):206-217
- Banati RB, Middleton RJ, Chan R, Hatty CR, Kam WW-Y, Quin C, Graeber MB, Parmar A, Zahra D, Callaghan P (2014) Positron emission tomography and functional characterization of a complete PBR/TSPO knockout. *Nature communications* 5:5452
- Barbiero JK, Santiago RM, Persike DS, da Silva Fernandes MJ, Tonin FS, da Cunha C, Boschen SL, Lima MM, Vital MA (2014) Neuroprotective effects of peroxisome proliferator-activated receptor alpha and gamma agonists in model of parkinsonism induced by intranigral 1-methyl-4-phenyl-1, 2, 3, 6-tetrahydropyridine. *Behavioural brain research* 274:390-399
- Barron AM, Garcia-Segura LM, Caruso D, Jayaraman A, Lee JW, Melcangi RC, Pike CJ (2013) Ligand for translocator protein reverses pathology in a mouse model of Alzheimer's disease. *J Neurosci* 33 (20):8891-8897. doi:10.1523/JNEUROSCI.1350-13.2013
- Barron AM, Ji B, Kito S, Suhara T, Higuchi M (2018) Steroidogenic abnormalities in translocator protein knockout mice and significance in the aging male. *Biochemical Journal* 475 (1):75-85
- Bartels AL, Leenders KL (2007) Neuroinflammation in the pathophysiology of Parkinson's disease: Evidence from animal models to human in vivo studies with [11C]-PK11195 PET. *Movement Disorders* 22 (13):1852-1856
- Bartels T, Choi JG, Selkoe DJ (2011)  $\alpha$ -Synuclein occurs physiologically as a helically folded tetramer that resists aggregation. *Nature* 477 (7362):107
- Beal MF (2001) Experimental models of Parkinson's disease. *Nature reviews neuroscience* 2 (5):325

- Becker C, Jick S, Meier C (2011) NSAID use and risk of Parkinson disease: a population-based case-control study. *European journal of neurology* 18 (11):1336-1342
- Bell-Temin H, Culver-Cochran AE, Chaput D, Carlson CM, Kuehl M, Burkhardt BR, Bickford PC, Liu B, Stevens SM (2015) Novel molecular insights into classical and alternative activation states of microglia as revealed by stable isotope labeling by amino acids in cell culture (SILAC)-based proteomics. *Molecular & Cellular Proteomics* 14 (12):3173-3184
- Belloli S, Pannese M, Buonsanti C, Maiorino C, Di Grigoli G, Carpinelli A, Monterisi C, Moresco RM, Panina-Bordignon P (2017) Early upregulation of 18-kDa translocator protein in response to acute neurodegenerative damage in TREM2-deficient mice. *Neurobiology of aging* 53:159-168
- Benarroch EE (2013) Microglia Multiple roles in surveillance, circuit shaping, and response to injury. *Neurology*:10.1212/WNL.1210b1013e3182a1214a1577
- Benavides J, Guilloux F, Allam D, Uzan A, Mizoule J, Renault C, Dubroeuq M, Gueremy C, Le Fur G (1984) Opposite effects of an agonist, R05-4864, and an antagonist, PK 11195, of the peripheral type benzodiazepine binding sites on audiogenic seizures in DBA/2J mice. *Life sciences* 34 (26):2613-2620
- Benavides J, Malgouris C, Imbault F, Begassat F, Uzan A, Renault C, Dubroeuq M, Gueremy C, Le GF (1983) "Peripheral type" benzodiazepine binding sites in rat adrenals: binding studies with [3H] PK 11195 and autoradiographic localization. *Archives internationales de pharmacodynamie et de therapie* 266 (1):38-49
- Bendor JT, Logan TP, Edwards RH (2013) The function of  $\alpha$ -synuclein. *Neuron* 79 (6):1044-1066
- Béraud D, Twomey M, Bloom B, Mittereder A, Neitzke K, Ton V, Chasovskikh S, Mhyre TR, Maguire-Zeiss KA (2011)  $\alpha$ -Synuclein alters toll-like receptor expression. *Frontiers in neuroscience* 5:80
- Bezard E, Gross CE, Fournier M-C, Dovero S, Bloch B, Jaber M (1999) Absence of MPTP-induced neuronal death in mice lacking the dopamine transporter. *Experimental neurology* 155 (2):268-273
- Billingsley K, Bandres-Ciga S, Saez-Atienzar S, Singleton A (2018) Genetic risk factors in Parkinson's disease. *Cell and tissue research* 373 (1):9-20
- Bindea G, Mlecnik B, Hackl H, Charoentong P, Tosolini M, Kirilovsky A, Fridman WH, Pages F, Trajanoski Z, Galon J (2009) ClueGO: a Cytoscape plug-in to decipher functionally grouped gene ontology and pathway annotation networks. *Bioinformatics* 25 (8):1091-1093. doi:10.1093/bioinformatics/btp101
- Block ML, Zecca L, Hong J-S (2007) Microglia-mediated neurotoxicity: uncovering the molecular mechanisms. *Nature Reviews Neuroscience* 8 (1):57
- Blume SR, Cass DK, Tseng KY (2009) Stepping test in mice: a reliable approach in determining forelimb akinesia in MPTP-induced Parkinsonism. *Experimental neurology* 219 (1):208-211
- Boche D, Perry V, Nicoll J (2013) Activation patterns of microglia and their identification in the human brain. *Neuropathology and applied neurobiology* 39 (1):3-18
- Boka G, Anglade P, Wallach D, Javoy-Agid F, Agid Y, Hirsch E (1994) Immunocytochemical analysis of tumor necrosis factor and its receptors in Parkinson's disease. *Neuroscience letters* 172 (1-2):151-154
- Bovolin P, Schlichting J, Miyata M, Ferrarese C, Guidotti A, Alho H (1990) Distribution and characterization of diazepam binding inhibitor (DBI) in peripheral tissues of rat. *Regulatory peptides* 29 (2-3):267-281
- Braak H, Bohl JR, Müller CM, Rüb U, de Vos RA, Del Tredici K (2006) Stanley Fahn Lecture 2005: The staging procedure for the inclusion body pathology associated with sporadic Parkinson's disease reconsidered. *Movement disorders: official journal of the Movement Disorder Society* 21 (12):2042-2051
- Braak H, Del Tredici K (2008) Invited Article: Nervous system pathology in sporadic Parkinson disease. *Neurology* 70 (20):1916-1925
- Braak H, Del Tredici K, Rüb U, De Vos RA, Steur ENJ, Braak E (2003) Staging of brain pathology related to sporadic Parkinson's disease. *Neurobiology of aging* 24 (2):197-211

- Braak H, Ghebremedhin E, Rüb U, Bratzke H, Del Tredici K (2004) Stages in the development of Parkinson's disease-related pathology. *Cell and tissue research* 318 (1):121-134
- Braestrup C, Squires RF (1977) Specific benzodiazepine receptors in rat brain characterized by high-affinity (3H)diazepam binding. *Proceedings of the National Academy of Sciences* 74 (9):3805-3809. doi:10.1073/pnas.74.9.3805
- Braun J, McHugh N, Singh A, Wajdula J, Sato R (2007) Improvement in patient-reported outcomes for patients with ankylosing spondylitis treated with etanercept 50 mg once-weekly and 25 mg twice-weekly.
- Brice A (2005) Genetics of Parkinson's disease: LRRK2 on the rise. *Brain* 128 (12):2760-2762
- Brissaud E (1895) *Leçons sur les maladies nerveuses* (Salpêtrière, 1893-94).
- Burré J, Sharma M, Tsetsenis T, Buchman V, Etherton MR, Südhof TC (2010)  $\alpha$ -Synuclein promotes SNARE-complex assembly in vivo and in vitro. *Science* 329 (5999):1663-1667
- Butovsky O, Talpalar AE, Ben-Yaakov K, Schwartz M (2005) Activation of microglia by aggregated  $\beta$ -amyloid or lipopolysaccharide impairs MHC-II expression and renders them cytotoxic whereas IFN- $\gamma$  and IL-4 render them protective. *Molecular and Cellular Neuroscience* 29 (3):381-393
- Calvello R, Cianiulli A, Nicolardi G, De Nuccio F, Giannotti L, Salvatore R, Porro C, Trotta T, Panaro MA, Lofrumento DD (2017) Vitamin D treatment attenuates neuroinflammation and dopaminergic neurodegeneration in an animal model of Parkinson's disease, shifting M1 to M2 microglia responses. *Journal of Neuroimmune Pharmacology* 12 (2):327-339
- Campolo M, Casili G, Biundo F, Crupi R, Cordaro M, Cuzzocrea S, Esposito E (2017) The neuroprotective effect of dimethyl fumarate in an MPTP-mouse model of Parkinson's disease: involvement of reactive oxygen species/nuclear factor- $\kappa$ B/nuclear transcription factor related to NF-E2. *Antioxidants & redox signaling* 27 (8):453-471
- CARLSSON A, WALDECK B (1958) A fluorimetric method for the determination of dopamine (3-hydroxytyramine.). *Acta physiologica scandinavica* 44 (3-4):293-298
- Casellas P, Galiegue S, Basile AS (2002) Peripheral benzodiazepine receptors and mitochondrial function. *Neurochemistry international* 40 (6):475-486
- Castro EMC, Waak J, Weber SS, Fiesel FC, Oberhettinger P, Schütz M, Autenrieth IB, Springer W, Kahle PJ (2010) Parkinson's disease-associated DJ-1 modulates innate immunity signaling in *Caenorhabditis elegans*. *Journal of neural transmission* 117 (5):599-604
- Chan CS, Guzman JN, Ilijic E, Mercer JN, Rick C, Tkatch T, Meredith GE, Surmeier DJ (2007) 'Rejuvenation' protects neurons in mouse models of Parkinson's disease. *Nature* 447 (7148):1081
- Chandra G, Roy A, Rangasamy SB, Pahan K (2017) Induction of adaptive immunity leads to nigrostriatal disease progression in MPTP mouse model of Parkinson's disease. *The Journal of Immunology* 198 (11):4312-4326
- Charcot J (1869) *De la paralysie agitante* (leçon 5). *oeuvres complètes* 1: 161-188. Bureaux du progrès médical
- Chartier-Harlin M-C, Kachergus J, Roumier C, Mouroux V, Douay X, Lincoln S, Levecque C, Larvor L, Andrieux J, Hulihan M (2004)  $\alpha$ -synuclein locus duplication as a cause of familial Parkinson's disease. *The Lancet* 364 (9440):1167-1169
- Chen M-K, Guilarte TR (2008) Translocator protein 18 kDa (TSPO): molecular sensor of brain injury and repair. *Pharmacology & therapeutics* 118 (1):1-17
- Cheng L, Quek CY, Hung LW, Sharples RA, Sherratt NA, Barnham KJ, Hill AF (2016) Gene dysregulation is restored in the Parkinson's disease MPTP neurotoxic mice model upon treatment of the therapeutic drug Cu II (atm). *Scientific reports* 6:22398
- Chhor V, Le Charpentier T, Lebon S, Oré M-V, Celador IL, Josseland J, Degos V, Jacotot E, Hagberg H, Sävman K (2013) Characterization of phenotype markers and neuronotoxic potential of polarised primary microglia in vitro. *Brain, behavior, and immunity* 32:70-85
- Christine CW (2015) NINDS Exploratory Trials in Parkinson Disease (NET-PD) FS-ZONE Investigators. Pioglitazone in early Parkinson's disease: a phase 2, multicentre, double-blind, randomised trial.(vol 14, pg 795, 2015). *LANCET NEUROLOGY* 14 (10):979-979

- Chung J-Y, Chen H, Midzak A, Burnett A, Papadopoulos V, Zirkin BR (2013) Drug ligand-induced activation of translocator protein (TSPO) stimulates steroid production by aged brown Norway rat Leydig cells. *Endocrinology* 154 (6):2156-2165
- Cicchetti F, Brownell A, Williams K, Chen Y, Livni E, Isacson O (2002) Neuroinflammation of the nigrostriatal pathway during progressive 6-OHDA dopamine degeneration in rats monitored by immunohistochemistry and PET imaging. *European Journal of Neuroscience* 15 (6):991-998
- Ciechanover A (2005) Proteolysis: from the lysosome to ubiquitin and the proteasome. *Nature reviews Molecular cell biology* 6 (1):79
- Clavier T, Tonon M-C, Foutel A, Besnier E, Lefevre-Scelles A, Morin F, Gandolfo P, Tuech J-J, Quillard M, Veber B (2014) Increased plasma levels of endozepines, endogenous ligands of benzodiazepine receptors, during systemic inflammation: a prospective observational study. *Critical Care* 18 (6):633
- Colla E, Jensen PH, Pletnikova O, Troncoso JC, Glabe C, Lee MK (2012) Accumulation of toxic  $\alpha$ -synuclein oligomer within endoplasmic reticulum occurs in  $\alpha$ -synucleinopathy in vivo. *Journal of Neuroscience* 32 (10):3301-3305
- Conrad AT, Dittel BN (2011) Taming of macrophage and microglial cell activation by microRNA-124. *Cell research* 21 (2):213
- Cosenza-Nashat M, Zhao ML, Suh HS, Morgan J, Natividad R, Morgello S, Lee SC (2009) Expression of the translocator protein of 18 kDa by microglia, macrophages and astrocytes based on immunohistochemical localization in abnormal human brain. *Neuropathology and applied neurobiology* 35 (3):306-328
- Costa B, Da Pozzo E, Cavallini C, Taliani S, Da Settimo F, Martini C (2016) Long residence time at the neurosteroidogenic 18 kDa translocator protein characterizes the anxiolytic ligand XBD173. *ACS chemical neuroscience* 7 (8):1041-1046
- Costa B, Pini S, Gabelloni P, Da Pozzo E, Abelli M, Lari L, Preve M, Lucacchini A, Cassano GB, Martini C (2009) The spontaneous Ala147Thr amino acid substitution within the translocator protein influences pregnenolone production in lymphomonocytes of healthy individuals. *Endocrinology* 150 (12):5438-5445
- Costa E, Guidotti A (1991) Diazepam binding inhibitor (DBI): a peptide with multiple biological actions. *Life sciences* 49 (5):325-344
- Couch Y, Alvarez-Erviti L, Sibson NR, Wood MJ, Anthony DC (2011) The acute inflammatory response to intranigral  $\alpha$ -synuclein differs significantly from intranigral lipopolysaccharide and is exacerbated by peripheral inflammation. *Journal of neuroinflammation* 8 (1):166
- Członkowska A, Kohutnicka M, Kurkowska-Jastrzębska I, Członkowski A (1996) Microglial reaction in MPTP (1-methyl-4-phenyl-1, 2, 3, 6-tetrahydropyridine) induced Parkinson's disease mice model. *Neurodegeneration* 5 (2):137-143
- D'Amato RJ, Alexander GM, Schwartzman RJ, Kitt CA, Price DL, Snyder SH (1987) Evidence for neuromelanin involvement in MPTP-induced neurotoxicity. *Nature* 327 (6120):324
- Da Pozzo E, Giacomelli C, Barresi E, Costa B, Taliani S, Passetti FDS, Martini C (2015) Targeting the 18-kDa translocator protein: recent perspectives for neuroprotection. *Biochemical Society Transactions* 43 (4):559-565
- Daubner SC, Le T, Wang S (2011) Tyrosine hydroxylase and regulation of dopamine synthesis. *Archives of biochemistry and biophysics* 508 (1):1-12
- Dauer W, Przedborski S (2003) Parkinson's disease: mechanisms and models. *neuron* 39 (6):889-909
- Davalos D, Grutzendler J, Yang G, Kim JV, Zuo Y, Jung S, Littman DR, Dustin ML, Gan W-B (2005) ATP mediates rapid microglial response to local brain injury in vivo. *Nature neuroscience* 8 (6):752
- Dawson TM, Golde TE, Lagier-Tourenne C (2018) Animal models of neurodegenerative diseases. *Nat Neurosci* 21:1370-1379
- Dawson TM, Ko HS, Dawson VL (2010) Genetic animal models of Parkinson's disease. *Neuron* 66 (5):646-661

- Decaudin D, Castedo M, Nemati F, Beurdeley-Thomas A, De Pinieux G, Caron A, Pouillart P, Wijdenes J, Rouillard D, Kroemer G (2002) Peripheral benzodiazepine receptor ligands reverse apoptosis resistance of cancer cells in vitro and in vivo. *Cancer research* 62 (5):1388-1393
- Dehmer T, Heneka MT, Sastre M, Dichgans J, Schulz JB (2004) Protection by pioglitazone in the MPTP model of Parkinson's disease correlates with I $\kappa$ B $\alpha$  induction and block of NF $\kappa$ B and iNOS activation. *Journal of neurochemistry* 88 (2):494-501
- Delavoie F, Li H, Hardwick M, Robert J-C, Giatzakis C, Péranzi G, Yao Z-X, Maccario J, Lacapere J-J, Papadopoulos V (2003) In vivo and in vitro peripheral-type benzodiazepine receptor polymerization: functional significance in drug ligand and cholesterol binding. *Biochemistry* 42 (15):4506-4519
- Dickson DW (2012) Parkinson's disease and parkinsonism: neuropathology. *Cold Spring Harbor perspectives in medicine*:a009258
- Dickson DW, Braak H, Duda JE, Duyckaerts C, Gasser T, Halliday GM, Hardy J, Leverenz JB, Del Tredici K, Wszolek ZK (2009) Neuropathological assessment of Parkinson's disease: refining the diagnostic criteria. *The Lancet Neurology* 8 (12):1150-1157
- Dickstein LP, Zoghbi SS, Fujimura Y, Imaizumi M, Zhang Y, Pike VW, Innis RB, Fujita M (2011) Comparison of 18 F-and 11 C-labeled aryloxyanilide analogs to measure translocator protein in human brain using positron emission tomography. *European journal of nuclear medicine and molecular imaging* 38 (2):352-357
- Dijkstra AA, Voorn P, Berendse HW, Groenewegen HJ, Bank NB, Rozemuller AJ, van de Berg WD (2014) Stage-dependent nigral neuronal loss in incidental Lewy body and Parkinson's disease. *Movement Disorders* 29 (10):1244-1251
- do Rego J-C, Orta M-H, Leprince J, Tonon M-C, Vaudry H, Costentin J (2007) Pharmacological characterization of the receptor mediating the anorexigenic action of the octadecaneuropeptide: evidence for an endozepinergic tone regulating food intake. *Neuropsychopharmacology* 32 (7):1641
- Domingo A, Klein C (2018) Genetics of Parkinson disease. In: *Handbook of clinical neurology*, vol 147. Elsevier, pp 211-227
- Dorsey E, Constantinescu R, Thompson J, Biglan K, Holloway R, Kieburtz K, Marshall F, Ravina B, Schifitto G, Siderowf A (2007) Projected number of people with Parkinson disease in the most populous nations, 2005 through 2030. *Neurology* 68 (5):384-386
- Du Y, Ma Z, Lin S, Dodel RC, Gao F, Bales KR, Triarhou LC, Chernet E, Perry KW, Nelson DL (2001) Minocycline prevents nigrostriatal dopaminergic neurodegeneration in the MPTP model of Parkinson's disease. *Proceedings of the National Academy of Sciences* 98 (25):14669-14674
- Duran-Aniotz C, Cornejo VH, Espinoza S, Ardiles AO, Medinas DB, Salazar C, Foley A, Gajardo I, Thielen P, Iwawaki T (2017a) IRE1 signaling exacerbates Alzheimer's disease pathogenesis. *Acta neuropathologica* 134 (3):489-506
- Duran-Aniotz C, Cornejo VH, Espinoza S, Ardiles AO, Medinas DB, Salazar C, Foley A, Gajardo I, Thielen P, Iwawaki T, Scheper W, Soto C, Palacios AG, Hoozemans JJM, Hetz C (2017b) IRE1 signaling exacerbates Alzheimer's disease pathogenesis. *Acta Neuropathol* 134 (3):489-506. doi:10.1007/s00401-017-1694-x
- Edwards JP, Zhang X, Frauwirth KA, Mosser DM (2006) Biochemical and functional characterization of three activated macrophage populations. *Journal of leukocyte biology* 80 (6):1298-1307
- Egawa N, Yamamoto K, Inoue H, Hikawa R, Nishi K, Mori K, Takahashi R (2011) The endoplasmic reticulum stress sensor, ATF6 $\alpha$ , protects against neurotoxin-induced dopaminergic neuronal death. *Journal of Biological Chemistry* 286 (10):7947-7957
- English C, Aloji JJ (2015) New FDA-approved disease-modifying therapies for multiple sclerosis. *Clinical therapeutics* 37 (4):691-715
- Færgeman NJ, Wadum M, Feddersen S, Burton M, Kragelund BB, Knudsen J (2007) Acyl-CoA binding proteins; structural and functional conservation over 2000 MYA. *Molecular and cellular biochemistry* 299 (1-2):55-65

- Fairweather D, Coronado MJ, Garton AE, Dziedzic JL, Bucek A, Cooper LT, Brandt JE, Alikhan FS, Wang H, Endres CJ (2014) Sex differences in translocator protein 18 kDa (TSPO) in the heart: implications for imaging myocardial inflammation. *Journal of cardiovascular translational research* 7 (2):192-202
- Fan J, Campioli E, Midzak A, Culty M, Papadopoulos V (2015) Conditional steroidogenic cell-targeted deletion of TSPO unveils a crucial role in viability and hormone-dependent steroid formation. *Proceedings of the National Academy of Sciences* 112 (23):7261-7266
- Fan J, Lindemann P, GJ Feuilloy M, Papadopoulos V (2012) Structural and functional evolution of the translocator protein (18 kDa). *Current molecular medicine* 12 (4):369-386
- Fan J, Liu J, Culty M, Papadopoulos V (2010) Acyl-coenzyme A binding domain containing 3 (ACBD3; PAP7; GCP60): an emerging signaling molecule. *Progress in lipid research* 49 (3):218-234
- Fan J, Wang K, Zirkin B, Papadopoulos V (2017) CRISPR/Cas9-mediated *Tspo* gene mutations lead to reduced mitochondrial membrane potential and steroid formation in MA-10 mouse tumor Leydig cells. *Endocrinology* 159 (2):1130-1146
- Faraco G, Pittelli M, Cavone L, Fossati S, Porcu M, Mascagni P, Fossati G, Moroni F, Chiarugi A (2009) Histone deacetylase (HDAC) inhibitors reduce the glial inflammatory response in vitro and in vivo. *Neurobiology of disease* 36 (2):269-279
- Fellner L, Irschick R, Schanda K, Reindl M, Klimaschewski L, Poewe W, Wenning GK, Stefanova N (2013) Toll-like receptor 4 is required for  $\alpha$ -synuclein dependent activation of microglia and astroglia. *Glia* 61 (3):349-360
- Ferrarese C, Appollonio I, Frigo M, Meregalli S, Piolti R, Tamma F, Frattola L (1990) Cerebrospinal fluid levels of diazepam-binding inhibitor in neurodegenerative disorders with dementia. *Neurology* 40 (4):632-632
- Fiorentino DF, Bond MW, Mosmann T (1989) Two types of mouse T helper cell. IV. Th2 clones secrete a factor that inhibits cytokine production by Th1 clones. *Journal of Experimental Medicine* 170 (6):2081-2095
- Fleming SM, Zhu C, Fernagut P-O, Mehta A, DiCarlo CD, Seaman RL, Chesselet M-F (2004) Behavioral and immunohistochemical effects of chronic intravenous and subcutaneous infusions of varying doses of rotenone. *Experimental neurology* 187 (2):418-429
- Fornai F, Schlüter OM, Lenzi P, Gesi M, Ruffoli R, Ferrucci M, Lazzeri G, Busceti CL, Pontarelli F, Battaglia G (2005) Parkinson-like syndrome induced by continuous MPTP infusion: convergent roles of the ubiquitin-proteasome system and  $\alpha$ -synuclein. *Proceedings of the National Academy of Sciences* 102 (9):3413-3418
- Franco R, Fernandez-Suarez D (2015) Alternatively activated microglia and macrophages in the central nervous system. *Progress in neurobiology* 131:65-86
- Frank W, Baar KM, Qudeimat E, Woriedh M, Alawady A, Ratnadewi D, Gremillon L, Grimm B, Reski R (2007) A mitochondrial protein homologous to the mammalian peripheral-type benzodiazepine receptor is essential for stress adaptation in plants. *The Plant Journal* 51 (6):1004-1018
- Frankola KA, Greig NH, Luo W, Tweedie D (2011) Targeting TNF- $\alpha$  to elucidate and ameliorate neuroinflammation in neurodegenerative diseases. *CNS Neurol Disord Drug Targets* 10 (3):391-403
- Friedman LK, Mytilineou C (1990) Neurochemical and toxic effects of 1-methyl-4-phenyl-1, 2, 3, 6-tetrahydropyridine and 1-methyl-4-phenylpyridine to rat serotonin neurons in dissociated cell cultures. *Journal of Pharmacology and Experimental Therapeutics* 253 (2):892-898
- Gainetdinov RR, Fumagalli F, Jones SR, Caron MG (1997) Dopamine transporter is required for in vivo MPTP neurotoxicity: evidence from mice lacking the transporter. *Journal of neurochemistry* 69 (3):1322-1325
- Gao H-M, Kotzbauer PT, Uryu K, Leight S, Trojanowski JQ, Lee VM-Y (2008) Neuroinflammation and oxidation/nitration of  $\alpha$ -synuclein linked to dopaminergic neurodegeneration. *Journal of Neuroscience* 28 (30):7687-7698

- Gao H-M, Liu B, Zhang W, Hong J-S (2003) Critical role of microglial NADPH oxidase-derived free radicals in the in vitro MPTP model of Parkinson's disease. *The FASEB Journal* 17 (13):1954-1956
- Gao X, Chen H, Schwarzschild MA, Ascherio A (2011) Use of ibuprofen and risk of Parkinson disease. *Neurology* 76 (10):863-869
- Garza-Contreras J, Duong P, Snyder B, Cunningham R (2017) Novel Androgen Receptor Protein in Brain: Implication for Parkinson's Disease.
- Gavioli E, Marzola G, Guerrini R, Bertorelli R, Zucchini S, De Lima TM, Rae G, Salvadori S, Regoli D, Calo G (2003) Blockade of nociceptin/orphanin FQ-NOP receptor signalling produces antidepressant-like effects: pharmacological and genetic evidences from the mouse forced swimming test. *European Journal of Neuroscience* 17 (9):1987-1990
- Gavish M, Bachman I, Shoukrun R, Katz Y, Veenman L, Weisinger G, Weizman A (1999) Enigma of the peripheral benzodiazepine receptor. *Pharmacological reviews* 51 (4):629-650
- Gerhard A, Pavese N, Hotton G, Turkheimer F, Es M, Hammers A, Eggert K, Oertel W, Banati RB, Brooks DJ (2006) In vivo imaging of microglial activation with [<sup>11</sup>C](R)-PK11195 PET in idiopathic Parkinson's disease. *Neurobiology of disease* 21 (2):404-412
- Gerhard A, Watts J, Trender-Gerhard I, Turkheimer F, Banati RB, Bhatia K, Brooks DJ (2004) In vivo imaging of microglial activation with [<sup>11</sup>C](R)-PK11195 PET in corticobasal degeneration. *Movement disorders: official journal of the Movement Disorder Society* 19 (10):1221-1226
- Giatti S, Pesaresi M, Cavaletti G, Bianchi R, Carozzi V, Lombardi R, Maschi O, Lauria G, Garcia-Segura LM, Caruso D (2009) Neuroprotective effects of a ligand of translocator protein-18kDa (Ro5-4864) in experimental diabetic neuropathy. *Neuroscience* 164 (2):520-529
- Gibb W, Lees A (1991) Anatomy, pigmentation, ventral and dorsal subpopulations of the substantia nigra, and differential cell death in Parkinson's disease. *Journal of Neurology, Neurosurgery & Psychiatry* 54 (5):388-396
- Gibrat C, Saint-Pierre M, Bousquet M, Lévesque D, Rouillard C, Cicchetti F (2009) Differences between subacute and chronic MPTP mice models: investigation of dopaminergic neuronal degeneration and  $\alpha$ -synuclein inclusions. *Journal of neurochemistry* 109 (5):1469-1482
- Gillardot F, Schmid R, Draheim H (2012) Parkinson's disease-linked leucine-rich repeat kinase 2 (R1441G) mutation increases proinflammatory cytokine release from activated primary microglial cells and resultant neurotoxicity. *Neuroscience* 208:41-48
- Giordano S, Lee J, Darley-Usmar VM, Zhang J (2012) Distinct effects of rotenone, 1-methyl-4-phenylpyridinium and 6-hydroxydopamine on cellular bioenergetics and cell death. *PLoS One* 7 (9):e44610. doi:10.1371/journal.pone.0044610
- Gispert S, Del Turco D, Garrett L, Chen A, Bernard DJ, Hamm-Clement J, Korf H-W, Deller T, Braak H, Auburger G (2003) Transgenic mice expressing mutant A53T human alpha-synuclein show neuronal dysfunction in the absence of aggregate formation. *Molecular and Cellular Neuroscience* 24 (2):419-429
- Giunti D, Parodi B, Cordano C, Uccelli A, Kerlero de Rosbo N (2014) Can we switch microglia's phenotype to foster neuroprotection? Focus on multiple sclerosis. *Immunology* 141 (3):328-339
- Glocker E-O, Kotlarz D, Boztug K, Gertz EM, Schäffer AA, Noyan F, Perro M, Diestelhorst J, Allroth A, Murugan D (2009) Inflammatory bowel disease and mutations affecting the interleukin-10 receptor. *New England Journal of Medicine* 361 (21):2033-2045
- Goedert M, Spillantini MG, Del Tredici K, Braak H (2013) 100 years of Lewy pathology. *Nature Reviews Neurology* 9 (1):13
- Goldberg N, Haack A, Lim N, Janson O, Meshul C (2011) Dopaminergic and behavioral correlates of progressive lesioning of the nigrostriatal pathway with 1-methyl-4-phenyl-1, 2, 3, 6-tetrahydropyridine. *Neuroscience* 180:256-271
- Goldman SM (2014) Environmental toxins and Parkinson's disease. *Annual review of pharmacology and toxicology* 54:141-164

- González H, Elgueta D, Montoya A, Pacheco R (2014) Neuroimmune regulation of microglial activity involved in neuroinflammation and neurodegenerative diseases. *Journal of neuroimmunology* 274 (1-2):1-13
- Guo Q, Colasanti A, Owen DR, Onega M, Kamalakaran A, Bennacef I, Matthews PM, Rabiner EA, Turkheimer FE, Gunn RN (2013) Quantification of the specific translocator protein signal of 18F-PBR111 in healthy humans: a genetic polymorphism effect on in vivo binding. *Journal of nuclear medicine* 54 (11):1915-1923
- Guo Y, Kalathur RC, Liu Q, Kloss B, Bruni R, Ginter C, Kloppmann E, Rost B, Hendrickson WA (2015) Structure and activity of tryptophan-rich TSPO proteins. *Science* 347 (6221):551-555
- Halliday GM, Holton JL, Revesz T, Dickson DW (2011) Neuropathology underlying clinical variability in patients with synucleinopathies. *Acta neuropathologica* 122 (2):187-204
- Hamre K, Tharp R, Poon K, Xiong X, Smeyne RJ (1999) Differential strain susceptibility following 1-methyl-4-phenyl-1, 2, 3, 6-tetrahydropyridine (MPTP) administration acts in an autosomal dominant fashion: quantitative analysis in seven strains of *Mus musculus*. *Brain research* 828 (1-2):91-103
- Hamza TH, Zabetian CP, Tenesa A, Laederach A, Montimurro J, Yearout D, Kay DM, Doheny KF, Paschall J, Pugh E (2010) Common genetic variation in the HLA region is associated with late-onset sporadic Parkinson's disease. *Nature genetics* 42 (9):781
- Haobam R, Sindhu KM, Chandra G, Mohanakumar KP (2005) Swim-test as a function of motor impairment in MPTP model of Parkinson's disease: a comparative study in two mouse strains. *Behavioural brain research* 163 (2):159-167
- Harms AS, Barnum CJ, Ruhn KA, Varghese S, Treviño I, Blesch A, Tansey MG (2011) Delayed dominant-negative TNF gene therapy halts progressive loss of nigral dopaminergic neurons in a rat model of Parkinson's disease. *Molecular Therapy* 19 (1):46-52
- Harms AS, Cao S, Rowse AL, Thome AD, Li X, Mangieri LR, Cron RQ, Shacka JJ, Raman C, Standaert DG (2013) MHCII is required for  $\alpha$ -synuclein-induced activation of microglia, CD4 T cell proliferation, and dopaminergic neurodegeneration. *Journal of Neuroscience* 33 (23):9592-9600
- Hassler R (1938) The pathology of paralysis agitans and post-encephalitic Parkinson's. *Journal fur Psychologie und Neurologie* 48:387-476
- Hetz C (2012) The unfolded protein response: controlling cell fate decisions under ER stress and beyond. *Nature reviews Molecular cell biology* 13 (2):89
- Hetz C, Martinon F, Rodriguez D, Glimcher LH (2011) The unfolded protein response: integrating stress signals through the stress sensor IRE1 $\alpha$ . *Physiological reviews* 91 (4):1219-1243
- Hetz C, Mollereau B (2014) Disturbance of endoplasmic reticulum proteostasis in neurodegenerative diseases. *Nature Reviews Neuroscience* 15 (4):233
- Hirsch EC, Hunot S (2009) Neuroinflammation in Parkinson's disease: a target for neuroprotection? *The Lancet Neurology* 8 (4):382-397
- Hofmann KW, Schuh AFS, Saute J, Townsend R, Fricke D, Leke R, Souza DO, Portela LV, Chaves MLF, Rieder CR (2009) Interleukin-6 serum levels in patients with Parkinson's disease. *Neurochemical research* 34 (8):1401-1404
- Hoozemans JJ, Van Haastert ES, Nijholt DA, Rozemuller AJ, Scheper W (2012) Activation of the unfolded protein response is an early event in Alzheimer's and Parkinson's disease. *Neurodegenerative Diseases* 10 (1-4):212-215
- Hu X, Ivashkiv LB (2009) Cross-regulation of signaling pathways by interferon- $\gamma$ : implications for immune responses and autoimmune diseases. *Immunity* 31 (4):539-550
- Iacono D, Geraci-Erck M, Rabin ML, Adler CH, Serrano G, Beach TG, Kurlan R (2015) Parkinson disease and incidental Lewy body disease: just a question of time? *Neurology* 85 (19):1670-1679
- Iannaccone S, Cerami C, Alessio M, Garibotto V, Panzacchi A, Olivieri S, Gelsomino G, Moresco R, Perani D (2013) In vivo microglia activation in very early dementia with Lewy bodies, comparison with Parkinson's disease. *Parkinsonism & related disorders* 19 (1):47-52

- Iglesias-González J, Sánchez-Iglesias S, Méndez-Álvarez E, Rose S, Hikima A, Jenner P, Soto-Otero R (2012) Differential toxicity of 6-hydroxydopamine in SH-SY5Y human neuroblastoma cells and rat brain mitochondria: protective role of catalase and superoxide dismutase. *Neurochemical research* 37 (10):2150-2160
- Imamura K, Hishikawa N, Sawada M, Nagatsu T, Yoshida M, Hashizume Y (2003) Distribution of major histocompatibility complex class II-positive microglia and cytokine profile of Parkinson's disease brains. *Acta neuropathologica* 106 (6):518-526
- Jackson-Lewis V, Jakowec M, Burke RE, Przedborski S (1995) Time course and morphology of dopaminergic neuronal death caused by the neurotoxin 1-methyl-4-phenyl-1, 2, 3, 6-tetrahydropyridine. *Neurodegeneration* 4 (3):257-269
- Jackson-Lewis V, Lester D, Kozina E, Przedborski S, Smeyne RJ (2015) From man to mouse: The MPTP model of Parkinson disease. In: *Movement Disorders*. Elsevier, pp 287-306
- Jafari M, Khodayari B, Felgner J, Bussel II, Rose MR, Mueller LD (2007) Pioglitazone: an anti-diabetic compound with anti-aging properties. *Biogerontology* 8 (6):639-651
- Jaipuria G, Leonov A, Giller K, Vasa SK, Jaremko L, Jaremko M, Linser R, Becker S, Zweckstetter M (2017) Cholesterol-mediated allosteric regulation of the mitochondrial translocator protein structure. *Nature communications* 8:14893
- Jaremko L, Jaremko M, Giller K, Becker S, Zweckstetter M (2014) Structure of the mitochondrial translocator protein in complex with a diagnostic ligand. *Science* 343 (6177):1363-1366
- Jellinger KA (2018) Is Braak staging valid for all types of Parkinson's disease? *Journal of Neural Transmission*:1-9
- Jenner P (2003) The contribution of the MPTP-treated primate model to the development of new treatment strategies for Parkinson's disease. *Parkinsonism & related disorders* 9 (3):131-137
- Jiang D, Niwa M, Koong AC Targeting the IRE1 $\alpha$ -XBP1 branch of the unfolded protein response in human diseases. In: *Seminars in cancer biology*, 2015. Elsevier, pp 48-56
- Joniec-Maciejak I, Ciesielska A, Wawer A, Szejder-Pacholek A, Schwenkgrub J, Cudna A, Hadaczek P, Bankiewicz KS, Członkowska A, Członkowski A (2014) The influence of AAV2-mediated gene transfer of human IL-10 on neurodegeneration and immune response in a murine model of Parkinson's disease. *Pharmacological reports* 66 (4):660-669
- Juárez Olguín H, Calderón Guzmán D, Hernández García E, Barragán Mejía G (2016) The role of dopamine and its dysfunction as a consequence of oxidative stress. *Oxidative medicine and cellular longevity* 2016
- Karchewski LA, Bloechlinger S, Woolf CJ (2004) Axonal injury-dependent induction of the peripheral benzodiazepine receptor in small-diameter adult rat primary sensory neurons. *European Journal of Neuroscience* 20 (3):671-683
- Karlstetter M, Nothdurfter C, Aslanidis A, Moeller K, Horn F, Scholz R, Neumann H, Weber BH, Rupprecht R, Langmann T (2014) Translocator protein (18 kDa)(TSPO) is expressed in reactive retinal microglia and modulates microglial inflammation and phagocytosis. *Journal of neuroinflammation* 11 (1):3
- Kaushik S, Cuervo AM (2015) Proteostasis and aging. *Nature medicine* 21 (12):1406
- Kawanokuchi J, Mizuno T, Takeuchi H, Kato H, Wang J, Mitsuma N, Suzumura A (2006) Production of interferon- $\gamma$  by microglia. *Multiple Sclerosis Journal* 12 (5):558-564
- Keller AF, Gravel M, Kriz J (2011) Treatment with minocycline after disease onset alters astrocyte reactivity and increases microgliosis in SOD1 mutant mice. *Experimental neurology* 228 (1):69-79
- Kemp DE, Ismail-Beigi F, Ganocy SJ, Conroy C, Gao K, Obral S, Fein E, Findling RL, Calabrese JR (2012) Use of insulin sensitizers for the treatment of major depressive disorder: a pilot study of pioglitazone for major depression accompanied by abdominal obesity. *Journal of Affective Disorders* 136 (3):1164-1173
- Khan MM, Kempuraj D, Thangavel R, Zaheer A (2013) Protection of MPTP-induced neuroinflammation and neurodegeneration by Pycnogenol. *Neurochemistry international* 62 (4):379-388

- Khasnavis S, Ghosh A, Roy A, Pahan K (2013) Castration induces Parkinson disease pathologies in young male mice via inducible nitric-oxide synthase. *Journal of Biological Chemistry* 288 (29):20843-20855
- Kierdorf K, Prinz M (2013) Factors regulating microglia activation. *Frontiers in cellular neuroscience* 7:44
- Kigerl KA, Gensel JC, Ankeny DP, Alexander JK, Donnelly DJ, Popovich PG (2009) Identification of two distinct macrophage subsets with divergent effects causing either neurotoxicity or regeneration in the injured mouse spinal cord. *Journal of Neuroscience* 29 (43):13435-13444
- Kim B, Yang M-S, Choi D, Kim J-H, Kim H-S, Seol W, Choi S, Jou I, Kim E-Y, Joe E-h (2012) Impaired inflammatory responses in murine Lrrk2-knockdown brain microglia. *PloS one* 7 (4):e34693
- Kim C, Ho D-H, Suk J-E, You S, Michael S, Kang J, Lee SJ, Masliah E, Hwang D, Lee H-J (2013) Neuron-released oligomeric  $\alpha$ -synuclein is an endogenous agonist of TLR2 for paracrine activation of microglia. *Nature communications* 4:1562
- Kim C, Ojo-Amaize E, Spencer B, Rockenstein E, Mante M, Desplats P, Wrasidlo W, Adame A, Nchekwube E, Oyemade O (2015) Hypoestoxide reduces neuroinflammation and  $\alpha$ -synuclein accumulation in a mouse model of Parkinson's disease. *Journal of neuroinflammation* 12 (1):236
- Kim SN, Son SC, Lee SM, Kim CS, Yoo DG, Lee SK, Hur GM, Park JB, Jeon BH (2006) Midazolam inhibits proinflammatory mediators in the lipopolysaccharide-activated macrophage. *Anesthesiology: The Journal of the American Society of Anesthesiologists* 105 (1):105-110
- Kim WS, Kågedal K, Halliday GM (2014) Alpha-synuclein biology in Lewy body diseases. *Alzheimer's research & therapy* 6 (5):73
- Kirov S, Ji R, Wang J, Zhang B (2014) Functional annotation of differentially regulated gene set using WebGestalt: a gene set predictive of response to ipilimumab in tumor biopsies. *Methods Mol Biol* 1101:31-42. doi:10.1007/978-1-62703-721-1\_3
- Kita A, Kinoshita T, Kohayakawa H, Furukawa K, Akaike A (2009) Lack of tolerance to anxiolysis and withdrawal symptoms in mice repeatedly treated with AC-5216, a selective TSPO ligand. *Progress in neuro-psychopharmacology & biological psychiatry* 33 (6):1040-1045
- Kita A, Kohayakawa H, Kinoshita T, Ochi Y, Nakamichi K, Kurumiya S, Furukawa K, Oka M (2004) Antianxiety and antidepressant-like effects of AC-5216, a novel mitochondrial benzodiazepine receptor ligand. *British journal of pharmacology* 142 (7):1059-1072
- Klemann CJ, Martens GJ, Poelmans G, Visser JE (2016) Validity of the MPTP-treated mouse as a model for Parkinson's disease. *Molecular neurobiology* 53 (3):1625-1636
- Kondratiuk I, Devijver H, Lechat B, Van Leuven F, Kaczmarek L, Filipkowski RK (2013) Glycogen synthase kinase-3 $\beta$  affects size of dentate gyrus and species-typical behavioral tasks in transgenic and knockout mice. *Behavioural brain research* 248:46-50
- Kopin I, Markey S (1988) MPTP toxicity: implications for research in Parkinson's disease. *Annual review of neuroscience* 11 (1):81-96
- Koprich JB, Kalia LV, Brotchie JM (2017) Animal models of  $\alpha$ -synucleinopathy for Parkinson disease drug development. *Nature Reviews Neuroscience* 18 (9):515
- Koshimori Y, Ko J-H, Mizrahi R, Rusjan P, Mabrouk R, Jacobs MF, Christopher L, Hamani C, Lang AE, Wilson AA (2015) Imaging striatal microglial activation in patients with Parkinson's disease. *PLoS One* 10 (9):e0138721
- Krug AK, Gutbier S, Zhao L, Poltl D, Kullmann C, Ivanova V, Forster S, Jagtap S, Meiser J, Lepar G, Schildknecht S, Adam M, Hiller K, Farhan H, Brunner T, Hartung T, Sachinidis A, Leist M (2014) Transcriptional and metabolic adaptation of human neurons to the mitochondrial toxicant MPP(+). *Cell death & disease* 5:e1222. doi:10.1038/cddis.2014.166
- Krüger R, Kuhn W, Müller T, Woitalla D, Graeber M, Kösel S, Przuntek H, Epplen JT, Schols L, Riess O (1998) AlaSOPro mutation in the gene encoding  $\alpha$ -synuclein in Parkinson's disease. *Nature genetics* 18 (2):106
- Kuo H-C, Lu C-C, Shen C-H, Tung S-Y, Hsieh MC, Lee K-C, Lee L-Y, Chen C-C, Teng C-C, Huang W-S (2016) *Hericium erinaceus* mycelium and its isolated erinacine A protection from MPTP-

- induced neurotoxicity through the ER stress, triggering an apoptosis cascade. *Journal of translational medicine* 14 (1):78
- Kusumi M, Nakashima K, Harada H, Nakayama H, Takahashi K (1996) Epidemiology of Parkinson's disease in Yonago City, Japan: comparison with a study carried out 12 years ago. *Neuroepidemiology* 15 (4):201-207
- Kwon M, Sung M, Kwon Y-J, Song YG, Lee S-W, Park M-C, Park Y-B, Lee S-K, Song JJ (2014) Active tuberculosis risk with tumor necrosis factor inhibitors after treating latent tuberculosis. *JCR: Journal of Clinical Rheumatology* 20 (2):68-73
- Lacapere J-J, Papadopoulos V (2003) Peripheral-type benzodiazepine receptor: structure and function of a cholesterol-binding protein in steroid and bile acid biosynthesis. *Steroids* 68 (7-8):569-585
- Langston JW (1985) The case of the tainted heroin. *The Sciences* 25 (1):34-42
- Langston JW, Ballard P, Tetrad JW, Irwin I (1983) Chronic Parkinsonism in humans due to a product of meperidine-analog synthesis. *Science* 219 (4587):979-980
- Lawson L, Perry V, Dri P, Gordon S (1990) Heterogeneity in the distribution and morphology of microglia in the normal adult mouse brain. *Neuroscience* 39 (1):151-170
- Le B, Chen H, Zirkin B, Burnett A (2014) New targets for increasing endogenous testosterone production: clinical implications and review of the literature. *Andrology* 2 (4):484-490
- Le Fur G, Perrier M, Vaucher N, Imbault F, Flamier A, Benavides J, Uzan A, Renault C, Dubroeuq M, Gueremy C (1983a) Peripheral benzodiazepine binding sites: effect of PK 11195, 1-(2-chlorophenyl)-N-methyl-N-(1-methylpropyl)-3-isoquinolinecarboxamide: I. In vitro studies. *Life sciences* 32 (16):1839-1847
- Le Fur G, Vaucher N, Perrier M, Flamier A, Benavides J, Renault C, Dubroeuq M, Gueremy C, Uzan A (1983b) Differentiation between two ligands for peripheral benzodiazepine binding sites, [3H] R05-4864 and [3H] PK 11195, by thermodynamic studies. *Life sciences* 33 (5):449-457
- Lee Y, Dawson VL, Dawson TM (2012) Animal models of Parkinson's disease: vertebrate genetics. *Cold Spring Harbor perspectives in medicine* 2 (10):a009324
- Leibson CL, Long KH, Maraganore DM, Bower JH, Ransom JE, O'Brien PC, Rocca WA (2006) Direct medical costs associated with Parkinson's disease: A population-based study. *Movement disorders: official journal of the Movement Disorder Society* 21 (11):1864-1871
- Lesage S, Anheim M, Letournel F, Bousset L, Honoré A, Rozas N, Pieri L, Madiona K, Dürr A, Melki R (2013) G51D  $\alpha$ -synuclein mutation causes a novel Parkinsonian-pyramidal syndrome. *Annals of neurology* 73 (4):459-471
- Leva G, Klein C, Benyounes J, Hallé F, Bihel F, Collongues N, De Seze J, Mensah-Nyagan A-G, Patte-Mensah C (2017) The translocator protein ligand XBD173 improves clinical symptoms and neuropathological markers in the SJL/J mouse model of multiple sclerosis. *Biochimica et Biophysica Acta (BBA)-Molecular Basis of Disease* 1863 (12):3016-3027
- Lewy F, Handb H (1912) Dementia with Lewy bodies. *Neurol*,
- Li F, Liu J, Zheng Y, Garavito RM, Ferguson-Miller S (2015) Crystal structures of translocator protein (TSPO) and mutant mimic of a human polymorphism. *Science* 347 (6221):555-558
- Li F, Xia Y, Meiler J, Ferguson-Miller S (2013) Characterization and modeling of the oligomeric state and ligand binding behavior of purified translocator protein 18 kDa from *Rhodobacter sphaeroides*. *Biochemistry* 52 (34):5884-5899
- Li H, Degenhardt B, Tobin D, Yao Z-x, Tasken K, Papadopoulos V (2001a) Identification, localization, and function in steroidogenesis of PAP7: a peripheral-type benzodiazepine receptor-and PKA (RI $\alpha$ )-associated protein. *Molecular Endocrinology* 15 (12):2211-2228
- Li H, Yao Z-x, Degenhardt B, Teper G, Papadopoulos V (2001b) Cholesterol binding at the cholesterol recognition/interaction amino acid consensus (CRAC) of the peripheral-type benzodiazepine receptor and inhibition of steroidogenesis by an HIV TAT-CRAC peptide. *Proceedings of the National Academy of Sciences* 98 (3):1267-1272

- Li Q, Cheng Z, Zhou L, Darmanis S, Neff NF, Okamoto J, Gulati G, Bennett ML, Sun LO, Clarke LE (2019) Developmental heterogeneity of microglia and brain myeloid cells revealed by deep single-cell RNA sequencing. *Neuron* 101 (2):207-223. e210
- Li Y, Tomiyama H, Sato K, Hatano Y, Yoshino H, Atsumi M, Kitaguchi M, Sasaki S, Kawaguchi S, Miyajima H (2005) Clinicogenetic study of PINK1 mutations in autosomal recessive early-onset parkinsonism. *Neurology* 64 (11):1955-1957
- Lin R, Rittenhouse D, Sweeney K, Potluri P, Wallace DC (2015) TSPO, a mitochondrial outer membrane protein, controls ethanol-related behaviors in *Drosophila*. *PLoS genetics* 11 (8):e1005366
- Liu J, Rone MB, Papadopoulos V (2006) Protein-protein interactions mediate mitochondrial cholesterol transport and steroid biosynthesis. *Journal of Biological Chemistry* 281 (50):38879-38893
- Liu M, Bachstetter AD, Cass WA, Lifshitz J, Bing G (2017) Pioglitazone attenuates neuroinflammation and promotes dopaminergic neuronal survival in the nigrostriatal system of rats after diffuse brain injury. *Journal of neurotrauma* 34 (2):414-422
- Lix LM, Hobson DE, Azimaee M, Leslie WD, Burchill C, Hobson S (2010) Socioeconomic variations in the prevalence and incidence of Parkinson's disease: a population-based analysis. *Journal of Epidemiology & Community Health* 64 (4):335-340
- Loane DJ, Byrnes KR (2010) Role of microglia in neurotrauma. *Neurotherapeutics* 7 (4):366-377
- Logan T, Bendor J, Toupin C, Thorn K, Edwards RH (2017)  $\alpha$ -Synuclein promotes dilation of the exocytotic fusion pore. *Nature neuroscience* 20 (5):681
- Lotharius J, Barg S, Wiekop P, Lundberg C, Raymon HK, Brundin P (2002) Effect of mutant alpha-synuclein on dopamine homeostasis in a new human mesencephalic cell line. *J Biol Chem* 277 (41):38884-38894. doi:10.1074/jbc.M205518200
- Love MI, Huber W, Anders S (2014) Moderated estimation of fold change and dispersion for RNA-seq data with DESeq2. *Genome biology* 15 (12):550
- Lu J, Cao Q, Zheng D, Sun Y, Wang C, Yu X, Wang Y, Lee VW, Zheng G, Tan TK (2013) Discrete functions of M2a and M2c macrophage subsets determine their relative efficacy in treating chronic kidney disease. *Kidney international* 84 (4):745-755
- Luchtman DW, Shao D, Song C (2009) Behavior, neurotransmitters and inflammation in three regimens of the MPTP mouse model of Parkinson's disease. *Physiology & behavior* 98 (1-2):130-138
- Lücking CB, Dürr A, Bonifati V, Vaughan J, De Michele G, Gasser T, Harhangi BS, Meo G, Denèfle P, Wood NW (2000) Association between early-onset Parkinson's disease and mutations in the parkin gene. *New England Journal of Medicine* 342 (21):1560-1567
- Luthman J, Fredriksson A, Sundström E, Jonsson G, Archer T (1989) Selective lesion of central dopamine or noradrenaline neuron systems in the neonatal rat: motor behavior and monoamine alterations at adult stage. *Behavioural brain research* 33 (3):267-277
- Ma B, Xu L, Pan X, Sun L, Ding J, Xie C, Koliatsos VE, Cai H (2016) LRRK2 modulates microglial activity through regulation of chemokine (C-X3-C) receptor 1-mediated signalling pathways. *Human molecular genetics* 25 (16):3515-3523
- Machado MMF, Bassani TB, Cópola-Segovia V, Moura ELR, Zanata SM, Andreatini R, Vital MABF (2018) PPAR- $\gamma$  agonist pioglitazone reduces microglial proliferation and NF- $\kappa$ B activation in the substantia nigra in the 6-hydroxydopamine model of Parkinson's disease. *Pharmacological Reports*
- Maeda J, Higuchi M, Inaji M, Ji B, Haneda E, Okauchi T, Zhang M-R, Suzuki K, Suhara T (2007) Phase-dependent roles of reactive microglia and astrocytes in nervous system injury as delineated by imaging of peripheral benzodiazepine receptor. *Brain research* 1157:100-111
- Mahad DJ, Ransohoff RM The role of MCP-1 (CCL2) and CCR2 in multiple sclerosis and experimental autoimmune encephalomyelitis (EAE). In: *Seminars in immunology*, 2003. vol 1. Elsevier, pp 23-32
- Marinus J, Zhu K, Marras C, Aarsland D, van Hilten JJ (2018) Risk factors for non-motor symptoms in Parkinson's disease. *The Lancet Neurology*

- Martin J, Franck M, Fischer M, Spies C (2006) Sedation and analgesia in German intensive care units: how is it done in reality? Results of a patient-based survey of analgesia and sedation. *Intensive care medicine* 32 (8):1137-1142
- Martinez-Vicente M, Talloczy Z, Kaushik S, Massey AC, Mazzulli J, Mosharov EV, Hodara R, Fredenburg R, Wu D-C, Follenzi A (2008) Dopamine-modified  $\alpha$ -synuclein blocks chaperone-mediated autophagy. *The Journal of clinical investigation* 118 (2):777-788
- Martinez FO, Gordon S (2014) The M1 and M2 paradigm of macrophage activation: time for reassessment. *F1000prime reports* 6
- Martinez FO, Helming L, Milde R, Varin A, Melgert BN, Draijer C, Thomas B, Fabbri M, Crawshaw A, Ho LP (2013) Genetic programs expressed in resting and IL-4 alternatively activated mouse and human macrophages: similarities and differences. *Blood: blood-2012-2006-436212*
- Martinez TN, Greenamyre JT (2012) Toxin models of mitochondrial dysfunction in Parkinson's disease. *Antioxidants & redox signaling* 16 (9):920-934
- Mascarenhas JO, Cross NC, Mesa RA (2014) The future of JAK inhibition in myelofibrosis and beyond. *Blood reviews* 28 (5):189-196
- Masuda-Suzukake M, Nonaka T, Hosokawa M, Oikawa T, Arai T, Akiyama H, Mann DM, Hasegawa M (2013) Prion-like spreading of pathological  $\alpha$ -synuclein in brain. *Brain* 136 (4):1128-1138
- Masuda T, Sankowski R, Staszewski O, Böttcher C, Amann L, Scheiwe C, Nessler S, Kunz P, van Loo G, Coenen VA (2019) Spatial and temporal heterogeneity of mouse and human microglia at single-cell resolution. *Nature*:1
- Matus S, Glimcher LH, Hetz C (2011) Protein folding stress in neurodegenerative diseases: a glimpse into the ER. *Current opinion in cell biology* 23 (2):239-252
- McCormack AL, Thiruchelvam M, Manning-Bog AB, Thiffault C, Langston JW, Cory-Slechta DA, Di Monte DA (2002) Environmental risk factors and Parkinson's disease: selective degeneration of nigral dopaminergic neurons caused by the herbicide paraquat. *Neurobiology of disease* 10 (2):119-127
- McCoy MK, Ruhn KA, Martinez TN, McAlpine FE, Blesch A, Tansey MG (2008) Intranigral lentiviral delivery of dominant-negative TNF attenuates neurodegeneration and behavioral deficits in hemiparkinsonian rats. *Molecular Therapy* 16 (9):1572-1579
- McDowell K, Chesselet M-F (2012) Animal models of the non-motor features of Parkinson's disease. *Neurobiology of disease* 46 (3):597-606
- McGeer P, Itagaki S, Boyes B, McGeer E (1988) Reactive microglia are positive for HLA-DR in the substantia nigra of Parkinson's and Alzheimer's disease brains. *Neurology* 38 (8):1285-1285
- McManus RM, Heneka MT (2017) Role of neuroinflammation in neurodegeneration: new insights. *Alzheimer's research & therapy* 9 (1):14
- Meiser J, Weindl D, Hiller K (2013) Complexity of dopamine metabolism. *Cell Communication and Signaling* 11 (1):34
- Mercado G, Castillo V, Vidal R, Hetz C (2015) ER proteostasis disturbances in Parkinson's disease: novel insights. *Frontiers in aging neuroscience* 7:39
- Meredith GE, Kang UJ (2006) Behavioral models of Parkinson's disease in rodents: a new look at an old problem. *Movement disorders* 21 (10):1595-1606
- Meredith GE, Rademacher DJ (2011) MPTP mouse models of Parkinson's disease: an update. *Journal of Parkinson's disease* 1 (1):19-33
- Michel PP, Hirsch EC, Hunot S (2016) Understanding dopaminergic cell death pathways in Parkinson disease. *Neuron* 90 (4):675-691
- Michell-Robinson MA, Touil H, Healy LM, Owen DR, Durafour BA, Bar-Or A, Antel JP, Moore CS (2015) Roles of microglia in brain development, tissue maintenance and repair. *Brain* 138 (5):1138-1159
- Michelucci A, Heurtaux T, Grandbarbe L, Morga E, Heuschling P (2009) Characterization of the microglial phenotype under specific pro-inflammatory and anti-inflammatory conditions: effects of oligomeric and fibrillar amyloid- $\beta$ . *Journal of neuroimmunology* 210 (1-2):3-12
- Miller GW (2007) Paraquat: the red herring of Parkinson's disease research. Oxford University Press,

- Mitra N, Mohanakumar K, Ganguly D (1994) Resistance of Golden Hamster to 1-Methyl-4-Phenyl-1, 2, 3, 6 Tetrahydropyridine: Relationship with Low Levels of Regional Monoamine Oxidase B. *Journal of neurochemistry* 62 (5):1906-1912
- Mittelbronn M, Dietz K, Schluesener H, Meyermann R (2001) Local distribution of microglia in the normal adult human central nervous system differs by up to one order of magnitude. *Acta neuropathologica* 101 (3):249-255
- Mocchetti I, Santi M (1991) Diazepam binding inhibitor peptide: cloning and gene expression. *Neuropharmacology* 30 (12):1365-1371
- Moehle MS, Webber PJ, Tse T, Sukar N, Standaert DG, DeSilva TM, Cowell RM, West AB (2012) LRRK2 inhibition attenuates microglial inflammatory responses. *Journal of Neuroscience* 32 (5):1602-1611
- Morales-García JA, Susín C, Alonso-Gil S, Pérez DI, Palomo V, Pérez C, Conde S, Santos A, Gil C, Martínez A (2012) Glycogen synthase kinase-3 inhibitors as potent therapeutic agents for the treatment of Parkinson disease. *ACS chemical neuroscience* 4 (2):350-360
- Moreno JA, Halliday M, Molloy C, Radford H, Verity N, Axten JM, Ortori CA, Willis AE, Fischer PM, Barrett DA (2013) Oral treatment targeting the unfolded protein response prevents neurodegeneration and clinical disease in prion-infected mice. *Science translational medicine* 5 (206):206ra138-206ra138
- Mount MP, Lira A, Grimes D, Smith PD, Faucher S, Slack R, Anisman H, Hayley S, Park DS (2007) Involvement of interferon-gamma in microglial-mediated loss of dopaminergic neurons. *J Neurosci* 27 (12):3328-3337. doi:10.1523/JNEUROSCI.5321-06.2007
- Murray CJ, Vos T, Lozano R, Naghavi M, Flaxman AD, Michaud C, Ezzati M, Shibuya K, Salomon JA, Abdalla S (2012) Disability-adjusted life years (DALYs) for 291 diseases and injuries in 21 regions, 1990–2010: a systematic analysis for the Global Burden of Disease Study 2010. *The lancet* 380 (9859):2197-2223
- Nakagawa Y, Chiba K (2015) Diversity and plasticity of microglial cells in psychiatric and neurological disorders. *Pharmacology & therapeutics* 154:21-35
- Nalls MA, Pankratz N, Lill CM, Do CB, Hernandez DG, Saad M, DeStefano AL, Kara E, Bras J, Sharma M (2014) Large-scale meta-analysis of genome-wide association data identifies six new risk loci for Parkinson's disease. *Nature genetics* 46 (9):989
- Neurath M (2014) New targets for mucosal healing and therapy in inflammatory bowel diseases. *Mucosal immunology* 7 (1):6
- Nicklas W, Vyas I, Heikkila RE (1985) Inhibition of NADH-linked oxidation in brain mitochondria by 1-methyl-4-phenyl-pyridine, a metabolite of the neurotoxin, 1-methyl-4-phenyl-1, 2, 5, 6-tetrahydropyridine. *Life sciences* 36 (26):2503-2508
- Nimmerjahn A, Kirchhoff F, Helmchen F (2005) Resting microglial cells are highly dynamic surveillants of brain parenchyma in vivo. *Science* 308 (5726):1314-1318
- Ning B, Deng M, Zhang Q, Wang N, Fang Y (2016)  $\beta$ -Asarone inhibits IRE1/XBP1 endoplasmic reticulum stress pathway in 6-OHDA-induced Parkinsonian rats. *Neurochemical research* 41 (8):2097-2101
- Nishijima H, Suzuki S, Kon T, Funamizu Y, Ueno T, Haga R, Suzuki C, Arai A, Kimura T, Suzuki C (2014) Morphologic changes of dendritic spines of striatal neurons in the levodopa-induced dyskinesia model. *Movement Disorders* 29 (3):336-343
- Nuber S, Rajsombath M, Minakaki G, Winkler J, Müller CP, Ericsson M, Caldarone B, Dettmer U, Selkoe DJ (2018) Abrogating native  $\alpha$ -synuclein tetramers in mice causes a L-DOPA-responsive motor syndrome closely resembling Parkinson's disease. *Neuron* 100 (1):75-90. e75
- Ogawa N, Hirose Y, Ohara S, Ono T, Watanabe Y (1985) A simple quantitative bradykinesia test in MPTP-treated mice. *Research communications in chemical pathology and pharmacology* 50 (3):435-441
- Olah M, Biber K, Vinet J, Wgm Boddeke H (2011) Microglia phenotype diversity. *CNS & Neurological Disorders-Drug Targets (Formerly Current Drug Targets-CNS & Neurological Disorders)* 10 (1):108-118

- Oliveras-Salvá M, Van der Perren A, Casadei N, Stroobants S, Nuber S, D'Hooge R, Van den Haute C, Baekelandt V (2013) rAAV2/7 vector-mediated overexpression of alpha-synuclein in mouse substantia nigra induces protein aggregation and progressive dose-dependent neurodegeneration. *Molecular neurodegeneration* 8 (1):44
- Oliveros JC (2007-2015) Venny. An interactive tool for comparing lists with Venn's diagrams. <http://bioinfogpcnbsices/tools/venny/indexhtml>
- Ouchi Y, Yoshikawa E, Sekine Y, Futatsubashi M, Kanno T, Ogusu T, Torizuka T (2005) Microglial activation and dopamine terminal loss in early Parkinson's disease. *Annals of neurology* 57 (2):168-175
- Owen DR, Fan J, Campioli E, Venugopal S, Midzak A, Daly E, Harlay A, Issop L, Libri V, Kalogiannopoulou D (2017) TSPO mutations in rats and a human polymorphism impair the rate of steroid synthesis. *Biochemical Journal* 474 (23):3985-3999
- Owen DR, Lewis AJ, Reynolds R, Rupprecht R, Eser D, Wilkins MR, Bennacef I, Nutt DJ, Parker CA (2011) Variation in binding affinity of the novel anxiolytic XBD173 for the 18 kDa translocator protein in human brain. *Synapse* 65 (3):257-259
- Owen DR, Yeo AJ, Gunn RN, Song K, Wadsworth G, Lewis A, Rhodes C, Pulford DJ, Bennacef I, Parker CA (2012) An 18-kDa translocator protein (TSPO) polymorphism explains differences in binding affinity of the PET radioligand PBR28. *Journal of Cerebral Blood Flow & Metabolism* 32 (1):1-5
- Pankratz N, Pauciulo MW, Elsaesser VE, Marek DK, Halter CA, Wojcieszek J, Rudolph A, Shults CW, Foroud T, Nichols WC (2006) Mutations in DJ-1 are rare in familial Parkinson disease. *Neuroscience letters* 408 (3):209-213
- Paolicelli R, Bolasco G, Pagnani F, Maggi L, Scianni M (2011) Synaptic Pruning by Microglia Is Necessary for Normal Brain Development. *Science*.
- Papadopoulos V, Amri H, Boujrad N, Cascio C, Culty M, Garnier M, Hardwick M, Li H, Vidic B, Brown A (1997) Peripheral benzodiazepine receptor in cholesterol transport and steroidogenesis. *Steroids* 62 (1):21-28
- Papadopoulos V, Baraldi M, Guilarte TR, Knudsen TB, Lacapère J-J, Lindemann P, Norenberg MD, Nutt D, Weizman A, Zhang M-R (2006) Translocator protein (18 kDa): new nomenclature for the peripheral-type benzodiazepine receptor based on its structure and molecular function. *Trends in pharmacological sciences* 27 (8):402-409
- Papadopoulos V, Berkovich A, Krueger K, Costa E, Guidotti A (1991) Diazepam binding inhibitor and its processing products stimulate mitochondrial steroid biosynthesis via an interaction with mitochondrial benzodiazepine receptors. *Endocrinology* 129 (3):1481-1488
- Papadopoulos V, Fan J, Zirkin B (2018) Translocator protein (18 kDa): an update on its function in steroidogenesis. *Journal of neuroendocrinology* 30 (2):e12500
- Papadopoulos V, Lecanu L (2009) Translocator protein (18 kDa) TSPO: an emerging therapeutic target in neurotrauma. *Experimental neurology* 219 (1):53-57
- Papadopoulos V, Liu J, Culty M (2007) Is there a mitochondrial signaling complex facilitating cholesterol import? *Molecular and cellular endocrinology* 265:59-64
- Parkinson J (1997) An Essay on the Shaking Palsy (Sherwood, Neely, and Jones, London, 1817); MH Polymeropoulos, et al. *Science* 276:2045-2047
- Parkinson J (2002) An essay on the shaking palsy. *The Journal of neuropsychiatry and clinical neurosciences* 14 (2):223-236
- Pena-Altamira E, Prati F, Massenzio F, Virgili M, Contestabile A, Bolognesi ML, Monti B (2016) Changing paradigm to target microglia in neurodegenerative diseases: from anti-inflammatory strategy to active immunomodulation. *Expert opinion on therapeutic targets* 20 (5):627-640
- Pennathur S, Jackson-Lewis V, Przedborski S, Heinecke JW (1999) Mass spectrometric quantification of 3-nitrotyrosine, ortho-tyrosine, and o, o'-dityrosine in brain tissue of 1-methyl-4-phenyl-1, 2, 3, 6-tetrahydropyridine-treated mice, a model of oxidative stress in Parkinson's disease. *Journal of Biological Chemistry* 274 (49):34621-34628

- Peter I, Dubinsky M, Bressman S, Park A, Lu C, Chen N, Wang A (2018) Anti-tumor necrosis factor therapy and incidence of Parkinson disease among patients with inflammatory bowel disease. *JAMA neurology* 75 (8):939-946
- Philippens IH (2018) Refinement of the MPTP model for Parkinson's disease in the marmoset. *Drug Discovery Today: Disease Models*
- Pinter B, Diem-Zangerl A, Wenning GK, Scherfler C, Oberaigner W, Seppi K, Poewe W (2015) Mortality in Parkinson's disease: a 38-year follow-up study. *Movement Disorders* 30 (2):266-269
- Plimack ER, LoRusso PM, McCoon P, Tang W, Krebs AD, Curt G, Eckhardt SG (2013) AZD1480: a phase I study of a novel JAK2 inhibitor in solid tumors. *The oncologist* 18 (7):819-820
- Poewe W, Seppi K, Tanner CM, Halliday GM, Brundin P, Volkmann J, Schrag A-E, Lang AE (2017) Parkinson disease. *Nature reviews Disease primers* 3:17013
- Polymeropoulos MH, Higgins JJ, Golbe LI, Johnson WG, Ide SE, Di Iorio G, Sanges G, Stenroos ES, Pho LT, Schaffer AA (1996) Mapping of a gene for Parkinson's disease to chromosome 4q21-q23. *Science* 274 (5290):1197-1199
- Polymeropoulos MH, Lavedan C, Leroy E, Ide SE, Dehejia A, Dutra A, Pike B, Root H, Rubenstein J, Boyer R (1997) Mutation in the  $\alpha$ -synuclein gene identified in families with Parkinson's disease. *science* 276 (5321):2045-2047
- Ponomarev ED, Maresz K, Tan Y, Dittel BN (2007) CNS-derived interleukin-4 is essential for the regulation of autoimmune inflammation and induces a state of alternative activation in microglial cells. *Journal of Neuroscience* 27 (40):10714-10721
- Potashkin J, Blume S, Runkle N (2011) Limitations of animal models of Parkinson's disease. *Parkinson's disease* 2011
- Prati F, De Simone A, Armirotti A, Summa M, Pizzirani D, Scarpelli R, Bertozzi SM, Perez DI, Andrisano V, Perez-Castillo A (2015) 3, 4-Dihydro-1, 3, 5-triazin-2 (1 H)-ones as the First Dual BACE-1/GSK-3 $\beta$  Fragment Hits against Alzheimer's Disease. *ACS chemical neuroscience* 6 (10):1665-1682
- Pringsheim T, Jette N, Frolkis A, Steeves TD (2014) The prevalence of Parkinson's disease: A systematic review and meta-analysis. *Movement disorders* 29 (13):1583-1590
- Purisai MG, McCormack AL, Langston WJ, Johnston LC, Di Monte DA (2005)  $\alpha$ -Synuclein expression in the substantia nigra of MPTP-lesioned non-human primates. *Neurobiology of disease* 20 (3):898-906
- Qin H, Buckley JA, Li X, Liu Y, Fox TH, Meares GP, Yu H, Yan Z, Harms AS, Li Y (2016) Inhibition of the JAK/STAT pathway protects against  $\alpha$ -synuclein-induced neuroinflammation and dopaminergic neurodegeneration. *Journal of Neuroscience* 36 (18):5144-5159
- Quinn L, Crook B, Hows M, Vidgeon-Hart M, Chapman H, Upton N, Medhurst A, Virley D (2008) The PPAR $\gamma$  agonist pioglitazone is effective in the MPTP mouse model of Parkinson's disease through inhibition of monoamine oxidase B. *British journal of pharmacology* 154 (1):226-233
- Ransohoff RM (2016) How neuroinflammation contributes to neurodegeneration. *Science* 353 (6301):777-783
- Rashid K, Geissl L, Wolf A, Karlstetter M, Langmann T (2018a) Transcriptional regulation of Translocator protein (18 kDa)(TSPO) in microglia requires Pu. 1, Ap1 and Sp factors. *Biochimica et Biophysica Acta (BBA)-Gene Regulatory Mechanisms* 1861 (12):1119-1133
- Rashid K, Wolf A, Langmann T (2018b) Microglia activation and immunomodulatory therapies for retinal degenerations. *Frontiers in cellular neuroscience* 12
- Ravikumar B, Crawford D, Dellovade T, Savinainen A, Graham D, Liere P, Oudinet J-P, Webb M, Hering H (2016) Differential efficacy of the TSPO ligands etifoxine and XBD-173 in two rodent models of Multiple Sclerosis. *Neuropharmacology* 108:229-237
- Rees K, Stowe R, Patel S, Ives N, Breen K, Clarke CE, Ben-Shlomo Y (2011) Non-steroidal anti-inflammatory drugs as disease-modifying agents for Parkinson's disease: evidence from observational studies. *Cochrane Database of Systematic Reviews* (11)

- Riachi NJ, Harik SI (1988) Strain differences in systematic 1-methyl-4-phenyl-1, 2, 3, 6-tetrahydropyridine neurotoxicity in mice correlate best with monoamine oxidase activity at the blood-brain barrier. *Life sciences* 42 (23):2359-2363
- Romeo E, Cavallaro S, Korneyev A, Kozikowski A, Ma D, Polo A, Costa E, Guidotti A (1993) Stimulation of brain steroidogenesis by 2-aryl-indole-3-acetamide derivatives acting at the mitochondrial diazepam-binding inhibitor receptor complex. *Journal of Pharmacology and Experimental Therapeutics* 267 (1):462-471
- Rone MB, Fan J, Papadopoulos V (2009) Cholesterol transport in steroid biosynthesis: role of protein-protein interactions and implications in disease states. *Biochimica et Biophysica Acta (BBA)-Molecular and Cell Biology of Lipids* 1791 (7):646-658
- Roussakis A-A, Piccini P (2018) Molecular Imaging of Neuroinflammation in Idiopathic Parkinson's Disease. *International review of neurobiology* 141:347-363
- Rupprecht R, Papadopoulos V, Rammes G, Baghai TC, Fan J, Akula N, Groyer G, Adams D, Schumacher M (2010) Translocator protein (18 kDa)(TSPO) as a therapeutic target for neurological and psychiatric disorders. *Nature reviews Drug discovery* 9 (12):971
- Rupprecht R, Rammes G, Eser D, Baghai TC, Schüle C, Nothdurfter C, Troxler T, Gentsch C, Kalkman HO, Chaperon F (2009) Translocator protein (18 kD) as target for anxiolytics without benzodiazepine-like side effects. *Science* 325 (5939):490-493
- Saal K-A, Koch JC, Tatenhorst L, Szegő ÉM, Ribas VT, Michel U, Bähr M, Tönges L, Lingor P (2015) AAV. shRNA-mediated downregulation of ROCK2 attenuates degeneration of dopaminergic neurons in toxin-induced models of Parkinson's disease in vitro and in vivo. *Neurobiology of disease* 73:150-162
- Sado M, Yamasaki Y, Iwanaga T, Onaka Y, Ibuki T, Nishihara S, Mizuguchi H, Momota H, Kishibuchi R, Hashimoto T (2009a) Protective effect against Parkinson's disease-related insults through the activation of XBP1. *Brain research* 1257:16-24
- Sado M, Yamasaki Y, Iwanaga T, Onaka Y, Ibuki T, Nishihara S, Mizuguchi H, Momota H, Kishibuchi R, Hashimoto T, Wada D, Kitagawa H, Watanabe TK (2009b) Protective effect against Parkinson's disease-related insults through the activation of XBP1. *Brain Res* 1257:16-24. doi:10.1016/j.brainres.2008.11.104
- Sánchez-Mejorada G, Rosales C (1998) Signal transduction by immunoglobulin Fc receptors. *Journal of leukocyte biology* 63 (5):521-533
- Sato T, Hanyu H, Hirao K, Kanetaka H, Sakurai H, Iwamoto T (2011) Efficacy of PPAR- $\gamma$  agonist pioglitazone in mild Alzheimer disease. *Neurobiology of aging* 32 (9):1626-1633
- Savica R, Grossardt BR, Bower JH, Ahlskog JE, Rocca WA (2013) Incidence and pathology of synucleinopathies and tauopathies related to parkinsonism. *JAMA neurology* 70 (7):859-866
- Scalzo P, Kümmer A, Cardoso F, Teixeira AL (2010) Serum levels of interleukin-6 are elevated in patients with Parkinson's disease and correlate with physical performance. *Neuroscience letters* 468 (1):56-58
- Scarf AM, Ittner LM, Kassiou M (2009) The translocator protein (18 kDa): central nervous system disease and drug design. *Journal of medicinal chemistry* 52 (3):581-592
- Schallert T, Fleming SM, Leasure JL, Tillerson JL, Bland ST (2000) CNS plasticity and assessment of forelimb sensorimotor outcome in unilateral rat models of stroke, cortical ablation, parkinsonism and spinal cord injury. *neuropharmacology* 39 (5):777-787
- Schallert T, Tillerson JL (2000) Intervention strategies for degeneration of dopamine neurons in parkinsonism. In: *Central nervous system diseases*. Springer, pp 131-151
- Schapansky J, Nardozi JD, Felizia F, LaVoie MJ (2014) Membrane recruitment of endogenous LRRK2 precedes its potent regulation of autophagy. *Human molecular genetics* 23 (16):4201-4214
- Schapira A, Emre M, Jenner P, Poewe W (2009) Levodopa in the treatment of Parkinson's disease. *European Journal of Neurology* 16 (9):982-989
- Schapira AH, Chaudhuri KR, Jenner P (2017) Non-motor features of Parkinson disease. *Nature Reviews Neuroscience* 18 (7):435

- Schmid CD, Melchior B, Masek K, Puntambekar SS, Danielson PE, Lo DD, Gregor Sutcliffe J, Carson MJ (2009) Differential gene expression in LPS/IFN $\gamma$  activated microglia and macrophages: in vitro versus in vivo. *Journal of neurochemistry* 109:117-125
- Schmidt N, Ferger B (2001) Neurochemical findings in the MPTP model of Parkinson's disease. *Journal of neural transmission* 108 (11):1263-1282
- Scholz D, Pörtl D, Genewsky A, Weng M, Waldmann T, Schildknecht S, Leist M (2011) Rapid, complete and large-scale generation of post-mitotic neurons from the human LUHMES cell line. *Journal of neurochemistry* 119 (5):957-971
- Scholz R, Caramoy A, Bhuckory MB, Rashid K, Chen M, Xu H, Grimm C, Langmann T (2015) Targeting translocator protein (18 kDa)(TSPO) dampens pro-inflammatory microglia reactivity in the retina and protects from degeneration. *Journal of neuroinflammation* 12 (1):201
- Schweitzer PJ, Fallon BA, Mann JJ, Kumar JD (2010) PET tracers for the peripheral benzodiazepine receptor and uses thereof. *Drug discovery today* 15 (21-22):933-942
- Schwenkgrub J, Joniec-Maciejak I, Szejder-Pacholek A, Wawer A, Ciesielska A, Bankiewicz K, Członkowska A, Członkowski A (2013) Effect of human interleukin-10 on the expression of nitric oxide synthases in the MPTP-based model of Parkinson's disease. *Pharmacological Reports* 65 (1):44-49
- Sedelis M, Hofele K, Auburger GW, Morgan S, Huston JP, Schwarting RK (2000) MPTP susceptibility in the mouse: behavioral, neurochemical, and histological analysis of gender and strain differences. *Behavior genetics* 30 (3):171-182
- Selvaraj S, Sun Y, Watt JA, Wang S, Lei S, Birnbaumer L, Singh BB (2012) Neurotoxin-induced ER stress in mouse dopaminergic neurons involves downregulation of TRPC1 and inhibition of AKT/mTOR signaling. *The Journal of clinical investigation* 122 (4):1354-1367
- Selvaraj V, Tu LN (2016) Current status and future perspectives: TSPO in steroid neuroendocrinology. *Journal of Endocrinology* 231 (1):R1-R30
- Shechter R, London A, Varol C, Raposo C, Cusimano M, Yovel G, Rolls A, Mack M, Pluchino S, Martino G (2009) Infiltrating blood-derived macrophages are vital cells playing an anti-inflammatory role in recovery from spinal cord injury in mice. *PLoS medicine* 6 (7):e1000113
- Shechter R, Miller O, Yovel G, Rosenzweig N, London A, Ruckh J, Kim K-W, Klein E, Kalchenko V, Bendel P (2013) Recruitment of beneficial M2 macrophages to injured spinal cord is orchestrated by remote brain choroid plexus. *Immunity* 38 (3):555-569
- Sherer TB, Betarbet R, Testa CM, Seo BB, Richardson JR, Kim JH, Miller GW, Yagi T, Matsuno-Yagi A, Greenamyre JT (2003) Mechanism of toxicity in rotenone models of Parkinson's disease. *Journal of Neuroscience* 23 (34):10756-10764
- Shin J-H, Kim I-D, Kim S-W, Lee H-K, Jin Y, Park J-H, Kim T-K, Suh C-K, Kwak J, Lee K-H (2014) Ethyl pyruvate inhibits HMGB1 phosphorylation and release by chelating calcium. *Molecular Medicine* 20 (1):649
- Sigel E, Steinmann ME (2012) Structure, function, and modulation of GABAA receptors. *Journal of Biological Chemistry* 287 (48):40224-40231
- Simon-Sanchez J, Schulte C, Bras JM, Sharma M, Gibbs JR, Berg D, Paisan-Ruiz C, Lichtner P, Scholz SW, Hernandez DG (2009) Genome-wide association study reveals genetic risk underlying Parkinson's disease. *Nature genetics* 41 (12):1308
- Simuni T, Kieburtz K, Tilley B, Elm JJ, Ravina B, Babcock D, Emborg M, Feigin A, Zweig R, Ninds Exploratory Trials P (2015) Pioglitazone in early Parkinson's disease: a phase 2, multicentre, double-blind, randomised trial. *Lancet Neurology* 14 (8)
- Singleton A, Farrer M, Johnson J, Singleton A, Hague S, Kachergus J, Hulihan M, Peuralinna T, Dutra A, Nussbaum R (2003)  $\alpha$ -Synuclein locus triplication causes Parkinson's disease. *science* 302 (5646):841-841
- Smeyne RJ, Jackson-Lewis V (2005) The MPTP model of Parkinson's disease. *Molecular brain research* 134 (1):57-66

- Soldner F, Stelzer Y, Shivalila CS, Abraham BJ, Latourelle JC, Barrasa MI, Goldmann J, Myers RH, Young RA, Jaenisch R (2016) Parkinson-associated risk variant in distal enhancer of  $\alpha$ -synuclein modulates target gene expression. *Nature* 533 (7601):95
- Sonsalla PK, Heikkila RE (1986) The influence of dose and dosing interval on MPTP-induced dopaminergic neurotoxicity in mice. *European journal of pharmacology* 129 (3):339-345
- Spillantini MG, Schmidt ML, Lee VM-Y, Trojanowski JQ, Jakes R, Goedert M (1997)  $\alpha$ -Synuclein in Lewy bodies. *Nature* 388 (6645):839
- Sriram K, Matheson JM, Benkovic SA, Miller DB, Luster MI, O'CALLAGHAN JP (2002) Mice deficient in TNF receptors are protected against dopaminergic neurotoxicity: implications for Parkinson's disease. *The FASEB journal* 16 (11):1474-1476
- Steeland S, Gorlé N, Vandendriessche C, Balusu S, Brkic M, Van Cauwenberghe C, Van Imschoot G, Van Wonterghem E, De Rycke R, Kremer A (2018) Counteracting the effects of TNF receptor-1 has therapeutic potential in Alzheimer's disease. *EMBO molecular medicine* 10 (4):e8300
- Steeland S, Puimège L, Vandenbroucke RE, Van Hauwermeiren F, Haustaete J, Devoogdt N, Hulpiau P, Leroux-Roels G, Laukens D, Meuleman P (2015) Generation and characterization of small single domain antibodies inhibiting human tumor necrosis factor receptor 1. *Journal of Biological Chemistry* 290 (7):4022-4037
- Stevens B, Allen NJ, Vazquez LE, Howell GR, Christopherson KS, Nouri N, Micheva KD, Mehalow AK, Huberman AD, Stafford B (2007) The classical complement cascade mediates CNS synapse elimination. *Cell* 131 (6):1164-1178
- Subramaniam SR, Federoff HJ (2017) Targeting microglial activation states as a therapeutic avenue in Parkinson's disease. *Frontiers in aging neuroscience* 9:176
- Świątkiewicz M, Zaremba M, Joniec I, Członkowski A, Kurkowska-Jastrzębska I (2013) Potential neuroprotective effect of ibuprofen, insights from the mice model of Parkinson's disease. *Pharmacological reports* 65 (5):1227-1236
- Szegő ÉM, Gerhardt E, Outeiro TF (2017) Sirtuin 2 enhances dopaminergic differentiation via the AKT/GSK-3 $\beta$ / $\beta$ -catenin pathway. *Neurobiology of aging* 56:7-16
- Tabas I, Ron D (2011) Integrating the mechanisms of apoptosis induced by endoplasmic reticulum stress. *Nature cell biology* 13 (3):184
- Takai T (2002) Roles of Fc receptors in autoimmunity. *Nature reviews immunology* 2 (8):580
- Takeda K, Akira S TLR signaling pathways. In: *Seminars in immunology*, 2004. vol 1. Elsevier, pp 3-9
- Tanabe Y, Suehara Y, Kohsaka S, Hayashi T, Akaike K, Mukaihara K, Kurihara T, Kim Y, Okubo T, Ishii M, Kazuno S, Kaneko K, Saito T (2018) IRE1 $\alpha$ -XBP1 inhibitors exerted anti-tumor activities in Ewing's sarcoma. *Oncotarget* 9 (18):14428-14443. doi:10.18632/oncotarget.24467
- Tanner CM, Kamel F, Ross GW, Hoppin JA, Goldman SM, Korell M, Marras C, Bhudhikanok GS, Kasten M, Chade AR (2011) Rotenone, paraquat, and Parkinson's disease. *Environmental health perspectives* 119 (6):866-872
- Tatton N, Kish S (1997) In situ detection of apoptotic nuclei in the substantia nigra compacta of 1-methyl-4-phenyl-1, 2, 3, 6-tetrahydropyridine-treated mice using terminal deoxynucleotidyl transferase labelling and acridine orange staining. *Neuroscience* 77 (4):1037-1048
- Team R (2008) R: A language and environment for statistical computing. R foundation for statistical computing, Vienna, Austria
- Tillerson JL, Miller GW (2002) Book Review: Forced Limb-Use and Recovery following Brain Injury. *The Neuroscientist* 8 (6):574-585
- Tokay T, Hachem R, Masmoudi-Kouki O, Gandolfo P, Desrues L, Leprince J, Castel H, Diallo M, Amri M, Vaudry H (2008) Beta-amyloid peptide stimulates endozepine release in cultured rat astrocytes through activation of N-formyl peptide receptors. *Glia* 56 (13):1380-1389
- Tönges L, Frank T, Tatenhorst L, Saal KA, Koch JC, Szegő ÉM, Bähr M, Weishaupt JH, Lingor P (2012) Inhibition of rho kinase enhances survival of dopaminergic neurons and attenuates axonal loss in a mouse model of Parkinson's disease. *Brain* 135 (11):3355-3370

- Tremblay M-È, Lowery RL, Majewska AK (2010) Microglial interactions with synapses are modulated by visual experience. *PLoS biology* 8 (11):e1000527
- Trétiakoff C (1919) Contribution a l'etude de l'Anatomie pathologique du Locus Niger de Soemmering avec quelques deduction relatives a la pathogenie des troubles du tonus musculaire et de la maladie de Parkinson. Theses de Paris
- Tsai S-J, Kuo W-W, Liu W-H, Yin M-C (2010) Antioxidative and anti-inflammatory protection from carnosine in the striatum of MPTP-treated mice. *Journal of agricultural and food chemistry* 58 (21):11510-11516
- Tsika E, Glauser L, Moser R, Fiser A, Daniel G, Sheerin U-M, Lees A, Troncoso JC, Lewis PA, Bandopadhyay R (2014) Parkinson's disease-linked mutations in VPS35 induce dopaminergic neurodegeneration. *Human molecular genetics* 23 (17):4621-4638
- Tu LN, Morohaku K, Manna PR, Pelton SH, Butler WR, Stocco DM, Selvaraj V (2014) Peripheral benzodiazepine receptor/translocator protein global knock-out mice are viable with no effects on steroid hormone biosynthesis. *Journal of Biological Chemistry* 289 (40):27444-27454
- Tu LN, Zhao AH, Hussein M, Stocco DM, Selvaraj V (2016) Translocator protein (TSPO) affects mitochondrial fatty acid oxidation in steroidogenic cells. *Endocrinology* 157 (3):1110-1121
- Tu LN, Zhao AH, Stocco DM, Selvaraj V (2015) PK11195 effect on steroidogenesis is not mediated through the translocator protein (TSPO). *Endocrinology* 156 (3):1033-1039
- Twelves D, Perkins KS, Counsell C (2003) Systematic review of incidence studies of Parkinson's disease. *Movement disorders: official journal of the Movement Disorder Society* 18 (1):19-31
- Uchino H, Minamikawa-Tachino R, Kristián T, Perkins G, Narazaki M, Siesjö BK, Shibasaki F (2002) Differential neuroprotection by cyclosporin A and FK506 following ischemia corresponds with differing abilities to inhibit calcineurin and the mitochondrial permeability transition. *Neurobiology of disease* 10 (3):219-233
- Urrea H, Dufey E, Lisbona F, Rojas-Rivera D, Hetz C (2013) When ER stress reaches a dead end. *Biochimica et Biophysica Acta (BBA)-Molecular Cell Research* 1833 (12):3507-3517
- Valdés P, Mercado G, Vidal RL, Molina C, Parsons G, Martinez A, Galleguillos D, Armentano D, Schneider BL, Hetz C (2014) Control of dopaminergic neuron survival by the unfolded protein response transcription factor XBP1. *Proceedings of the National Academy of Sciences*:201321845
- Valera E, Mante M, Anderson S, Rockenstein E, Masliah E (2015) Lenalidomide reduces microglial activation and behavioral deficits in a transgenic model of Parkinson's disease. *Journal of neuroinflammation* 12 (1):93
- Van Den Eeden SK, Tanner CM, Bernstein AL, Fross RD, Leimpeter A, Bloch DA, Nelson LM (2003) Incidence of Parkinson's disease: variation by age, gender, and race/ethnicity. *American journal of epidemiology* 157 (11):1015-1022
- Van der Perren A, Macchi F, Toelen J, Carlon MS, Maris M, de Loor H, Kuypers DR, Gijsbers R, Van den Haute C, Debyser Z (2015) FK506 reduces neuroinflammation and dopaminergic neurodegeneration in an  $\alpha$ -synuclein-based rat model for Parkinson's disease. *Neurobiology of aging* 36 (3):1559-1568
- Van der Perren A, Van den Haute C, Baekelandt V (2014) Viral vector-based models of Parkinson's disease. In: *Behavioral Neurobiology of Huntington's Disease and Parkinson's Disease*. Springer, pp 271-301
- Vanhee C, Zapotoczny G, Masquelier D, Ghislain M, Batoko H (2011) The Arabidopsis multistress regulator TSPO is a heme binding membrane protein and a potential scavenger of porphyrins via an autophagy-dependent degradation mechanism. *The Plant Cell*:tpc. 110.081570
- Varga B, Markó K, Hádinger N, Jelítai M, Demeter K, Tihanyi K, Vas Á, Madarász E (2009) Translocator protein (TSPO 18 kDa) is expressed by neural stem and neuronal precursor cells. *Neuroscience letters* 462 (3):257-262
- Varley CD, Deodhar AA, Ehst BD, Bakke A, Blauvelt A, Vega R, Yamashita S, Winthrop KL (2013) Persistence of *Staphylococcus aureus* colonization among individuals with immune-mediated inflammatory diseases treated with TNF- $\alpha$  inhibitor therapy. *Rheumatology* 53 (2):332-337

- Veenman L, Vainshtein A, Yasin N, Azrad M, Gavish M (2016) Tetrapyrroles as endogenous TSPO ligands in eukaryotes and prokaryotes: comparisons with synthetic ligands. *International journal of molecular sciences* 17 (6):880
- Verdile G, Asih PR, Barron AM, Wahjoepramono EJ, Ittner LM, Martins RN (2015) The impact of luteinizing hormone and testosterone on beta amyloid (A $\beta$ ) accumulation: Animal and human clinical studies. *Hormones and behavior* 76:81-90
- Verleye M, Akwa Y, Liere P, Ladurelle N, Pianos A, Eychenne B, Schumacher M, Gillardin J-M (2005) The anxiolytic etifoxine activates the peripheral benzodiazepine receptor and increases the neurosteroid levels in rat brain. *Pharmacology Biochemistry and Behavior* 82 (4):712-720
- Verma A, Nye JS, Snyder SH (1987) Porphyrins are endogenous ligands for the mitochondrial (peripheral-type) benzodiazepine receptor. *Proceedings of the National Academy of Sciences* 84 (8):2256-2260
- Verma A, Snyder S (1988) Characterization of porphyrin interactions with peripheral type benzodiazepine receptors. *Molecular pharmacology* 34 (6):800-805
- Verstovsek S, Hoffman R, Mascarenhas J, Soria J-C, Bahleda R, McCoon P, Tang W, Cortes J, Kantarjian H, Ribrag V (2015) A phase I, open-label, multi-center study of the JAK2 inhibitor AZD1480 in patients with myelofibrosis. *Leukemia research* 39 (2):157-163
- Vila M, Vukosavic S, Jackson-Lewis V, Neystat M, Jakowec M, Przedborski S (2000)  $\alpha$ -Synuclein Up-Regulation in Substantia Nigra Dopaminergic Neurons Following Administration of the Parkinsonian Toxin MPTP. *Journal of neurochemistry* 74 (2):721-729
- Visanji NP, Brochie JM, Kalia LV, Koprich JB, Tandon A, Watts JC, Lang AE (2016)  $\alpha$ -Synuclein-based animal models of Parkinson's disease: challenges and opportunities in a new era. *Trends in neurosciences* 39 (11):750-762
- Vivash L, O'Brien TJ (2016) Imaging microglial activation with TSPO PET: lighting up neurologic diseases. *J Nucl Med* 57 (2):165-168
- Vogel DY, Vereyken EJ, Glim JE, Heijnen PD, Moeton M, van der Valk P, Amor S, Teunissen CE, van Horssen J, Dijkstra CD (2013) Macrophages in inflammatory multiple sclerosis lesions have an intermediate activation status. *Journal of neuroinflammation* 10 (1):809
- Volpicelli-Daley LA, Abdelmotilib H, Liu Z, Stoyka L, Daher JPL, Milnerwood AJ, Unni VK, Hirst WD, Yue Z, Zhao HT (2016) G2019S-LRRK2 expression augments  $\alpha$ -synuclein sequestration into inclusions in neurons. *Journal of Neuroscience* 36 (28):7415-7427
- Vos T, Flaxman AD, Naghavi M, Lozano R, Michaud C, Ezzati M, Shibuya K, Salomon JA, Abdalla S, Aboyans V (2012) Years lived with disability (YLDs) for 1160 sequelae of 289 diseases and injuries 1990–2010: a systematic analysis for the Global Burden of Disease Study 2010. *The lancet* 380 (9859):2163-2196
- Waak J, Weber SS, Waldenmaier A, Görner K, Alunni-Fabroni M, Schell H, Vogt-Weisenhorn D, Pham T-T, Reumers V, Baekelandt V (2009) Regulation of astrocyte inflammatory responses by the Parkinson's disease-associated gene DJ-1. *The FASEB Journal* 23 (8):2478-2489
- Wadsworth H, Jones PA, Chau W-F, Durrant C, Fouladi N, Passmore J, O'Shea D, Wynn D, Morisson-Iveson V, Ewan A (2012) [18 F] GE-180: a novel fluorine-18 labelled PET tracer for imaging translocator protein 18kDa (TSPO). *Bioorganic & medicinal chemistry letters* 22 (3):1308-1313
- Wang F, Cui N, Yang L, Shi L, Li Q, Zhang G, Wu J, Zheng J, Jiao B (2015a) Resveratrol rescues the impairments of hippocampal neurons stimulated by microglial over-activation in vitro. *Cellular and molecular neurobiology* 35 (7):1003-1015
- Wang G, Shi Y, Jiang X, Leak RK, Hu X, Wu Y, Pu H, Li W-W, Tang B, Wang Y (2015b) HDAC inhibition prevents white matter injury by modulating microglia/macrophage polarization through the GSK3 $\beta$ /PTEN/Akt axis. *Proceedings of the National Academy of Sciences* 112 (9):2853-2858
- Wang J, Duncan D, Shi Z, Zhang B (2013) WEB-based GEne SeT AnaLysis Toolkit (WebGestalt): update 2013. *Nucleic Acids Res* 41 (Web Server issue):W77-83. doi:10.1093/nar/gkt439

- Wang M, Wang X, Zhao L, Ma W, Rodriguez IR, Fariss RN, Wong WT (2014) Macroglia-microglia interactions via TSPO signaling regulates microglial activation in the mouse retina. *Journal of Neuroscience* 34 (10):3793-3806
- Wang Q, Liu Y, Zhou J (2015c) Neuroinflammation in Parkinson's disease and its potential as therapeutic target. *Translational neurodegeneration* 4 (1):19
- Weimers P, Halfvarson J, Sachs MC, Saunders-Pullman R, Ludvigsson JF, Peter I, Burisch J, Olén O (2018) Inflammatory bowel disease and parkinson's disease: a nationwide swedish cohort study. *Inflammatory bowel diseases* 25 (1):111-123
- Weisser SB, McLarren KW, Kuroda E, Sly LM (2013) Generation and characterization of murine alternatively activated macrophages. In: *Basic Cell Culture Protocols*. Springer, pp 225-239
- Wendler G, Lindemann P, Lacapère J-J, Papadopoulos V (2003) Protoporphyrin IX binding and transport by recombinant mouse PBR. *Biochemical and biophysical research communications* 311 (4):847-852
- Wichmann T, DeLONG MR (2003) Pathophysiology of Parkinson's disease: the MPTP primate model of the human disorder. *Annals of the New York Academy of Sciences* 991 (1):199-213
- Wilms H, Claasen J, Röhl C, Sievers J, Deuschl G, Lucius R (2003a) Involvement of benzodiazepine receptors in neuroinflammatory and neurodegenerative diseases: evidence from activated microglial cells in vitro. *Neurobiology of disease* 14 (3):417-424
- Wilms H, Rosenstiel P, Sievers J, DEUSCHL GN, Zecca L, Lucius R (2003b) Activation of microglia by human neuromelanin is NF- $\kappa$ B dependent and involves p38 mitogen-activated protein kinase: implications for Parkinson's disease. *The FASEB journal* 17 (3):500-502
- Winner BM, Zhang H, Farthing MM, Karchalla LM, Lookingland KJ, Goudreau JL (2017) Metabolism of Dopamine in Nucleus Accumbens Astrocytes Is Preserved in Aged Mice Exposed to MPTP. *Frontiers in aging neuroscience* 9:410
- Wisseman WT, Hill-Burns EM, Zabetian CP, Factor SA, Patsopoulos N, Hoglund B, Holcomb C, Donahue RJ, Thomson G, Erlich H (2013) Association of Parkinson disease with structural and regulatory variants in the HLA region. *The American Journal of Human Genetics* 93 (5):984-993
- Wolf L, Bauer A, Melchner D, Hallof-Buestrich H, Stoertebecker P, Haen E, Kreutz M, Sarubin N, Milenkovic V, Wetzel C (2015) Enhancing neurosteroid synthesis—relationship to the pharmacology of translocator protein (18 kDa)(TSPO) ligands and benzodiazepines. *Pharmacopsychiatry* 48 (02):72-77
- Wong YC, Krainc D (2017)  $\alpha$ -synuclein toxicity in neurodegeneration: mechanism and therapeutic strategies. *Nature medicine* 23 (2):1
- Wu H-F, Kao L-T, Shih J-H, Kao H-H, Chou Y-C, Li I-H, Kao S (2018) Pioglitazone use and Parkinson's disease: a retrospective cohort study in Taiwan. *BMJ open* 8 (8):e023302
- Xilouri M, Brekk OR, Stefanis L (2013) Alpha-synuclein and protein degradation systems: a reciprocal relationship. *Molecular neurobiology* 47 (2):537-551
- Yun SP, Kam T-I, Panicker N, Kim S, Oh Y, Park J-S, Kwon S-H, Park YJ, Karuppagounder SS, Park H (2018) Block of A1 astrocyte conversion by microglia is neuroprotective in models of Parkinson's disease. *Nature medicine* 24 (7):931
- Zambelli F, Pesole G, Pavesi G (2009) Pscan: finding over-represented transcription factor binding site motifs in sequences from co-regulated or co-expressed genes. *Nucleic Acids Res* 37 (Web Server issue):W247-252. doi:10.1093/nar/gkp464
- Zarranz JJ, Alegre J, Gómez-Esteban JC, Lezcano E, Ros R, Ampuero I, Vidal L, Hoenicka J, Rodriguez O, Atarés B (2004) The new mutation, E46K, of  $\alpha$ -synuclein causes parkinson and Lewy body dementia. *Annals of Neurology: Official Journal of the American Neurological Association and the Child Neurology Society* 55 (2):164-173
- Zhang B, Kirov S, Snoddy J (2005a) WebGestalt: an integrated system for exploring gene sets in various biological contexts. *Nucleic Acids Res* 33 (Web Server issue):W741-748. doi:10.1093/nar/gki475

- Zhang W, Wang T, Pei Z, Miller DS, Wu X, Block ML, Wilson B, Zhang W, Zhou Y, Hong J-S (2005b) Aggregated  $\alpha$ -synuclein activates microglia: a process leading to disease progression in Parkinson's disease. *The FASEB Journal* 19 (6):533-542
- Zhang W, Zecca L, Wilson B, Ren R, Wang Y-j, Wang X-m, Hong J-S (2013) Human neuromelanin: an endogenous microglial activator for dopaminergic neuron death. *Frontiers in bioscience (Elite edition)* 5:1
- Zhang Z, Zhang Z-Y, Schittenhelm J, Wu Y, Meyermann R, Schluesener HJ (2011) Parenchymal accumulation of CD163+ macrophages/microglia in multiple sclerosis brains. *Journal of neuroimmunology* 237 (1-2):73-79
- Zhang Z, Zhang Z-Y, Wu Y, Schluesener HJ (2012) Lesional accumulation of CD163+ macrophages/microglia in rat traumatic brain injury. *Brain research* 1461:102-110
- Zhao AH, Tu LN, Mukai C, Sirivelu MP, Pillai VV, Morohaku K, Cohen R, Selvaraj V (2016a) Mitochondrial translocator protein (TSPO) function is not essential for heme biosynthesis. *Journal of Biological Chemistry* 291 (4):1591-1603
- Zhao Q, Wu X, Yan S, Xie X, Fan Y, Zhang J, Peng C, You Z (2016b) The antidepressant-like effects of pioglitazone in a chronic mild stress mouse model are associated with PPAR $\gamma$ -mediated alteration of microglial activation phenotypes. *Journal of neuroinflammation* 13 (1):259
- Zhou X, Spittau B, Kriegstein K (2012) TGF $\beta$  signalling plays an important role in IL4-induced alternative activation of microglia. *Journal of neuroinflammation* 9 (1):210
- Zhu X-C, Jiang T, Zhang Q-Q, Cao L, Tan M-S, Wang H-F, Ding Z-Z, Tan L, Yu J-T (2015) Chronic metformin preconditioning provides neuroprotection via suppression of NF- $\kappa$ B-mediated inflammatory pathway in rats with permanent cerebral ischemia. *Molecular neurobiology* 52 (1):375-385
- Zimprich A, Benet-Pagès A, Struhal W, Graf E, Eck SH, Offman MN, Haubenberger D, Spielberger S, Schulte EC, Lichtner P (2011) A mutation in VPS35, encoding a subunit of the retromer complex, causes late-onset Parkinson disease. *The American Journal of Human Genetics* 89 (1):168-175

## 7 Curriculum Vitae

Jing Gong

Date of birth: 21, September 1988

Place of birth: Hubei, China

Email address: [jinggong24@gmail.com](mailto:jinggong24@gmail.com)

### Education

11/2013 - Present

#### **Georg-August-Universität Göttingen**

Ph.D. Thesis “Translocator protein 18 ligand Emapunil protects against neurodegeneration in the MPTP mouse model of Parkinsonism” in the Translational Dementia Research Department, German Center for Neurodegenerative Diseases (DZNE), Bonn, under the supervision of Prof. Dr. Anja Schneider

09/2010 – 06/2013

#### **Huazhong Agricultural University**

Master Thesis “Molecular mechanism study on an antimony-resistant bacterium Ts44” in the State key laboratory of agricultural microbiology, under the supervision of Prof. Dr. Gejiao Wang

09/2007 – 06/2011

#### **Huazhong Agricultural University**

Bachelor Thesis “The complex regulatory mode of arsenic oxidation controlled by  $\delta$ -54 promotor” in the colleague of life science, under the supervision of Prof. Dr. Gejiao Wang

### Publications:

**Gong, J.\***, Szegő, É.M.\*, Leonov, A., Benito, E., Becker, S., Fischer, A., Zweckstetter, M., Outeiro, T. and Schneider, A., 2019. Translocator protein ligand protects against neurodegeneration in the MPTP mouse model of Parkinsonism. *Journal of Neuroscience*, pp.2070-18.

Kunadt, M., Eckermann, K., Stuendl, A., **Gong, J.**, Russo, B., Strauss, K., Rai, S., Kügler, S., Lockhart, L.F., Schwalbe, M. and Krumova, P., 2015. Extracellular vesicle sorting of  $\alpha$ -Synuclein is regulated by sumoylation. *Acta neuropathologica*, 129(5), pp.695-713.